

UNCLASSIFIED

AD NUMBER

ADB113186

NEW LIMITATION CHANGE

TO

**Approved for public release, distribution
unlimited**

FROM

**Distribution: Further dissemination only
as directed by U.S. Army Medical Research
and Development Command, Fort Detrick, MD
21701-5012 or higher DoD authority.**

AUTHORITY

USAMRDC SGRD-RMI-S ltr, 31 Jul 1992

THIS PAGE IS UNCLASSIFIED

DTIC FILE COPY

L ①

AD-B113 186

Preformulation and Formulation of Investigational New Drugs

Annual Progress Report

John L. Lach
Douglas R. Flanagan
Lloyd E. Matheson, Jr.

July 1985

Supported by

U.S. Army Medical Research and
Development Command
Fort Detrick
Frederick, Maryland 21701-5012

Contract No. DAMD17-85-C-5003

College of Pharmacy
University of Iowa
Iowa City, Iowa 52242

Further dissemination only as directed by Commander, US Army Medical Research and Development Command, ATTN: SGRD-RMI-S, Fort Detrick, Frederick, Maryland 21701-5012, 16 September 1986, or higher DOD authority.

The findings in this report are not to be construed as an Official Department of the Army position unless so designated by other authorized documents.



SECURITY CLASSIFICATION OF THIS PAGE

Form Approved
OMB No 0704-0188
Exp Date Jun 30, 1986

AD-B113 186

ITIVE MARKINGS

1a REPORT SECURITY CLASSIFICATION
UNCLASSIFIED

2a SECURITY CLASSIFICATION AUTHORITY

2b. DECLASSIFICATION/DOWNGRADING SCHEDULE

4. PERFORMING ORGANIZATION REPORT NUMBER(S)

6a. NAME OF PERFORMING ORGANIZATION
College of Pharmacy
University of Iowa

6c. ADDRESS (City, State, and ZIP Code)

Iowa City, Iowa 52242

8a. NAME OF FUNDING/SPONSORING
ORGANIZATION U.S. Army Medical
Research & Development Command8c. ADDRESS (City, State, and ZIP Code)
Fort Detrick
Frederick, Maryland 21701-50126b. OFFICE SYMBOL
(If applicable)8b. OFFICE SYMBOL
(If applicable)
SGRD-RMI-S

3. DISTRIBUTION/AVAILABILITY OF REPORT

Further dissemination only as directed by
Commander, US Army Medical Research and
Development Command, ATTN: SGRD-RMI-S.

5. MONITORING ORGANIZATION REPORT NUMBER(S)

7a. NAME OF MONITORING ORGANIZATION

7b. ADDRESS (City, State, and ZIP Code)

9. PROCUREMENT INSTRUMENT IDENTIFICATION NUMBER

DAMD17-85-C-5003

10. SOURCE OF FUNDING NUMBERS

PROGRAM ELEMENT NO. 63764A	PROJECT NO. 3M4- 63764D995	TASK NO. ✓	WORK UNIT ACCESSION NO. BB 049
-------------------------------	----------------------------------	---------------	--------------------------------------

11. TITLE (Include Security Classification)

(U) Preformulation and Formulation of Investigational New Drugs

12. PERSONAL AUTHOR(S)

Lach, John L., Douglas R. Flanagan, and Lloyd E. Matheson, Jr.

13a. TYPE OF REPORT
Annual13b. TIME COVERED
FROM 10/3/84 TO 10/2/8514 DATE OF REPORT (Year, Month, Day)
1985 July15. PAGE COUNT
161

16. SUPPLEMENTARY NOTATION

17. COSATI CODES

FIELD	GROUP	SUB-GROUP
06	05	
06	15	

18. SUBJECT TERMS (Continue on reverse if necessary and identify by block number)

WR249,943; MMB-4·2Cl, stability, stabilization, bromides;
WR249,655; HI-6·2Cl; Preformulation; Antioxidants; Antidiarrheal;
WR142,490·HCl; Mefloquine HCl; Solid-State; Pyridostigmine;

19. ABSTRACT (Continue on reverse if necessary and identify by block number)

This annual report contains preformulation and formulation studies on WR249,655·2Cl (HI-6·2Cl), WR238,605, WR171,669·HCl (Halofantrine HCl), WR249,943·2Cl (MMB-4·2Cl), WR142,490·HCl (Mefloquine HCl) and Pyridostigmine Bromide. These studies include stability studies on WR249,655·2Cl and WR249,943·2Cl; physicochemical characterization of WR238,605; investigation of solid-state properties of various lots of WR171,669·HCl and WR142,490·HCl; initial development studies for a sustained release pyridostigmine bromide tablet. *Prepared by [Signature]*

20. DISTRIBUTION/AVAILABILITY OF ABSTRACT

 UNCLASSIFIED/UNLIMITED SAME AS RPT DTIC USERS

21. ABSTRACT SECURITY CLASSIFICATION

UNCLASSIFIED

22a. NAME OF RESPONSIBLE INDIVIDUAL
Mary Frances Bostian22b. TELEPHONE (Include Area Code)
301/663-732522c. OFFICE SYMBOL
SGRD-RMI-S

3. Distribution/Availability of Report (continued)

Fort Detrick, Frederick, Maryland 21701-5012, 16 September 1986, or higher authority.

18. Subject Terms (continued)

Sustained release

Accession For		
NTIS	CRA&I	<input type="checkbox"/>
DHIC	TAB	<input checked="" type="checkbox"/>
Unauthorized		<input type="checkbox"/>
Justification		
By		
Distribution /		
Availability Codes		
Dist	Avail and/or Special	
F-5		



Summary

This annual progress report represents preformulation and formulation projects on the following drugs:

WR249,655·2Cl (HI-6·2Cl)
WR238,605
WR171,669·HCl (Halofantrine HCl)
WR249,943·2Cl (MMB-4·2Cl)
WR142,490·HCl (Mefloquine HCl)
Pyridostigmine Bromide

This work consisted of degradation kinetics of WR249,655·2Cl and WR249,943·2Cl in solution; various attempts to stabilize these systems and the development of a stable aqueous solution formulation for WR249,943·2Cl. Also included are the physicochemical properties of WR238,605; a comparison of the solid state properties of various lots of WR171,669·HCl; a comparison of the solid state properties of various lots of WR142,490·HCl and the initial development of a sustained release tablet of pyridostigmine bromide.

TABLE OF CONTENTS

	<u>Page</u>
Abstract	i
Title Page	ii
Summary	iii
Quarterly Report No. 20	1
Quarterly Report No. 21	76
Quarterly Report No. 22	97
Quarterly Report No. 23	121

AD

Quarterly Report Number 20

- Part I: Solution Stability of the Cholinesterase Reactivator Oxime WR249,655·2C1 (HI-6·2C1)
Part II: Physico-chemical Properties of WR238,605
Part III: Comparison of the Solid State Properties of Lots AC, AD, AE, AG, AL and AM of WR171,669·HCl (Halo-fantrine Hydrochloride)

Submitted by:

John L. Lach, Principal Investigator
Douglas R. Flanagan, Assistant Principal Investigator
Lloyd E. Matheson, Jr., Assistant Principal Investigator

October 1984

Supported by:

U.S. Army Medical Research and Development Command
Fort Detrick
Frederick, Maryland 21701-5012

Contract No. DAMD 17-85-C-5003

College of Pharmacy
University of Iowa
Iowa City, IA 52242
(319/353-4520)

Further dissemination only as directed by Commander, US Army Medical Research and Development Command, ATTN: SGRD-RMI-S, Fort Detrick, Frederick, Maryland 21701-5012, 16 September, 1986, or higher DOD authority.

The findings in this report are not to be construed as an Official Department of the Army position unless so designated by other authorized documents.

Table of Contents

	<u>Page</u>
List of Tables	3
List of Figures	4
Resumé of Progress	7
PART I: Solution Stability of the Cholinesterase Reactivator Oxime WR249,655·2Cl (HI-6·2Cl)	
Objective	8
Summary	8
Methodology	9
Results	12
Conclusions	21
PART II: Physico-chemical Properties of WR238,605	
Solid Properties	24
Solution Properties	29
PART III: Comparison of the Solid State Properties of Lots AC, AD, AE, AG, AL and AM of WR171,669·HCl (Halofantrine Hydro- chloride)	
Objective	44
Summary	44
Solid State Properties	44
Conclusion	45

List of Tables

<u>Table</u>	<u>Title</u>	<u>Page</u>
1	Degradation of Dilute Solutions (1 mg/ml) of HI-6 at 40°C in Various pH Citrate Buffers and Their Apparent Kinetic Parameters	13
2	Degradation of Dilute Solutions (1 mg/ml) of HI-6 at 60°C in Various pH Citrate Buffers and Their Apparent Kinetic Parameters	14
3	Effect of Concentration (1 mg/ml vs. 100 mg/ml) of HI-6 on its Stability in Citrate Buffer	16
4	Degradation of Concentrated Solutions (25 mg/ml) of HI-6 in pH 5.72 Citrate Buffer at 60°C and its Apparent Kinetic Parameters	17
5	Degradation of Concentrated Solutions (100 mg/ml) of HI-6 in Glycine Buffer at 40°C (pH 1.93 and 2.94) and 60°C (pH 1.96 and 2.96) and Their Apparent Kinetic Parameters	19
6	Effect of Varying Concentrations of Sodium Lauryl Sulfate (SLS) on the Degradation of Dilute Solutions (0.5 mg/ml) of HI-6 in pH 5.74 Citrate Buffer at 60°C and Their Apparent Kinetic Parameters	20
7	Effect of 20% Sodium Taurocholate on the Degradation of Concentrated Solutions (100 mg/ml) of HI-6 in Citrate Buffer at 40°C (pH 2.69) and 60°C (pH 2.71) and Their Apparent Kinetic Parameters	22
8	X-Ray Diffraction Data for WR238,605 AC	29
9	X-Ray Diffraction Data for Halofantrine Hydrochloride (Lot AC)	65
10	X-Ray Diffraction Data for Halofantrine Hydrochloride (Lot AD)	67
11	X-Ray Diffraction Data for Halofantrine Hydrochloride (Lot AE)	69
12	X-Ray Diffraction Data for Halofantrine Hydrochloride (Lot AG)	71
13	X-Ray Diffraction Data for Halofantrine Hydrochloride (Lot AL)	73
14	X-Ray Diffraction Data for Halofantrine Hydrochloride (Lot AM)	75

List of Figures

<u>Figure</u>	<u>Description</u>	<u>Page</u>
1	pH Profiles for HI-6·2Cl in Citrate Buffer at 40°C	15
2a	Photomicrograph of WR238,605 AC at a 200X Magnification	25
2b	Photomicrograph of WR238,605 AC at a 400X Magnification	25
3	Thermogram of WR238,605 AC	26
4	X-Ray Diffraction Pattern for WR238,605 AC	27
5	Infrared Spectrum of WR238,605 AC	28
6	Ultraviolet Spectrum WR238,605 AC in Distilled Water	31
7	Ultraviolet Spectrum for WR238,605 AC in 0.01 N HCl	32
8	Ultraviolet Spectrum for WR238,605 AC in 95% Ethanol	33
9	Ultraviolet Spectrum for WR238,605 AC in Methanol	34
10	Ultraviolet Spectrum for WR238,605 AC in Isopropanol	35
11	Ultraviolet Spectrum for WR238,605 AC in Chloroform	36
12	NMR Spectrum of WR238,605 AC	37
13	Size distribution obtained for WR238,605 AC (1 mg/ml) cooled in 10°C increments from 80°C to 20°C	39
14	Size distribution obtained for WR238,605 AC (1 mg/ml) cooled quickly from 60°C to 20°C	40
15	Size distribution obtained for WR238,605 AC (1 mg/ml) in 1% gelatin cooled in 10°C increments from 80°C to 40°C	41
16	Size distribution obtained for WR238,605 AC (1 mg/ml) cooled in 10°C increments from 85°C to 25°C	42
17a	Photomicrograph of Halofantrine Hydrochloride (Lot AC) Magnified 100X	46
17b	Photomicrograph of Halofantrine Hydrochloride (Lot AC) Magnified 1000X	46
18a	Photomicrograph of Halofantrine Hydrochloride (Lot AD) Magnified 400X	47
18b	Photomicrograph of Halofantrine Hydrochloride (Lot AD) Magnified 2000X	47

<u>Figure</u>	<u>Description</u>	<u>Page</u>
19a	Photomicrograph of Halofantrine Hydrochloride (Lot AE) Magnified 400X	48
19b	Photomicrograph of Halofantrine Hydrochloride (Lot AE) Magnified 2000X	48
20a	Photomicrograph of Halofantrine Hydrochloride (Lot AG) Magnified 60X	49
20b	Photomicrograph of Halofantrine Hydrochloride (Lot AG) Magnified 3000X	49
21a	Photomicrograph of Halofantrine Hydrochloride (Lot AL) Magnified 200X	50
21b	Photomicrograph of Halofantrine Hydrochloride (Lot AL) Magnified 3000X	50
22a	Photomicrograph of Halofantrine Hydrochloride (Lot AM) Magnified 300X	51
22b	Photomicrograph of Halofantrine Hydrochloride (Lot AM) Magnified 1000X	51
23	Infrared Spectrum of Halofantrine Hydrochloride (Lot AC) (KBr Pellet)	52
24	Infrared Spectrum of Halofantrine Hydrochloride (Lot AD) (KBr Pellet)	53
25	Infrared Spectrum of Halofantrine Hydrochloride (Lot AE) (KBr Pellet)	54
26	Infrared Spectrum of Halofantrine Hydrochloride (Lot AG) (KBr Pellet)	55
27	Infrared Spectrum of Halofantrine Hydrochloride (Lot AL) (KBr Pellet)	56
28	Infrared Spectrum of Halofantrine Hydrochloride (Lot AM) (KBr Pellet)	57
29	Thermogram of Halofantrine Hydrochloride (Lot AC)	58
30	Thermogram of Halofantrine Hydrochloride (Lot AD)	59
31	Thermogram of Halofantrine Hydrochloride (Lot AE)	60
32	Thermogram of Halofantrine Hydrochloride (Lot AG)	61
33	Thermogram of Halofantrine Hydrochloride (Lot AL)	62

<u>Figure</u>	<u>Description</u>	<u>Page</u>
34	Thermogram of Halofantrine Hydrochloride (Lot AM)	63
35	X-Ray Powder Diffraction Pattern for Halofantrine Hydrochloride (Lot AC)	64
36	X-Ray Powder Diffraction Pattern for Halofantrine Hydrochloride (Lot AD)	66
37	X-Ray Powder Diffraction Pattern for Halofantrine Hydrochloride (Lot AE)	68
38	X-Ray Powder Diffraction Pattern for Halofantrine Hydrochloride (Lot AG)	70
39	X-Ray Powder Diffraction Pattern for Halofantrine Hydrochloride (Lot AL)	72
40	X-Ray Powder Diffraction Pattern for Halofantrine Hydrochloride (Lot AM)	74

Resumé of Progress

Work is beginning on a screen of antioxidant materials for use in stabilizing WR249,943·2C1 (MMB-4·2C1) and WR249,655·2C1 (HI-6·2C1).

Part I: Solution Stability of the Cholinesterase Reactivator

Objective

The objectives of this work were to 1) examine the stability of HI-6·2Cl (4-Carbamoyl-2'-hydroxyiminomethyl-1,1'-oxydimethylene-di (pyridinium chloride) in solution under a variety of pH and temperature conditions; 2) attempt to stabilize the drug in solution by retarding its hydrolysis rate.

Summary

The degradation of dilute solutions of HI-6·2Cl was followed in citrate buffers ranging in pH from approximately 2 to 6 at both 40° and 60°C. The most stable pH appears to be about 2.7. The $t_{1/2}$ at 25°C extrapolates to only 250 days. When concentrated (25 mg/mL or 100 mg/mL) solutions were studied it was observed that the concentrated solutions were less stable by a factor of five at 40°C and about 2.5 at 60°C. The $t_{1/2}$ at 25°C extrapolates to only 37 days. MMB-4·2Cl appears on the basis of limited data at pH 5.72, 60°C and a concentration of 25 mg/mL to be somewhat more stable than HI-6·2Cl. The use of glycine buffer at approximately pH 2 and 3 produced similar stability compared to the citrate buffer. It was noted that a dark green color develops in the concentrated HI-6·2Cl solutions. This suggests that an antioxidant may be useful. Stability was enhanced by the use of sodium lauryl sulfate but not by the use of sodium taurocholate.

MethodologyReagents

HI-6·2C1, (WRAIR); tetrahydrofuran, UV grade (Burdick and Jackson); 1-octane-sulfonic acid, sodium salt (Eastman Kodak); glacial acetic acid, A.C.S., methyl paraben, sodium hydroxide, citric acid monohydrate, concentrated hydrochloric acid, sodium chloride (Mallinckrodt); sodium lauryl sulfate, (Pfaltz and Bauer); glycine (Fisher). All reagents were at least reagent grade and were used as received.

Apparatus

The high pressure liquid chromatographic system consisted of: a Waters system with a Model 6000A pump and a Model 440 absorbance detector; a Fisher Recordall Series 5000 recorder; a Rheodyne 7125 injector with a 20 μ L loop and an Altex Ultrasphere I.P. 5 μ (25 cm x 4.6 mm I.D.) column. All dilute solution kinetic studies were carried out in 2 ml amber ampules (Wheaton). The concentrated solution kinetic studies were carried out by placing the drug solution into clear 1 mL vials (Pierce Chemical) sealed with Teflon®/Silicone discs (Pierce Chemical). The vials were, in turn, were placed into amber bottles and stored in the appropriate waterbath. An adjustable sampler system (Oxford) was used to pipet the required volumes. A Fisher pH meter was used for pH measurements. Haake E2 heater circulators were used to maintain waterbath temperature.

Solution Preparation

Citrate Buffers. Solution A was prepared by dissolving 21.01 grams of citric acid monohydrate and 8 grams of sodium hydroxide in enough distilled water to make 1000 mL of a pH 5.0 solution. Solution B was prepared by diluting concentrated hydrochloric acid to 0.1N (8.33 mL per liter) to produce a solution of pH 1.0. Solution C was prepared by dissolving 4.0 grams of sodium hydroxide in one liter (0.1N) of distilled water. The pH 2.0 buffer was prepared by

mixing 75.5 mL of solution A with enough solution B to make 250 mL of solution. The pH 3.0 buffer was prepared by mixing 99.8 mL of solution A with enough solution B to make 250 mL of solution. The pH 4.0 buffer was prepared by mixing 137.8 mL of solution A with enough solution B to make 250 mL of solution. The pH 6.0 buffer was prepared by mixing 150.8 mL of solution A with enough solution C to make 250 mL of solution. These pH values are theoretical values. Actual pH values were measured at 40° and 60°C.

Glycine Buffers. Solution A was prepared by dissolving 7.507 grams of glycine (0.1M) and 5.844 grams of sodium chloride (0.1M) in enough distilled water to make one liter of solution. Solution B was prepared by diluting concentrated hydrochloric acid to 0.1N (8.33 mL per liter). The pH 2.0 buffer was prepared by mixing 50.7 mL of solution A with enough solution B to make 100 mL of solution. The pH 3.0 buffer was prepared by mixing 81.0 mL of solution A with enough solution B to make 100 mL of solution. These pH values are theoretical values. Actual pH values were measured at 40° and 60°C.

Internal Standard. The stock solution was prepared by dissolving 16 mg of methyl paraben in 2-3 mL of methanol and bringing up to a volume of 1000 mL with distilled water.

HI-6·2C1 Standard Curve Stock Solution. Twenty milligrams of drug was dissolved in distilled water in a 100 mL volumetric flask diluted to the mark. This is a 20 mg % solution.

Standard Curve Solution. Four concentrations of HI-6·2C1 were prepared in distilled water mixing in a 50 mL volumetric flask either 0.5, 2, 4 or 5 mL of stock solution with 10.0 mL of internal standard solution and enough distilled water to make 50 mL. These dilutions resulted in concentrations of 0.2, 0.8,

1.6 and 2.0 mg %, respectively, and a constant concentration of 0.32 mg % of internal standard.

Kinetic Working Solution. The kinetics of degradation were followed in dilute solutions of either 0.5 or 1.0 mg/mL initial concentration of HI-6·2Cl and in concentrated solutions of either 25 mg/mL or 100 mg/mL.

Mobile Phase. This solution is prepared by dissolving 4.325 gram of 1-octanesulfonic acid, sodium salt in a solvent system consisting of 300 mL of tetrahydrofuran, 21 mL of glacial acetic acid and enough distilled water to make a volume of one liter.

Assay Method

The apparatus and mobile phase have been previously described. The analytical wavelength was 280 nm; the flow rate was 1.0 mL/min. and the chart speed was one cm/min. The diluted working kinetic solutions were analyzed by removing 0.5 mL of the solution from an ampule and adding it to a 25 mL volumetric flask containing 5 mL of the internal standard solution. The flasks were brought to volume with distilled water. The contents of two ampules were quantitated each time. The 25 mg/mL concentrated working kinetic solutions were analyzed by removing 40 μ L of solution from a vial and adding it to a 50 mL volumetric flask containing 10 mL of internal standard solution. The flasks were brought to volume with distilled water. Two samples were analyzed each time. The 100 mg/mL concentrated working kinetic solutions were analyzed by removing 10 μ L of solution from a vial and adding it to a 50 mL volumetric flask containing 10 mL of internal standard solution. Again the flasks were brought to volume with distilled water and carried out in duplicate.

Stabilization Studies

In addition to determining the pH of greatest stability, anionic surfactants were added to the kinetic working solutions. In the first, sodium lauryl sulfate

was dissolved in pH 5.74 citrate buffer in concentrations of either 0.25, 0.5, 1, 2, or 4 % w/v. The study was carried out at 60°C. In the second case, 20 % w/v sodium taurocholate was added to pH 2.69 citrate buffer. The study was carried out at both 40° and 60°C.

Results

Kinetic Studies

Hydrolysis Studies. The effects of temperature and pH on dilute solutions are easily seen in the data in Tables 1 and 2. HI-6·2Cl is considerably more stable at about pH 2.7 as seen in Figure 1 than at either lower or higher pH values. The apparent activation energy for the process causing the loss of HI-6·2Cl at pH 2.68 is approximately 23 Kcal per mole. This extrapolates to a $t_{\frac{1}{2}}$ at 25°C of about 4.5 years, but a $t_{.90}$ (i.e., time for 10% to degrade) of only 250 days.

Data in Table 3 shows the effect of the concentration of HI-6·2Cl (100 mg/mL vs. 1 mg/mL) on its degradation rate at 40° and 60°C. The more concentrated solutions are several times less stable. This has also been reported for 2-PAM by Ellin (1). The apparent activation energy for the process is about 15.4 kcal per mole which extrapolated to a $t_{\frac{1}{2}}$ at 25°C of about 177 days and $t_{.90}$ of only 37 days. Obviously, additional measures must be taken to stabilize HI-6 in addition to buffering at pH 2.7.

The degradation of solutions of HI-6·2Cl (25 mg/mL) at pH 5.72 in citrate buffer at 60°C are presented in Table 4. The $t_{\frac{1}{2}}$ is about 30 hours which may be compared to the $t_{\frac{1}{2}}$ for MMB-4·2Cl under these conditions of about 41 hours (2).

In dilute solutions, a $t_{\frac{1}{2}}$ of 1.3 years at pH 2.67 and 40°C has been previously reported for MMB-4·2Cl (2) compared to a $t_{\frac{1}{2}}$ for HI-6·2Cl under these conditions of 0.7 years from the data in Table 1 in this report. It appears

Table 1. Degradation of Dilute Solutions (1 mg/mL) of HI-6 at 40°C in Various pH Citrate Buffers and Their Apparent Kinetic Parameters

Time(Days)	Percent Remaining				
	pH 1.78	pH 2.68	pH 3.67	pH 4.80	pH 5.70
0	100*	100*	100	100	100*
4	93.2*	93.2*	98.3	81.8	67.7*
11	91.7*	89.8*	97.2	72.5*	29.8*
18	-	-	-	66.1*	14.5*
25	-	-	-	61.3*	5.0*
39	87.7*	-	92.9*	51.2*	-
60	64.9	79.3*	81.3*	39.1*	-
81	68.9*	79.0*	73.4*	32.0*	-
115	55.7*	69.5*	60.7*	19.8*	-
r	-.9589	-.9726	-.9991	-.9990	-.9971
k(days ⁻¹)	.00490	.00271	.00553	.0123	.118
t _{1/2} (days)	141	255	125	56	6

*Points used in regression line to calculate kinetic parameters

Table 2. Degradation of Dilute Solutions (1 mg/mL) of HI-6 at 60°C in Various pH Citrate Buffers and Their Apparent Kinetic Parameters

Time(Days)	Percent Remaining			
	pH 1.78	pH 2.71	pH 3.69	pH 4.81
0	100*	100*	100*	100*
4	84.9*	88.7*	82.7*	55.7*
11	69.0*	78.5*	60.7*	32.5*
18	59.8*	68.0*	44.5*	21.0*
25	52.3*	57.8*	31.0*	11.9*
39	25.1*	36.7*	7.8	-
60	11.8	22.5*	-	-
r	.9806	.9971	.9995	.9917
k(days ⁻¹)	.0330	.0251	.0463	.0808
t _{1/2} (days)	21	27.6	15	8.6

*Points used in regression line to calculate kinetic parameters

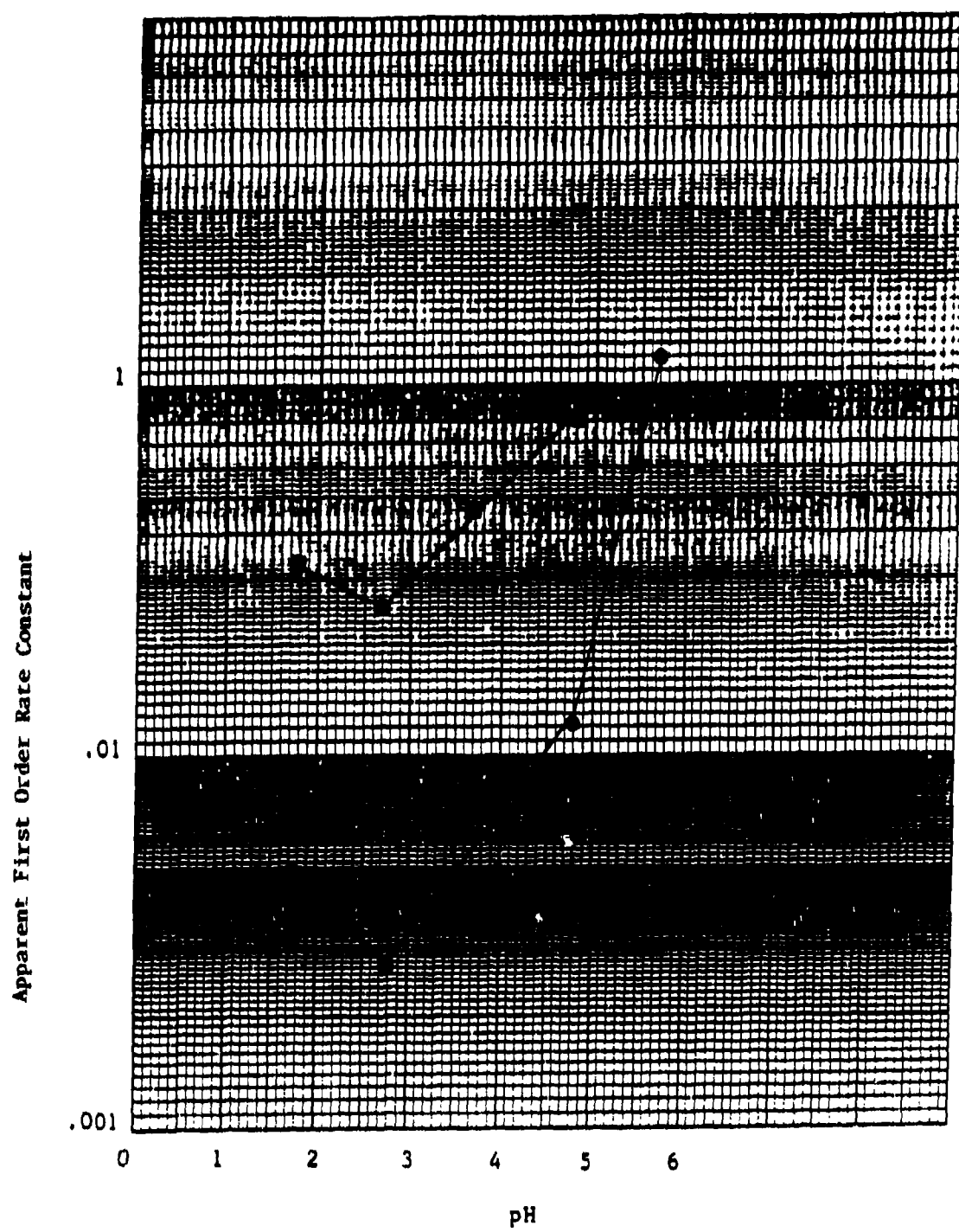


Figure 1. pH profile for HI-6·2Cl in Citrate Buffer at 40°C
● ; 60°C □ .

Table 3. Effect of Concentration (1 mg/mL vs. 100 mg/mL) of HI-6
on its Stability in Citrate Buffer

Time(Days)	Percent Remaining			
	1 mg/mL		100 mg/mL	
	40°C (pH 2.68)	60°C (pH 2.71)	40°C (pH 2.69)	60°C (pH 2.71)
0	100	100	100	100
4	93.2	88.7	-	-
11	89.8	78.5	-	-
14	-	-	87.6	34.7
18	-	68.0	-	-
25	-	57.8	-	-
34	-	-	64.1	9.5
39	-	36.7	-	-
48	-	-	53.0	5.7
60	79.3	22.5	-	-
81	79.0	-	-	-
115	69.5	-	-	-
r	.9726	.9971	.9963	.9921
k(days ⁻¹)	.00271	.0251	.0136	.0600
t _{1/2} (days)	255	27.6	51	11.5

Table 4. Degradation of Concentrated Solutions (25 mg/mL) of HI-6 in pH 5.72 Citrate Buffer at 60°C and Its Apparent Kinetic Parameters

Time(Hrs)	Percent Remaining
0	100
3	90
5	86.4
7	78.3
10	72.1
24	56.5
r	.9820
k(hrs ⁻¹)	.0232
t _{1/2} (hrs)	29.8

as though the MMB-4·2Cl is more stable than HI-6·2Cl although this is being examined further.

Glycine buffers at about pH 2 and 3 were used to determine if they might be more suitable than citrate buffers. From the data in Table 5, it can be seen that little change in stability occurs.

Apparent Oxidation of HI-6·2Cl solutions. When earlier work on the stability of HI-6·2Cl was carried out it was only done at low concentrations. In this work done at higher concentrations, it was noted that colorless solutions of HI-6·2Cl eventually became dark green. This suggests that the kinetics of degradation in acidic media are much more complex than earlier suspected. The dilute solutions of HI-6·2Cl contained so little drug that no color change was observed.

Other workers (3) have suggested that under acidic conditions that an equilibrium exists between the oxime and the degradation products - hydroxylamine and an aldehyde. Aldehydes are easily oxidized, so it appears that it will be necessary to find an antioxidant that will protect the aldehyde degradation product so that the equilibrium will not be shifted to the right causing further loss of HI-6·2Cl as the aldehyde is further reacted. In addition, it may be possible to shift the equilibrium to the left by including hydroxylamine in the initial formulation. These studies are currently underway and will be reported when this report is finalized.

Stabilization Studies

Effect of Sodium Lauryl Sulfate. Since it has been previously reported that inclusion of the negatively charged surfactant, sodium lauryl sulfate, improved the stability of MMB-4·2Cl (2), it was also added to solutions of HI-6·2Cl. The data is presented in Table 6. As before, the half-life steadily

Table 5. Degradation of Concentrated Solutions (100 mg/mL) of HI-6 in Glycine Buffer at 40°C (pH 1.93 and 2.94) and 60°C (pH 1.96 and 2.96) and Their Apparent Kinetic Parameters

Time(Days)	Percent Remaining			
	40°C		60°C	
	pH 1.93	pH 2.94	pH 1.96	pH 2.96
0	100	100	100	100
13	79.6	89.3	30.8	38.8
27	61.9	78.5	11.2	15.6
r	-.9999	-.9999	-.9979	-.9995
k(days ⁻¹)	1.78x10 ⁻²	8.98x10 ⁻³	8.09x10 ⁻²	6.89x10 ⁻²
t _{1/2} (days)	39	77.3	8.5	10.1

Table 6. Effect of Varying Concentrations of Sodium Lauryl Sulfate (SLS) on the Degradation of Dilute Solutions (0.5 mg/mL) of HI-6 in pH 5.74 Citrate Buffer at 60°C and Their Apparent Kinetic Parameters

Time(Hrs)	Percent Remaining					
	No SLS	0.25% SLS	0.5% SLS	1% SLS	2% SLS	4% SLS
0	100	100	100	100	100	100
2	92.6	-	98.1	-	-	-
4	77.8	-	-	-	-	-
6	64.4	85.8	88.9	-	-	-
10	44.4	68.7	77.3	-	-	-
24	13.2	-	-	-	-	-
25	-	42.3	57.4	-	-	-
26	-	-	-	73.1	75.9	23.6
47	-	25.1	38.6	-	-	-
73	-	-	-	33.3	51.4	56.4
125	-	-	-	18.6	32.9	37.9
169	-	-	-	11.2	21.2	25.9
r	.9988	.9938	.9966	.9970	.9994	.9997
k(hrs^{-1})	.0867	.0298	.0206	.0131	.0090	.0080
$t_{\frac{1}{2}}$ (hrs)	8	23.2	33.7	52.8	77	86.6

increased to about 87 hours at 4% w/v levels of sodium lauryl sulfate. Unfortunately, this surfactant is irritating and somewhat toxic. An even larger drawback, however, is the instability (hydrolysis) of the sodium lauryl sulfate itself at low pH values where the HI-6·2Cl is more stable. This instability manifests itself as a precipitate of lauric acid as previously reported (2). Nevertheless, it does suggest that the technique may be beneficial if a more stable and less toxic surfactant can be found. Other surfactants are being screened.

Effect of Sodium Taurocholate. The effect of 20% w/v sodium taurocholate on the degradation of concentrated solutions of HI-6·2Cl is shown in Table 7. Approximately a 20% increase in stability is noted at 40°C while only a slight effect is noted at 60°C. This suggests that sodium taurocholate is unsuitable as a stability enhancer for HI-6·2Cl solutions.

Conclusions

HI-6·2Cl is apparently most stable at a pH of about 2.7. Additional measures other than just buffering will be needed to stabilize HI-6·2Cl. The addition of the anionic surfactant, sodium lauryl sulfate, enhances stability, but cannot be used due to its own instability, particularly at low pH where HI-6·2Cl is more stable. Oxidation of the aldehyde hydrolysis degradation products will have to be slowed in order to help stabilize the system and prevent color formation.

Table 7. Effect of 20% Sodium Taurocholate on the Degradation of Concentrated Solutions (100 mg/mL) of HI-6 in Citrate Buffer at 40°C (pH 2.69) and 60°C (pH 2.71) and Their Apparent Kinetic Parameters

Time (days)	Percent Remaining				
	40°C		60°C		
	No Taurocholate	20% Taurocholate	No Taurocholate	20% Taurocholate	
0	100	100	100	100	
14	87.6	90.4	34.7	36.2	
34	64.1	68.5	9.5	12.0	
48	53.0	60.3	5.7	6.3	
r	.9963	.9938	.9921	.9960	
k (days ⁻¹)	1.36×10^{-2}	1.10×10^{-2}	6.0×10^{-2}	5.74×10^{-2}	
t _{1/2} (days)	51	62.8	11.5	12.1	

References

1. Ellin, R.I., J. Pharm. Sci., 71(9) 1057 (1982).
2. Lach, J.L., Flanagan, D.R., and Matheson, L.E., Annual Report No. 5, Contract No. DAMD 17-79-C-9136, July, 1984, College of Pharmacy, University of Iowa.
3. Ellin, R.I., Carlese, J.S., Kondritzer, A.A., J. Pharm. Sci., 51(2) 141 (1962).

Part II: Physico-Chemical Properties of WR238,605

DATA SHEET SUMMARY

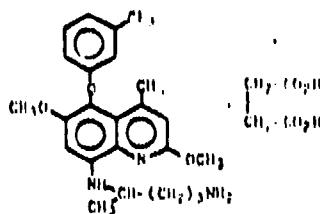
Compound - WR238,605 AC

Lot - 840941A1

Bottle Number - BK 73252

Molecular Weight - 581.59

Structure



8-[(4-Amino-1-methylbutyl)amino]-2,6-dimethoxy-4-methyl-5-(3-trifluoromethyl-phenoxy)quinoline succinate

A. Solid-State Properties

1. Color - milky white
2. Odor - none
3. Taste - bitter
4. Appearance - fine crystalline powder
5. Scanning Electron Micrographs (SEM) - taken on a Jeol 35C scanning electron micrograph (see Figures 2a and 2b)
6. Particle Size - in the range from 5-80 microns.
7. Differential Scanning Calorimetry (DSC) - taken on a Perkin-Elmer DSC-2C at 10°C/min (see Figure 3). Melting point - 151.6°C with decomposition after melting.
8. X-Ray Powder Diffraction - taken on Phillips APD 3500 automated diffractometer. The powder diffractogram (Figure 4) was obtained at 2 θ angles of 2-40°. Table I gives the 2 θ angles, D values (Å) and relative intensities (I/I') for all diffraction maxima in this range.
9. Infra-red Spectrum - taken as a KBr pellet at 1% concentration₁ on a Beckman Model 4240 infrared spectrometer at a speed of 150 cm⁻¹/min (see Figure 5).

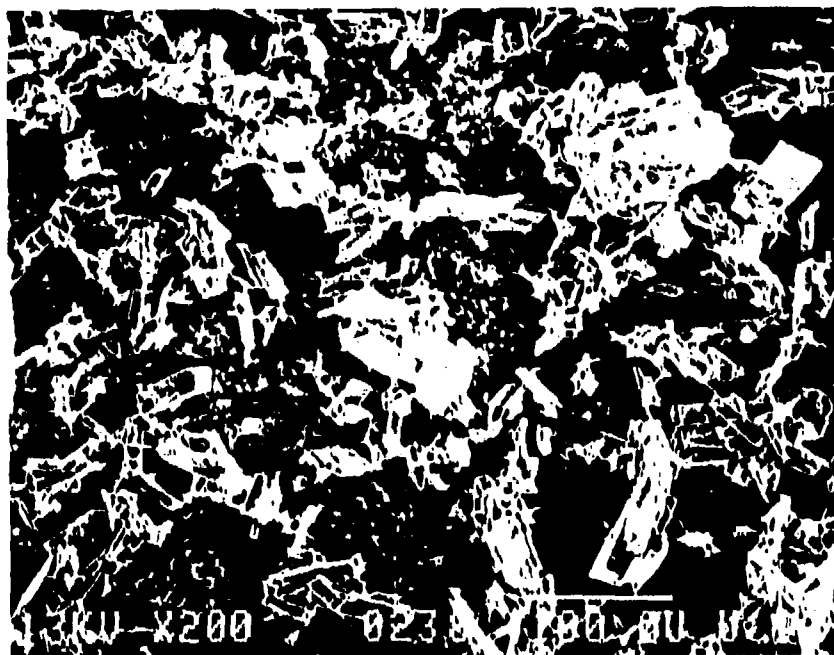


Figure 2a. Photomicrograph of WR238,605 AC at a 200 X magnification.



Figure 2b. Photomicrograph of WR238,605 AC at a 400 X magnification.

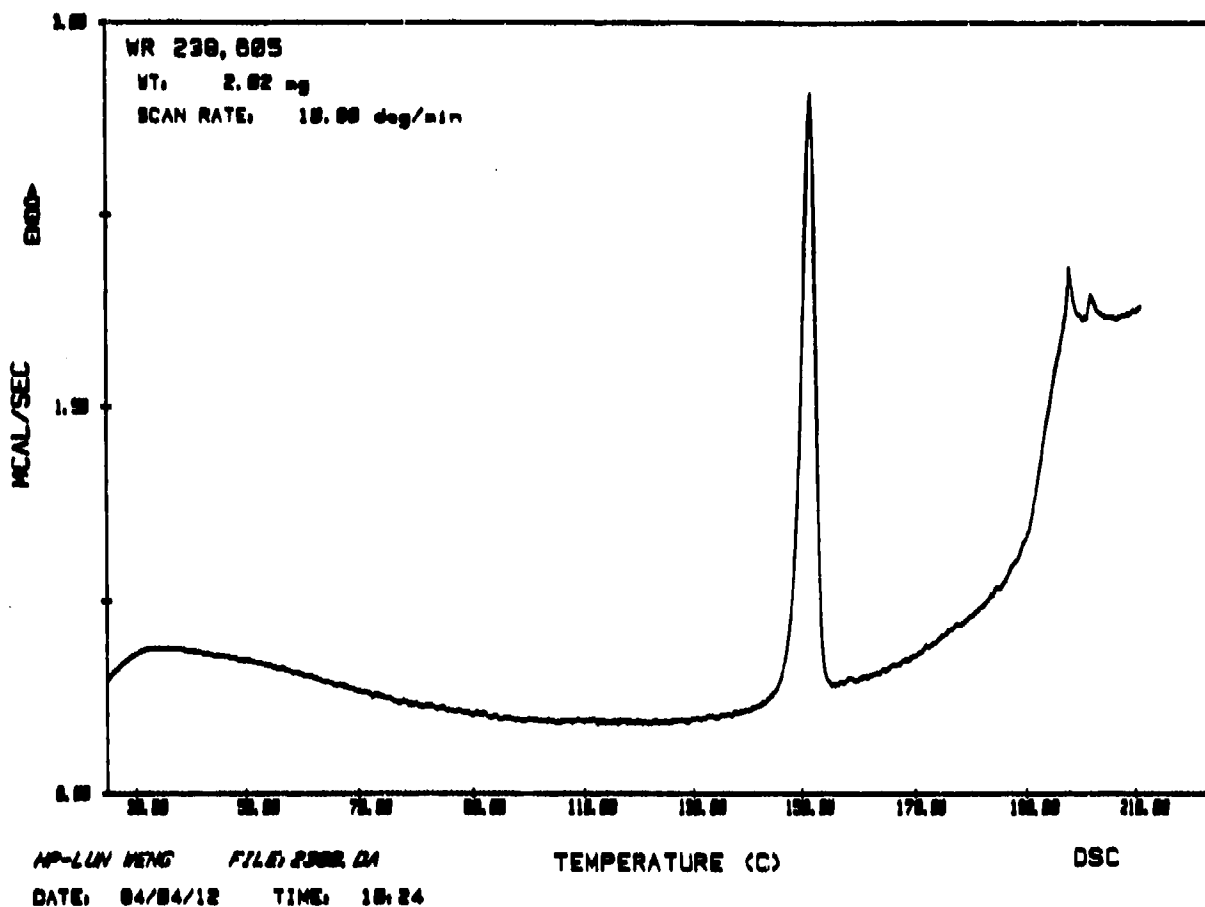


Figure 3. Thermogram of WR238,605 AC.

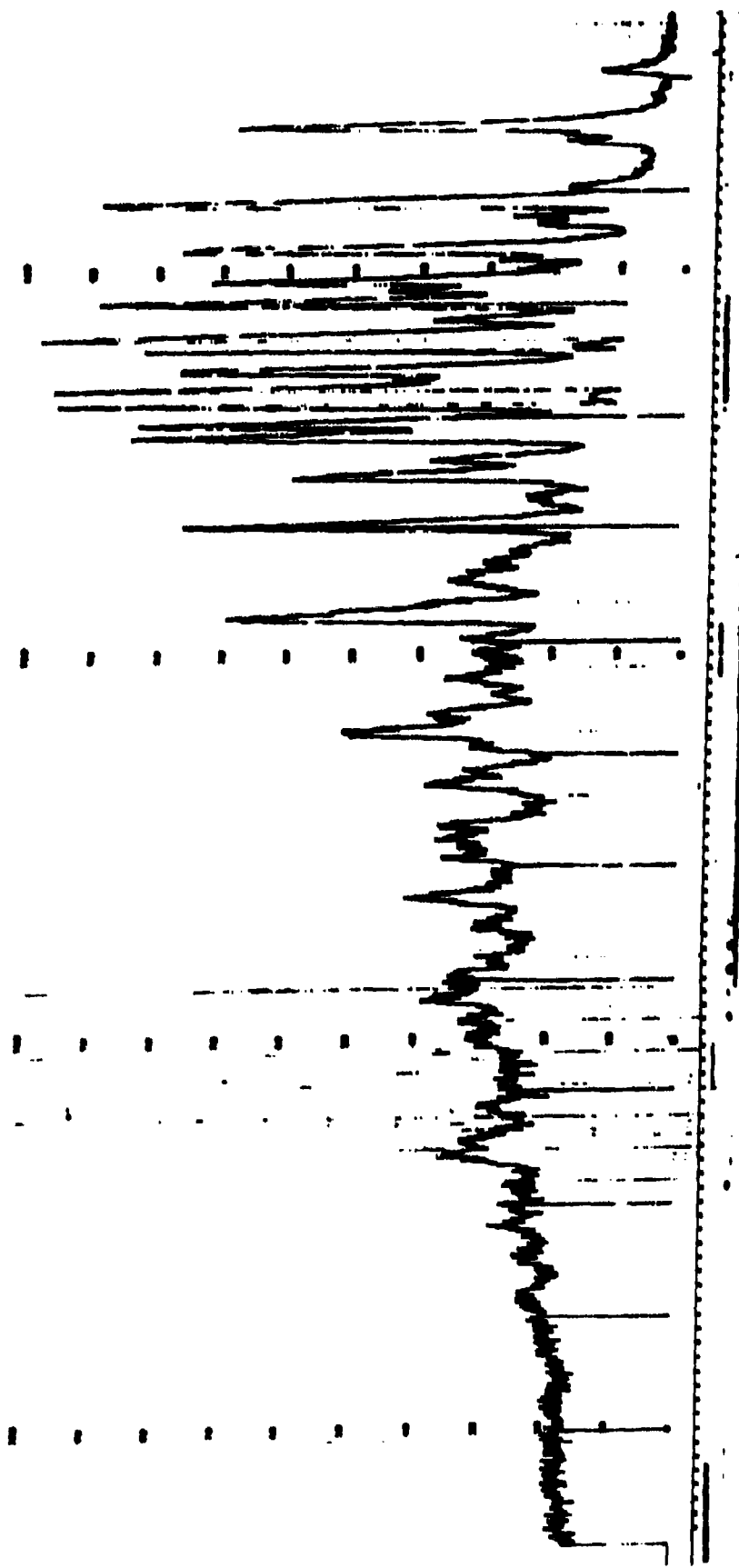


Figure 4. K-ray powder diffraction pattern for VR238,605 AC.

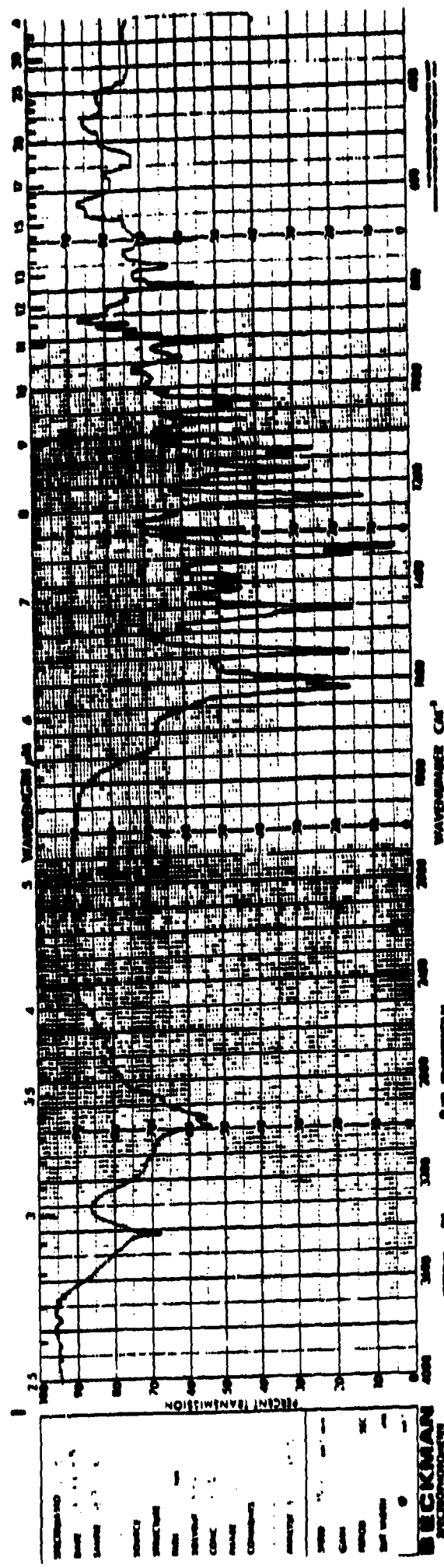


Figure 5. Infrared spectrum of WR238,605 AC.

Table 8. X-Ray Diffraction Data for WR238,605 AC

Background	Intensity(I)	Two-Theta Angle	D(Å)	I/I'(x100%)
156	1224	1.980	44.618	10
252	855	9.683	9.134	7
340	4308	11.719	7.551	38
340	1138	12.001	7.374	10
340	1060	12.257	7.221	9
340	1117	13.896	6.372	9
872	5553	14.409	6.147	49
872	4680	16.081	5.511	41
872	4368	17.196	5.156	38
872	2863	17.524	5.061	25
1372	5639	17.965	4.937	50
1372	11278(I')	19.532	4.545	100
1372	4939	20.347	4.365	44
1372	9346	21.321	4.167	83
1236	5085	22.274	3.991	45
1236	5072	22.727	3.913	45
1236	3664	24.204	3.677	42
1360	4850	25.992	3.428	42
1360	4335	29.165	3.062	38

B. Solution Properties

1. Solubilities

Solvent	Temperature(°C)	Solubility (mg/mL)
Water	25	between 0.64 (clear) and 0.826 (cloudy)
Acetone	25	>25
Propylene Glycol	25	54.186
Isopropanol	25	4.158
95% Ethanol	25	54.439
pH 6.6 Phosphate Buffer	30	0.0215
pH 6.0 Phosphate Buffer	30	0.0352
pH 5.6 Phosphate Buffer	30	0.0548
pH 5.0 Phosphate Buffer	30	0.0980

2. UV Spectral Data

<u>Solvent</u>	<u>Wavelength (nm)</u>	<u>Molar Absorptivity(ε)</u>
Water	261	26,887
0.01 N HCl	236	38,786
95% Ethanol	268	30,394
Methanol	269	29,318
Isopropanol	269	30,992
Chloroform	267	26,457

The spectra are shown in Figures 6, 7, 8, 9, 10 and 11.

3. Proton Magnetic Resonance Spectrum (NMR)

Spectrum taken in DMSO-d₆ on a Varian Model EM-360 NMR Spectrometer.
(See Figure 12.)

C. Colloidal Dispersion Properties

Since WR238,605 has the unique characteristic of forming colloidal dispersions in aqueous solutions, the size distribution of such dispersions was evaluated under a variety of conditions. The size distributions were all submicron and required the use of a Nicomp Model 200 Laser Particle Sizer (See Appendix A for a description of this technique) to characterize them. Samples of WR238,605 in aqueous solutions were prepared at elevated temperature to obtain complete dissolution and the cell holder temperature of the laser particle sizer set to various temperatures and particle size distributions obtained after waiting sufficient time for particles to grow.

At a WR238,605 concentration of 1 mg/mL, the laser particle sizer could not detect enough particles (i.e., not enough to detect a light scattering signal) to size at 80°C or 70°C. As the sample temperature is decreased in 10°C increments (i.e., 60°C, 50°C, etc.) adequate light scattering signal was obtained to get reliable size distributions. The size distributions were bimodal with one distribution mean being centered at

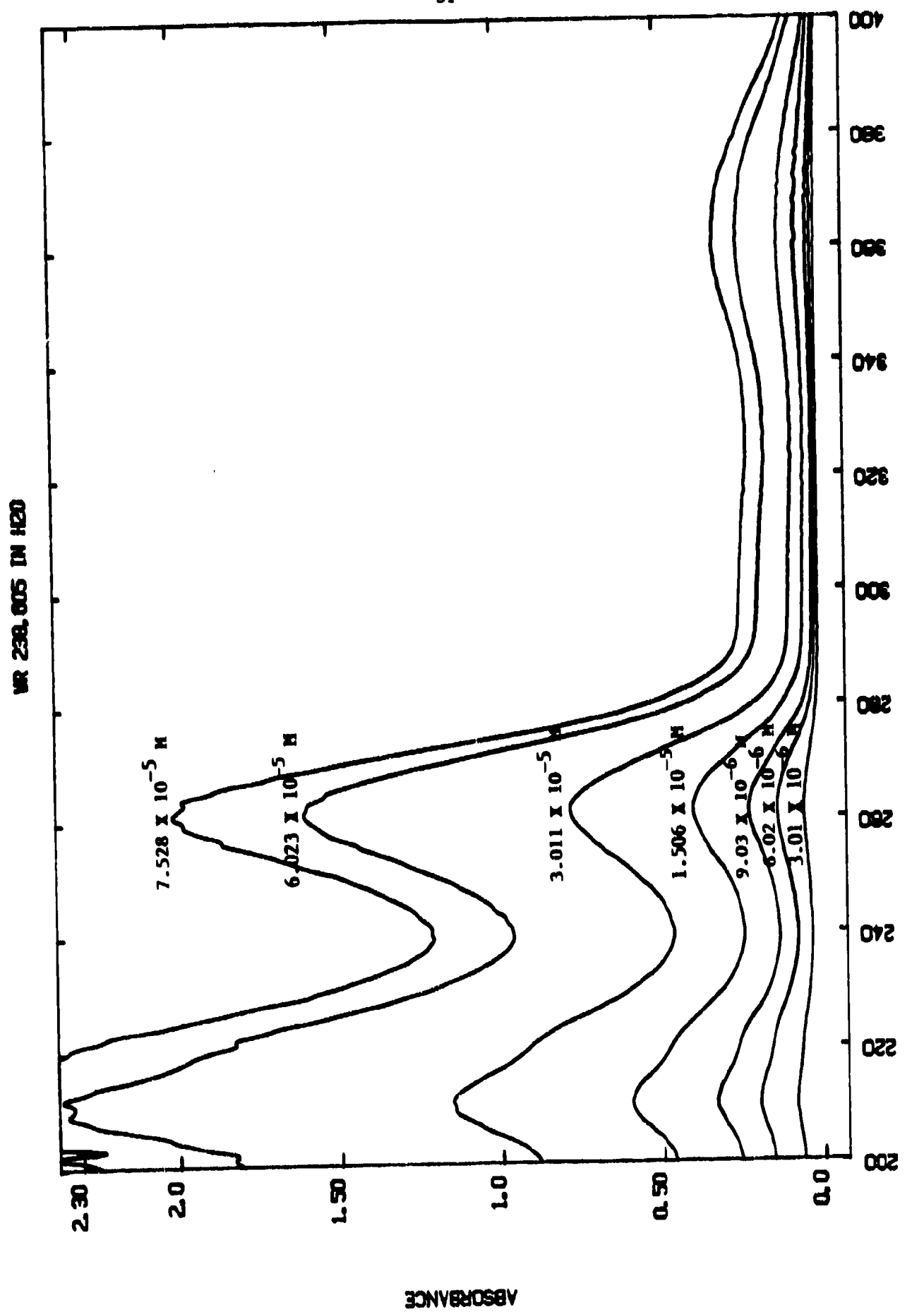


Figure 6. Ultraviolet spectrum of WR238,605 AC in distilled water.

WR 238,605 IN 0.01 N HCl.

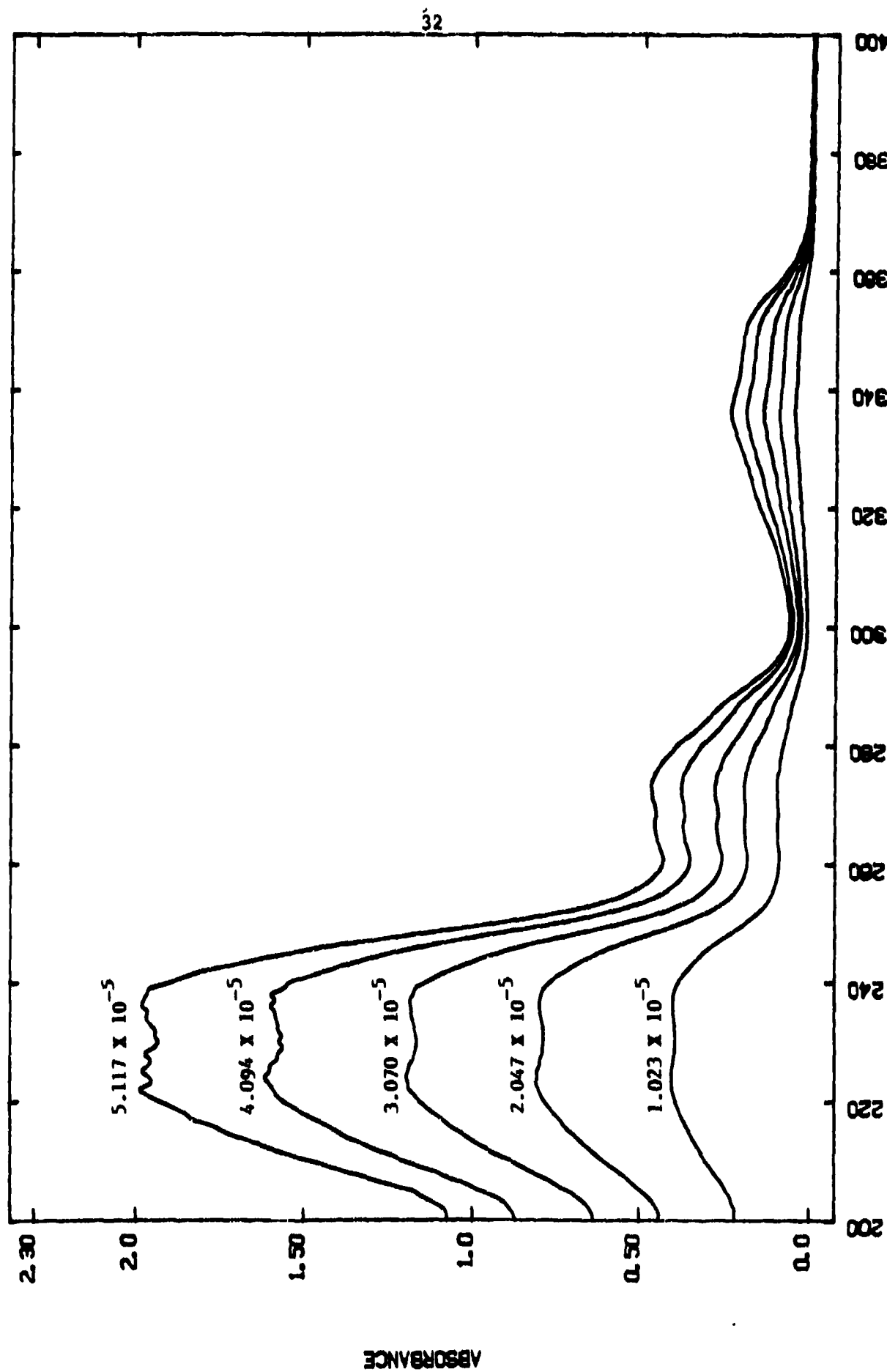


Figure 7. Ultraviolet spectrum of WR238,605 AC in 0.01 N HCl.

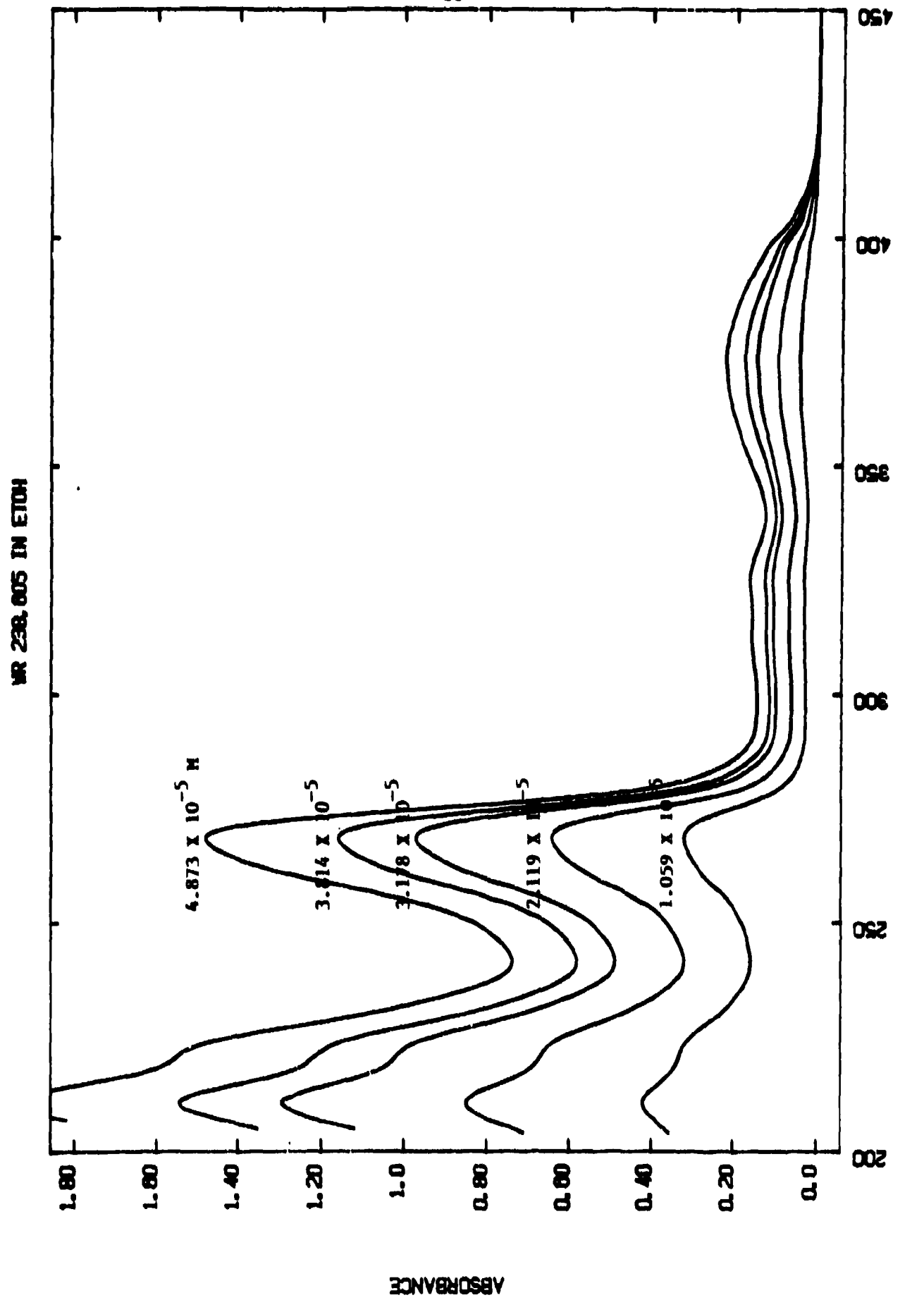


Figure 8. Ultraviolet spectrum of **UR238.605 AC in 95% Ethanol**.

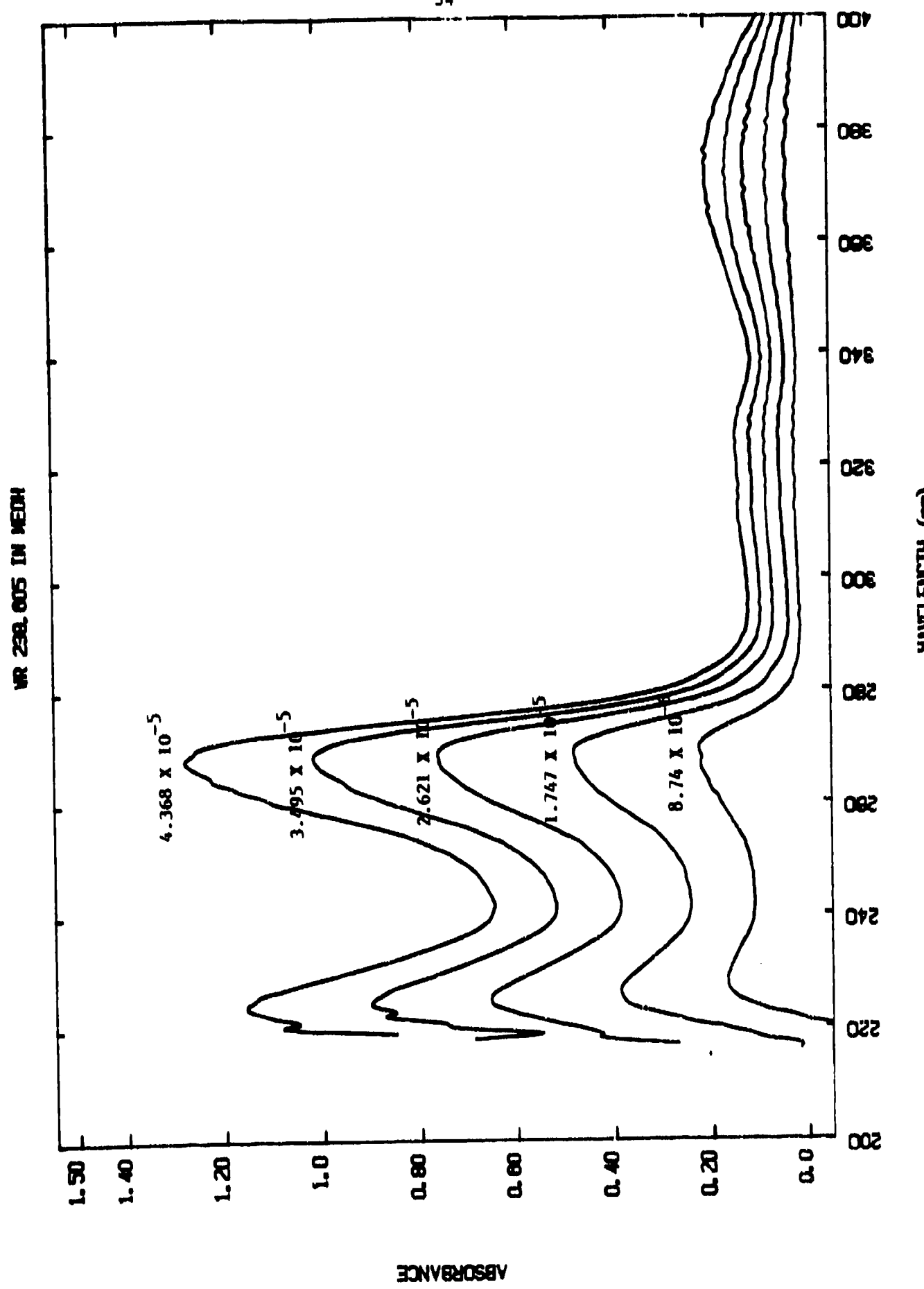


Figure 9. Ultraviolet spectrum of TR238,605 AC in Methanol.

MR 238.605 IN IPA

35

450

WAVELENGTH (nm)

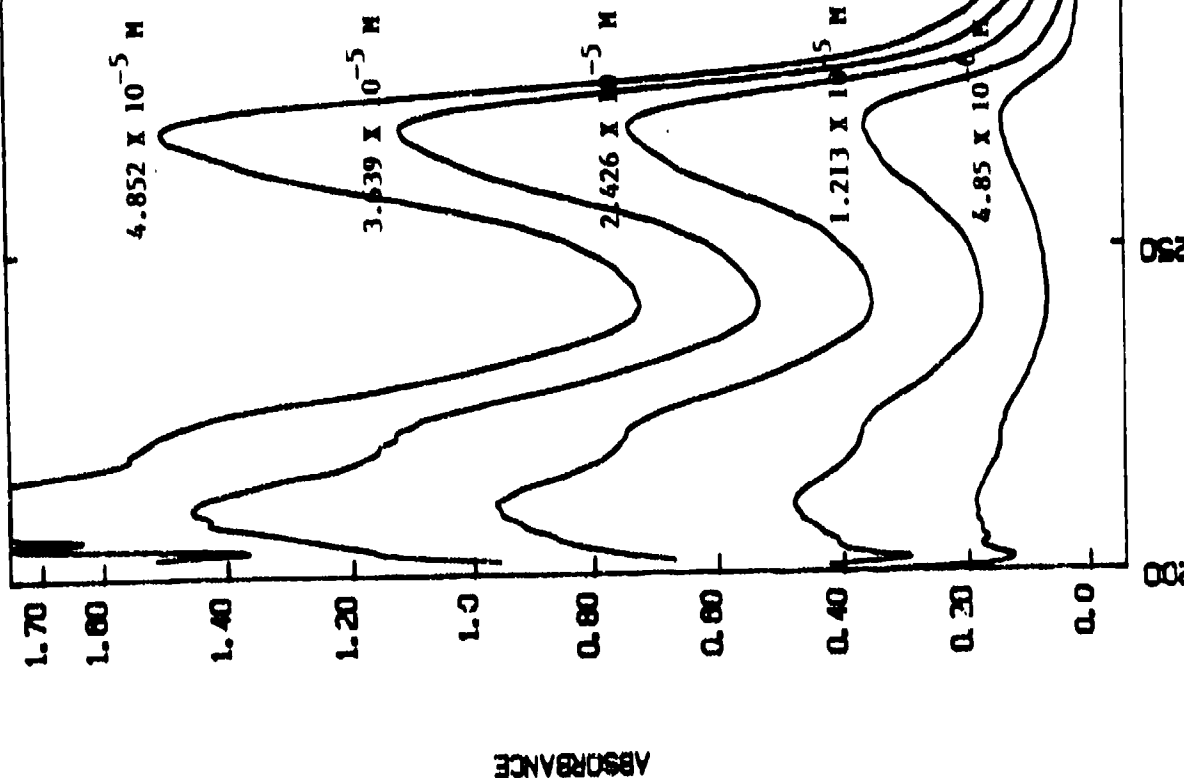


Figure 10. Ultraviolet spectrum of MR 238.605 AC in Isopropanol.

WR 238, 605 IN CHLOROFORM

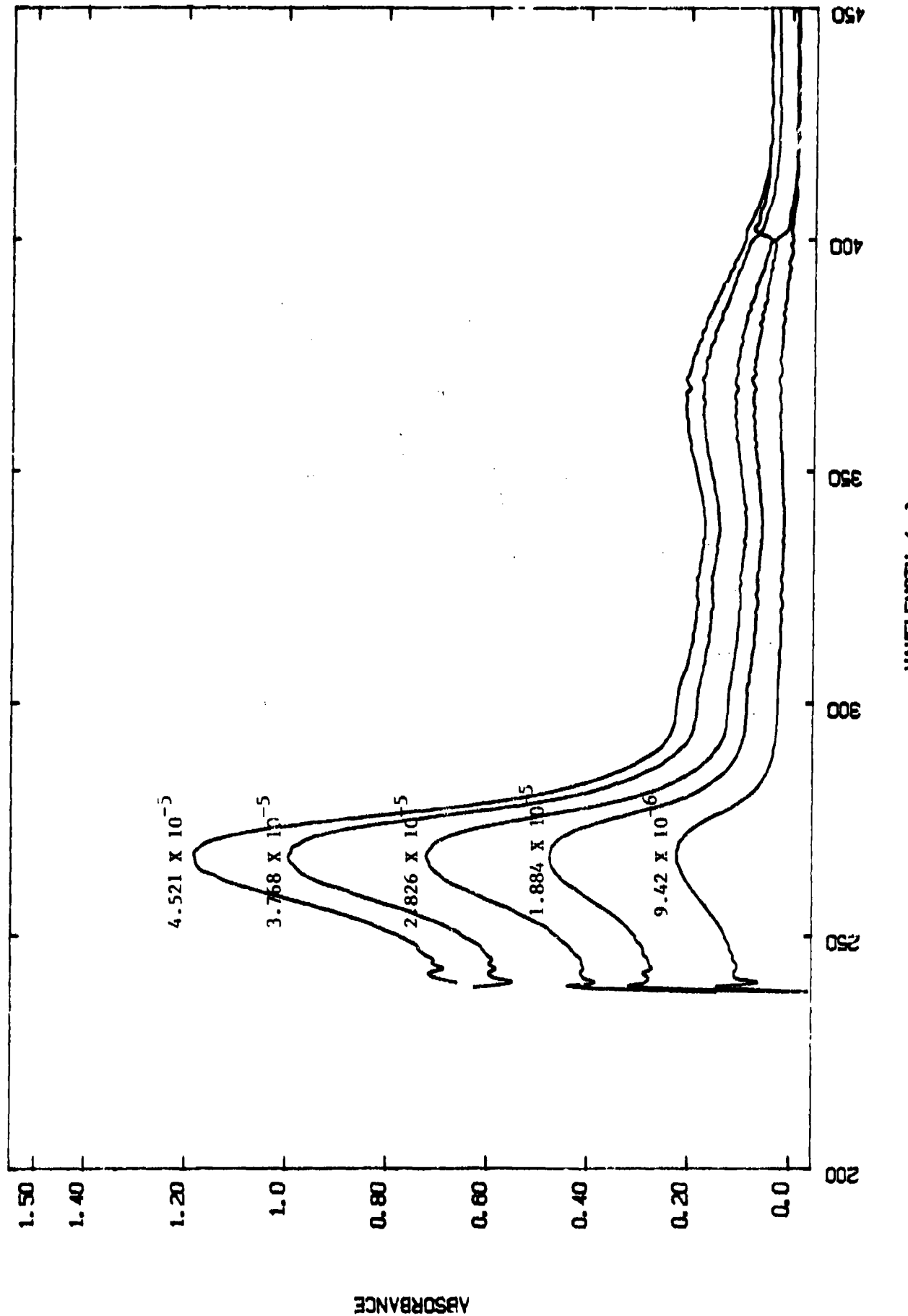


Figure 11. Ultraviolet spectrum at WR238,605 AC in Chloroform.

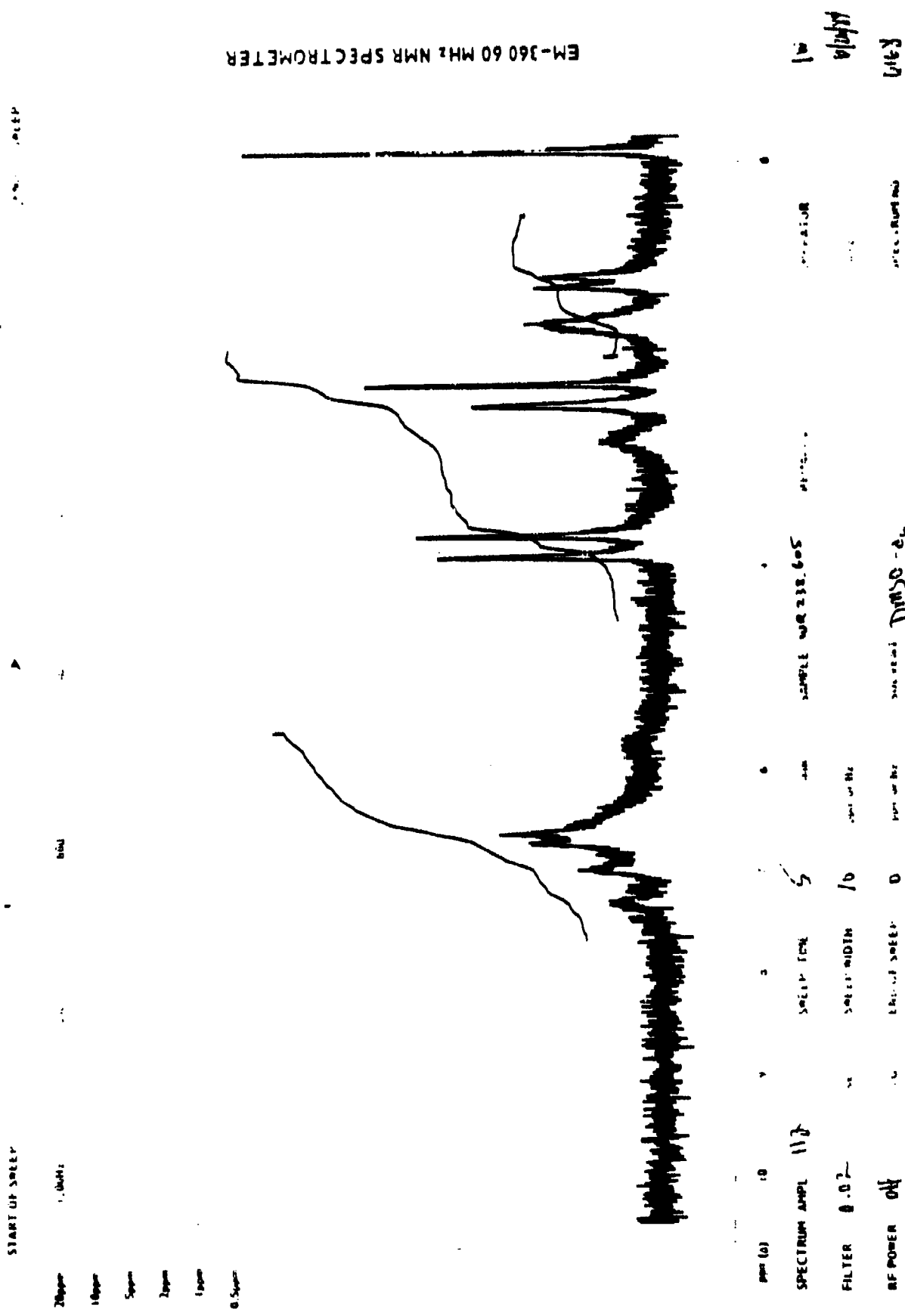


Figure 12. NMR spectrum of WR238, 605 AC.

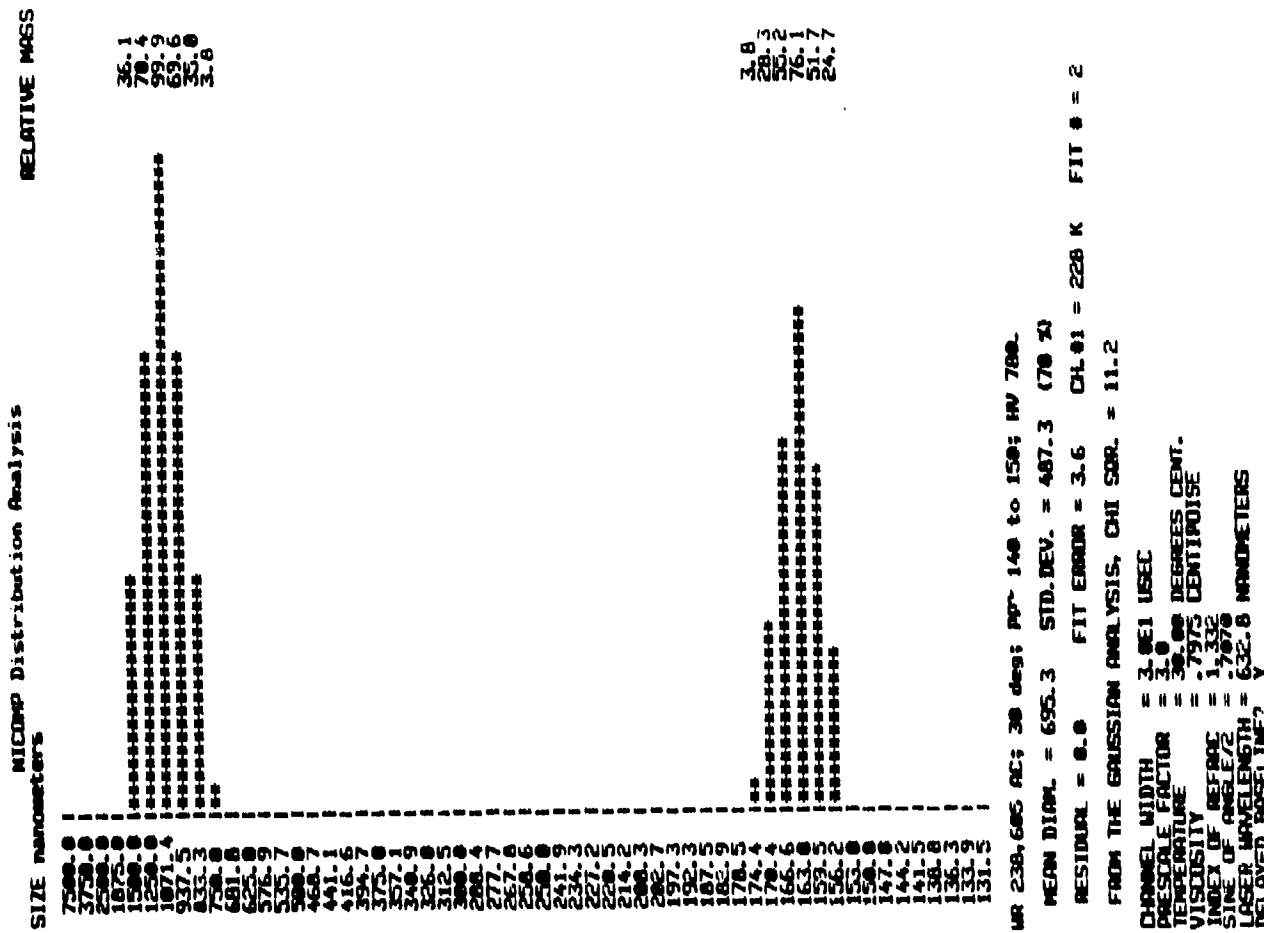
100-160 nanometers (0.1-0.16 microns) and the other centered at 750-1100 nanometers (0.75-1.10 microns). Figure 13 is an example of the final size distribution obtained at 30°C. As can be seen the largest particle size detected is 1500 nanometers (1.5 microns) on the largest distribution. If the solution of WR238,605 is cooled quickly to 20°C instead of cooling in 10°C increments the two size distributions have lower means (Figure 14).

The largest particle size is 857.1 nanometers (0.8571 microns) in this case. Such behavior is expected because the incremented slow cooling permits particle growth (i.e., crystal ripening) while the quick cooling gives less crystal growth but generates more particles for a given amount of material.

Various crystal growth inhibitors were added to the WR238,605 solutions to determine if they would alter the particle size distributions obtained on cooling or prevent crystallization completely.

A 1% w/v gelatin solution was used with 1 mg/mL WR238,605. Figure 15 is the final bimodal size distribution obtained at 40°C. As can be seen both distributions are larger than that obtained in water. No lower temperatures were studied since the mean size of each distribution would be expected to increase.

A 0.25% w/v polyvinylalcohol (PVA) was used with 1 mg/mL WR238,605. Figure 16 is the final bimodal size distribution obtained at 25°C. The smaller distribution is of lower size than that obtained in water but the higher distribution is slightly larger than that in water. It was concluded that PVA didn't affect the size distributions sufficiently to warrant further study.



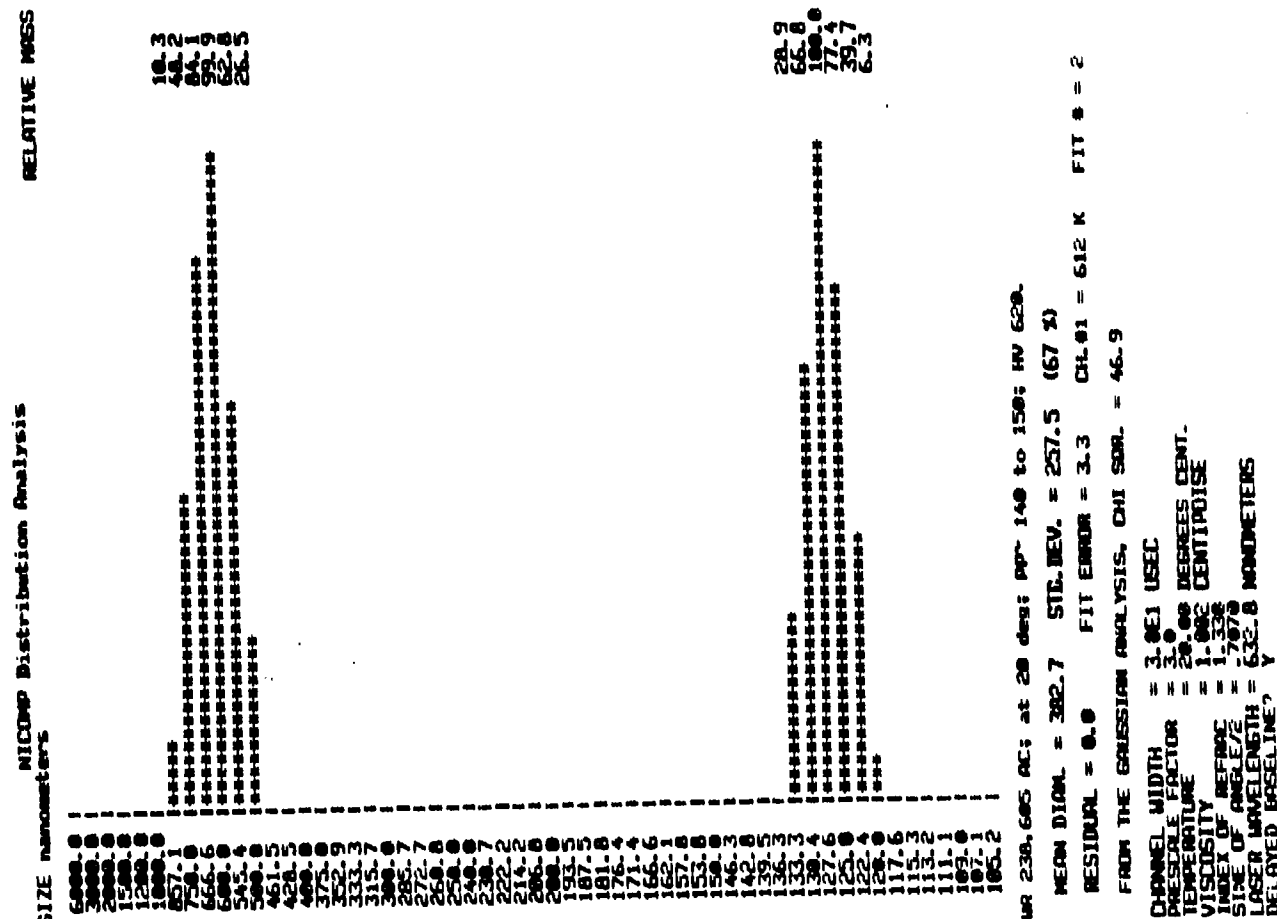


Figure 14. Size distribution obtained for WR238,605 AC (1 mg/mL) cooled quickly from 60°C to 20°C.

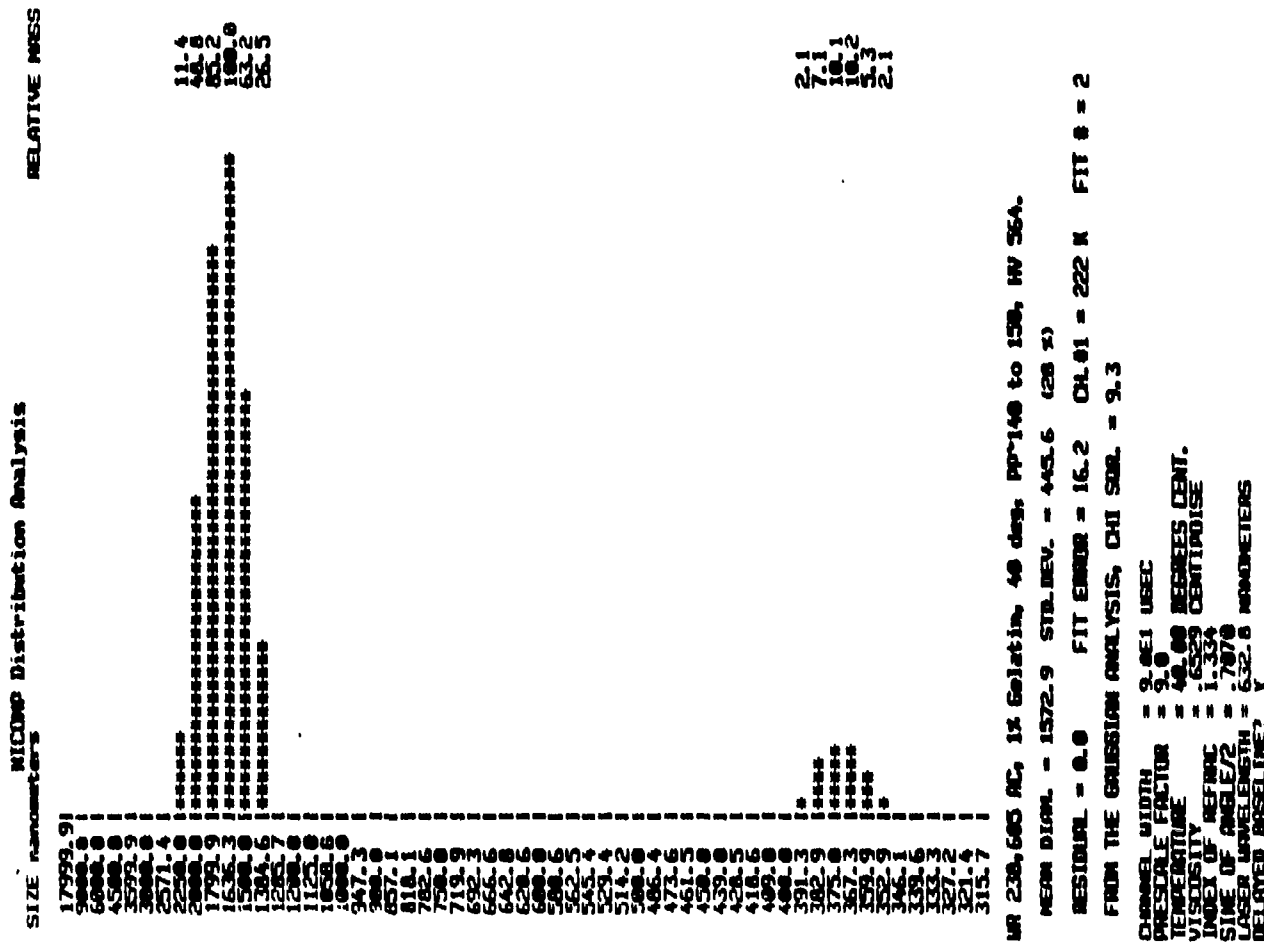


Figure 15. Size distribution obtained for WR238,605 AC (1 mg/mL) in 1% gelatin cooled in 10°C increments from 80°C to 40°C.

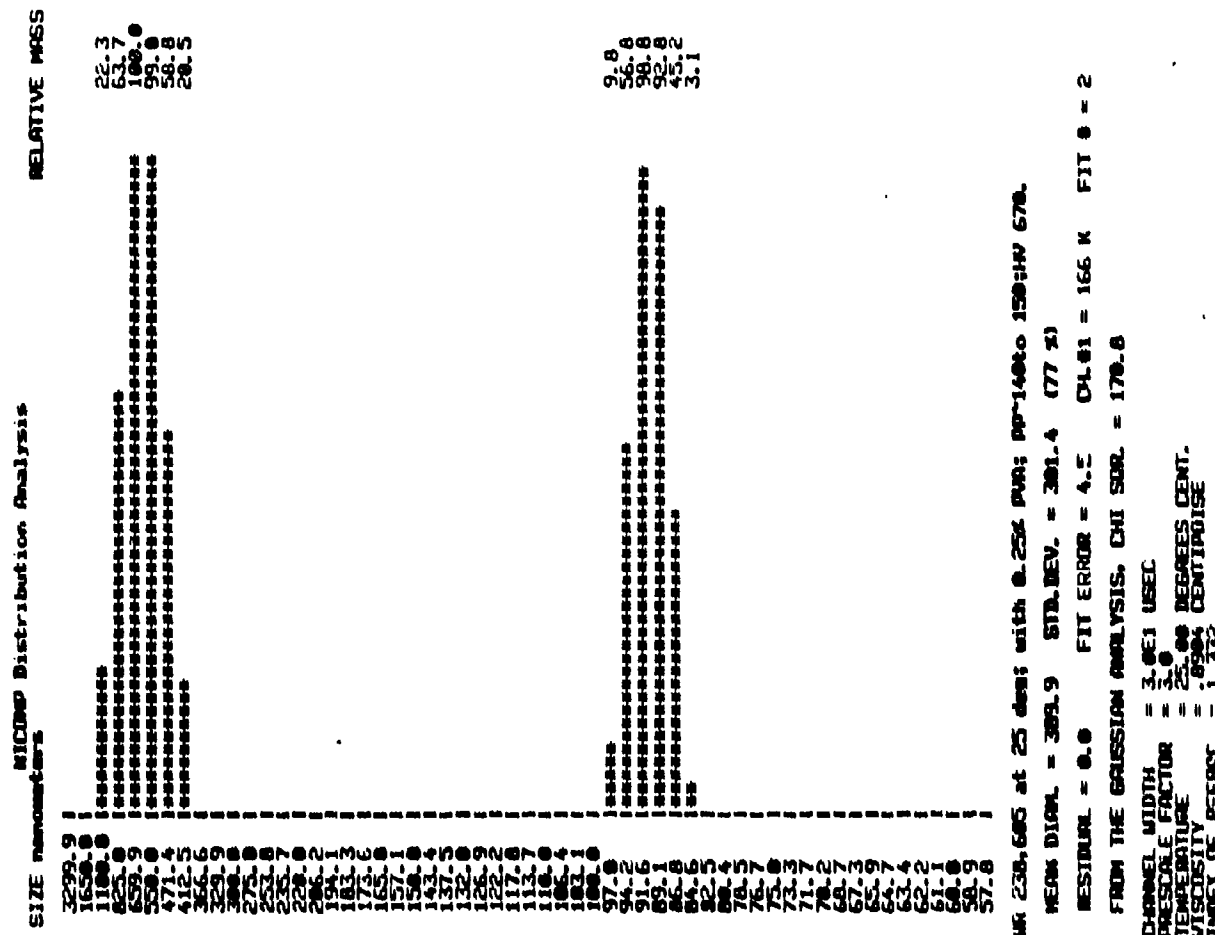


Figure 16. Size distribution obtained for WR238,605 AC (1 mg/mL) cooled in 10°C increments from 85°C to 25°C.

Polyvinylpyrrolidone (PVP) solutions were prepared at 0.5% and 1%. Two different molecular weight PVP's were employed - one with a molecular weight of 2500 (Kollidon[®] 12 PF) and the other with a molecular weight of 25,000 (Kollidon[®] 25). The laser particle size could not obtain adequate scattering signal when 1 mg/mL WR238,605 solutions containing 0.5% or 1.0% Kollidon[®] 12 PF or Kollidon[®] 25 were cooled from 80°C to 25°C. After two days at room temperature there was no detectable particle growth indicating that PVP either solubilizes WR238,605 by complexation or inhibits crystal growth completely. A 2 mg/mL solution of WR238,605 was prepared in 1% Kollidon[®] 25 and cooled from 80°C to 25°C. Again no visible particle growth occurred and the laser particle sizer could not detect sufficient signal to give any significant size distribution. Further studies are warranted on PVP's ability to maintain WR238,605 in solution.

Part III: Comparison of the Solid State Properties of Lots AC, AD, AE, AG, AL and AM of WR171,669·HCl (Halofantrine Hydrochloride)

Objective

The objective of this work was to determine if there were any differences in the solid state properties of various lots of halofantrine hydrochloride WR171,669·HCl. The lots studied were Lots AC, AD, AE, AG, AL and AM.

Summary

The solid state properties of halofantrine hydrochloride determined include color, odor, taste, appearance, particle size, thermal behavior, infrared spectrum and X-ray diffraction pattern. One lot, lot AG, appears to be a different polymorph than the other lots.

Solid State Properties

All six lots were white, bitter powders with no odor.

Scanning electron micrographs are shown for each lot at two magnifications in Figures 1-6. All lots seem to be composed of needle-like crystals, but crystals of lot AG shown in Figures 4a and 4b seem flatter and less needle-like.

The infrared spectra in Figures 7-12 are all very similar except that the spectrum of lot AG shown in Figure 10 contains a doublet between 12.5 and 13.0 μm that is not present in the other spectra.

The most convincing evidence of a difference in crystal habit between lot AG and the others is shown in the DSC thermograms in Figures 13-18. The melting point of lot AG is about 168°C as seen in Figure 16. The heat of fusion is only 16.67 calories per gram. All other lots have melting points between 202°C and 204°C and substantially higher heats of fusion.

The X-ray powder diffraction patterns are shown in Figures 19-24. The 2θ angles, D values (\AA) and relative intensities (I/I') for all diffraction maxima over $2-40^\circ$ are given in Tables I-VI. The doublet between 25° an 26° is missing in Figure 22 for lot AG, but is present in all other lots. Again this indicates the presence of a change in crystal form.

Conclusion

WR171,669 AG appears to possess a different crystal habit than the other lots examined. Based on its lower melting point, it should have a faster dissolution rate. It would be of interest to examine the history of the production of Lot AG such as recrystallizing solvents, etc.

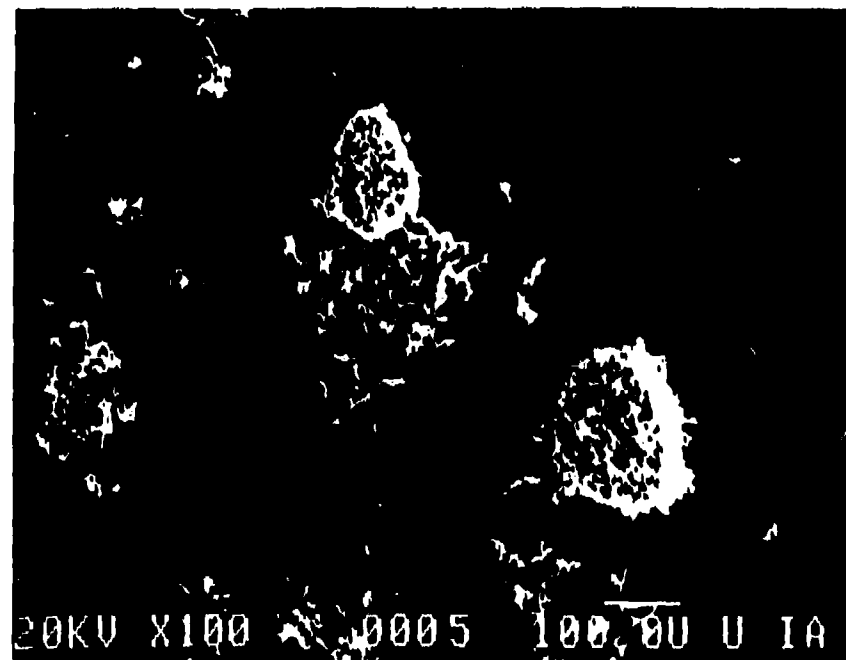


Figure 17a. Photomicrograph of Halofantrine Hydrochloride (Lot AC) magnified 100X



Figure 17b. Photomicrograph of Halofantrine Hydrochloride (Lot AC) magnified 1000X

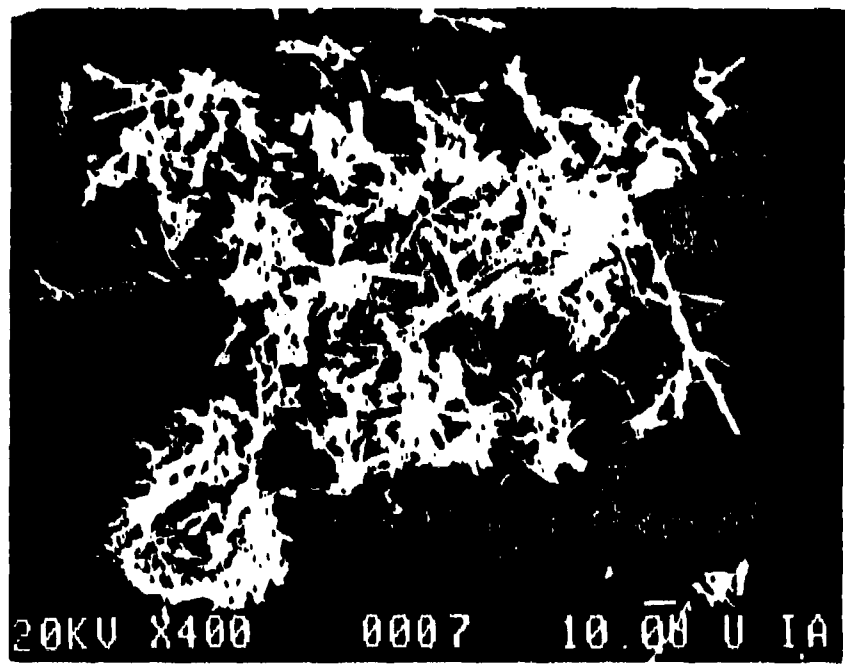


Figure 18a. Photomicrograph of Halofantrine Hydrochloride (Lot AD) magnified 400X



Figure 18b. Photomicrograph of Halofantrine Hydrochloride (Lot AD) magnified 2000X

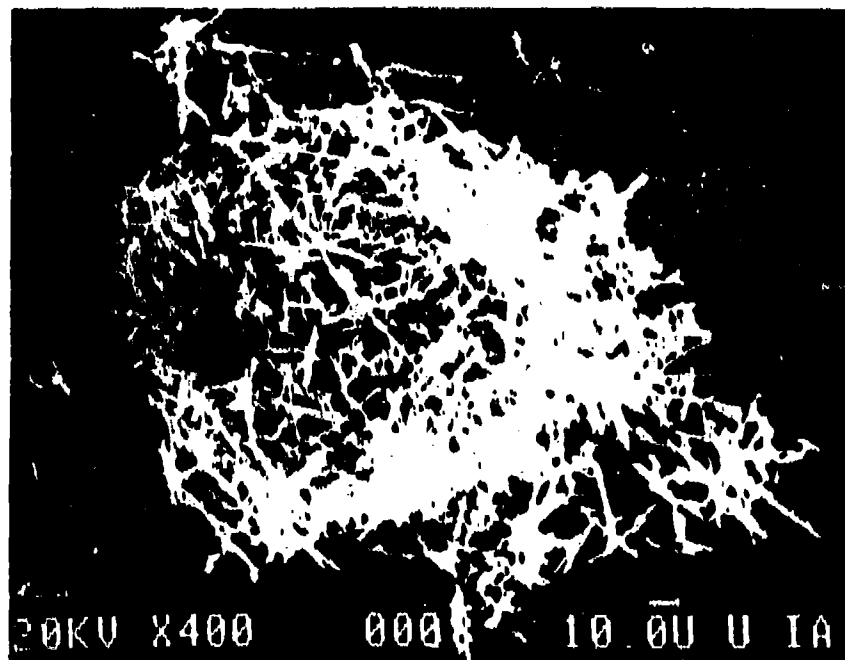


Figure 19a. Photomicrograph of Halofantrine Hydrochloride
(Lot AE) magnified 400X



Figure 19b. Photomicrograph of Halofantrine Hydrochloride
(Lot AE) magnified 2000X

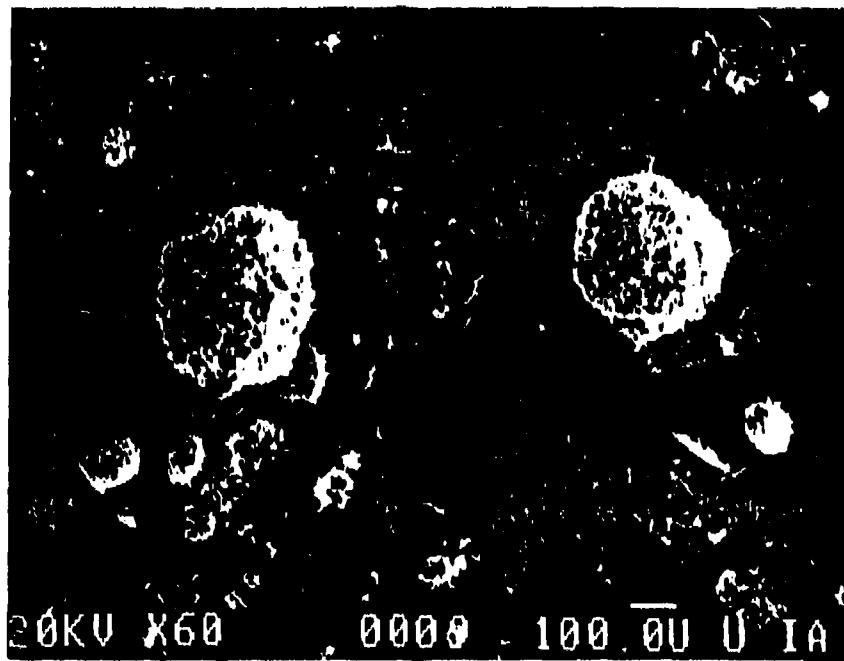


Figure 20a. Photomicrograph of Halofantrine Hydrochloride (Lot AG) magnified 60X



Figure 20b. Photomicrograph of Halofantrine Hydrochloride (Lot AG) magnified 3000X

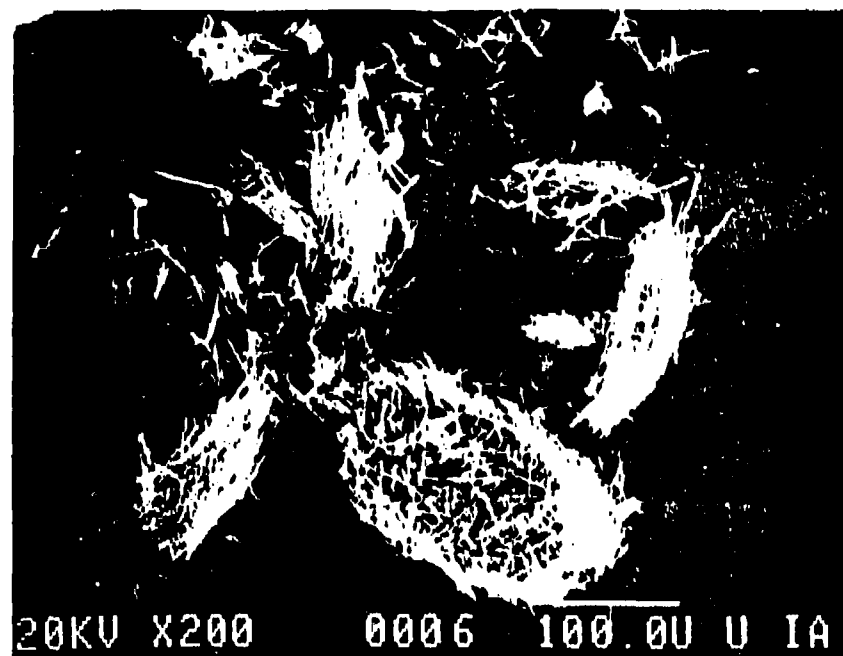


Figure 21a. Photomicrograph of Halofantrine Hydrochloride (Lot AL) magnified 200X



Figure 21b. Photomicrograph of Halofantrine Hydrochloride (Lot AL) magnified 3000X

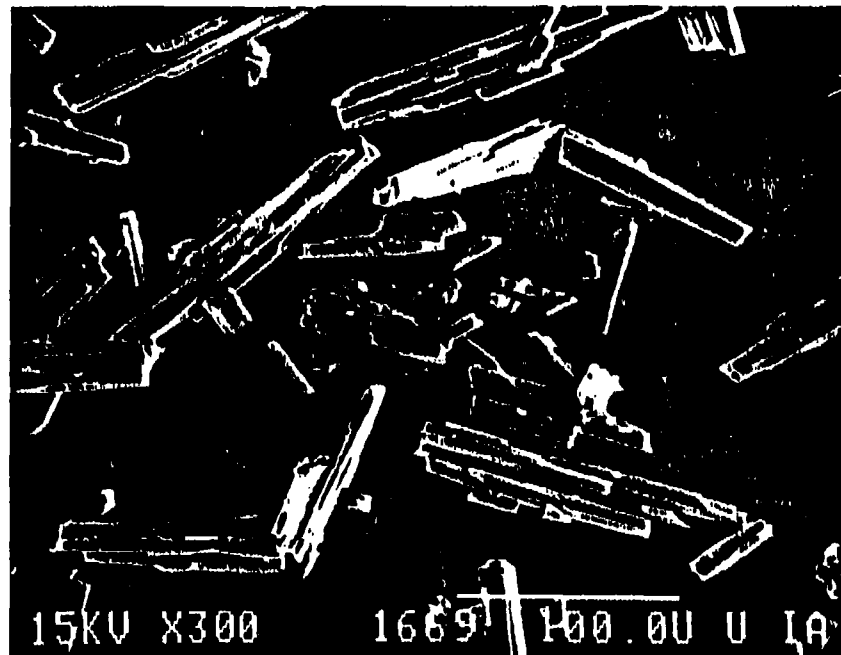


Figure 22a. Photomicrograph of Halofantrine Hydrochloride
(Lot AM) magnified 300X

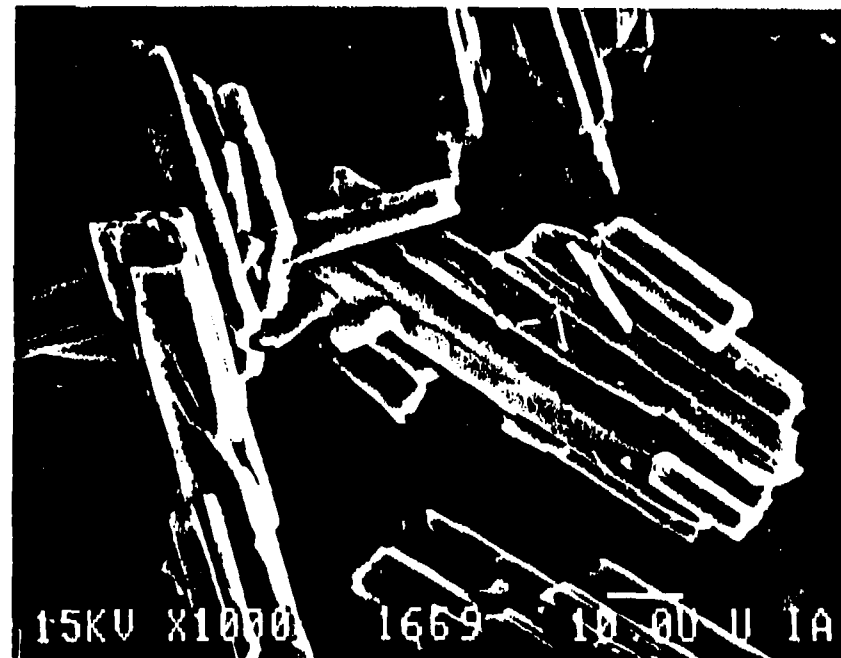


Figure 22b. Photomicrograph of Halofantrine Hydrochloride
(Lot AM) magnified 1000X

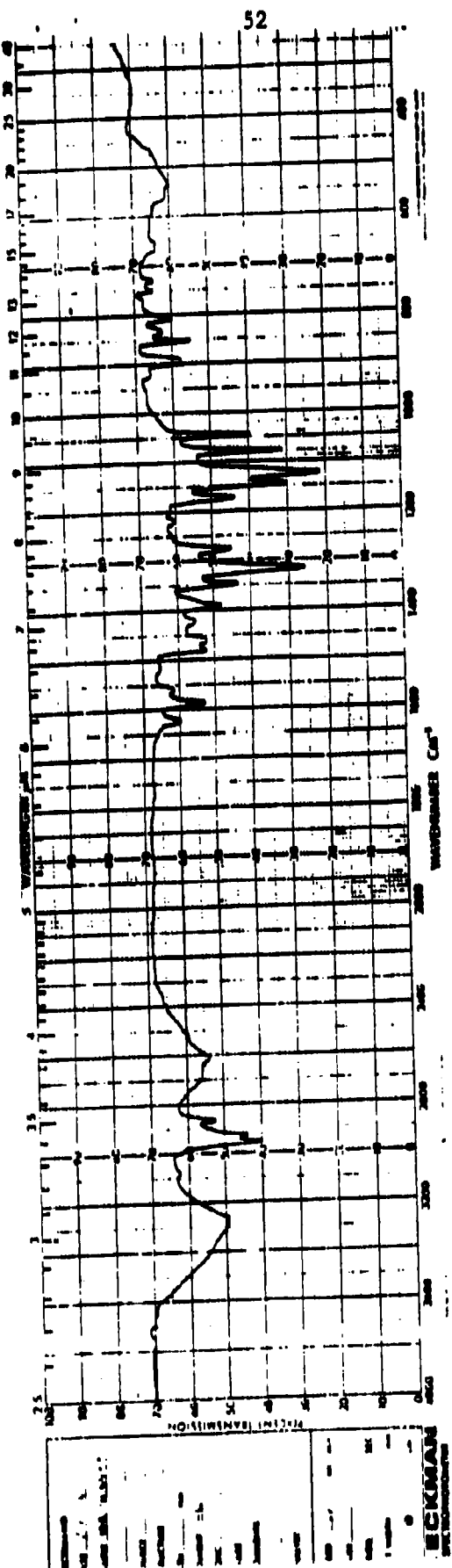


Figure 23. Infrared spectrum of Halofantrine Hydrochloride (Lot AC) (KBr pellet)

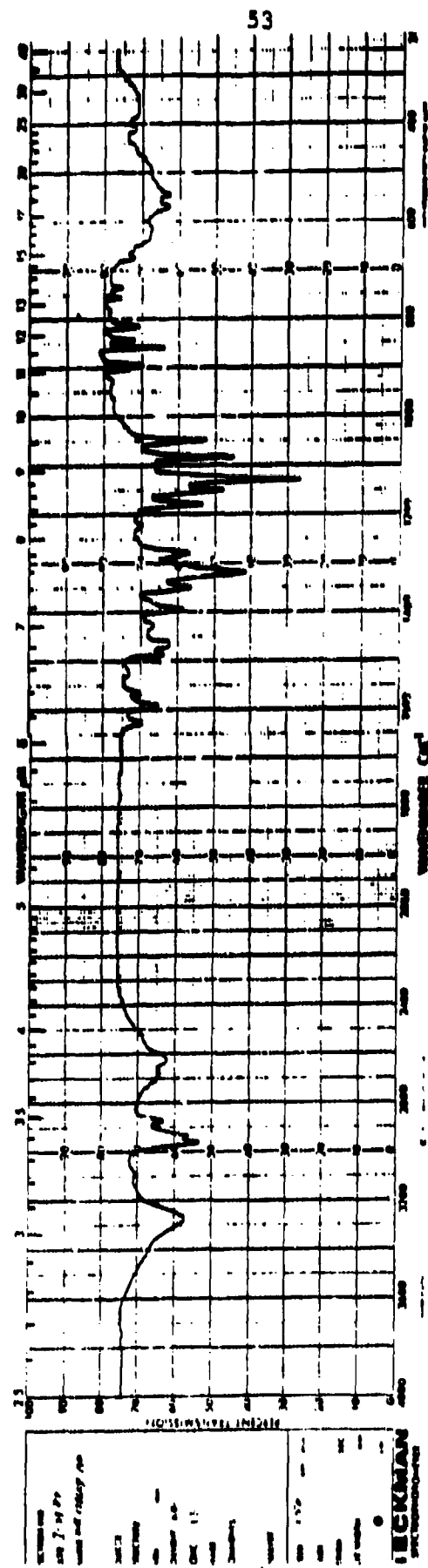


Figure 24. Infrared spectrum of Balfantrine Hydrochloride (Lot A) (KBr pellet)

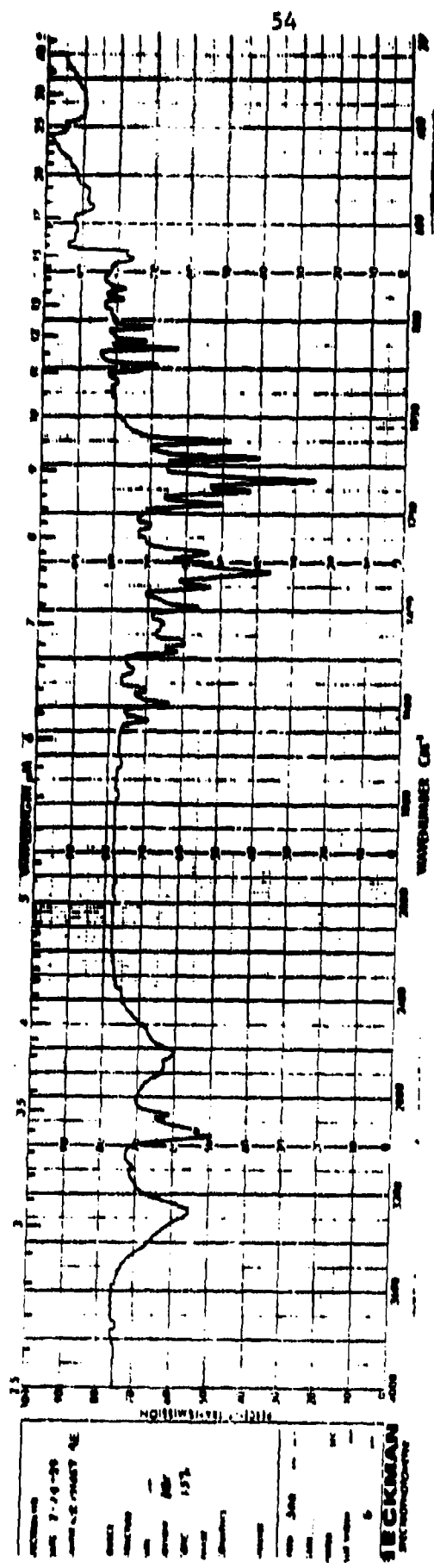


Figure 25. Infrared spectrum of Halofantrine Hydrochloride (Lot AE) (KBr pellet)

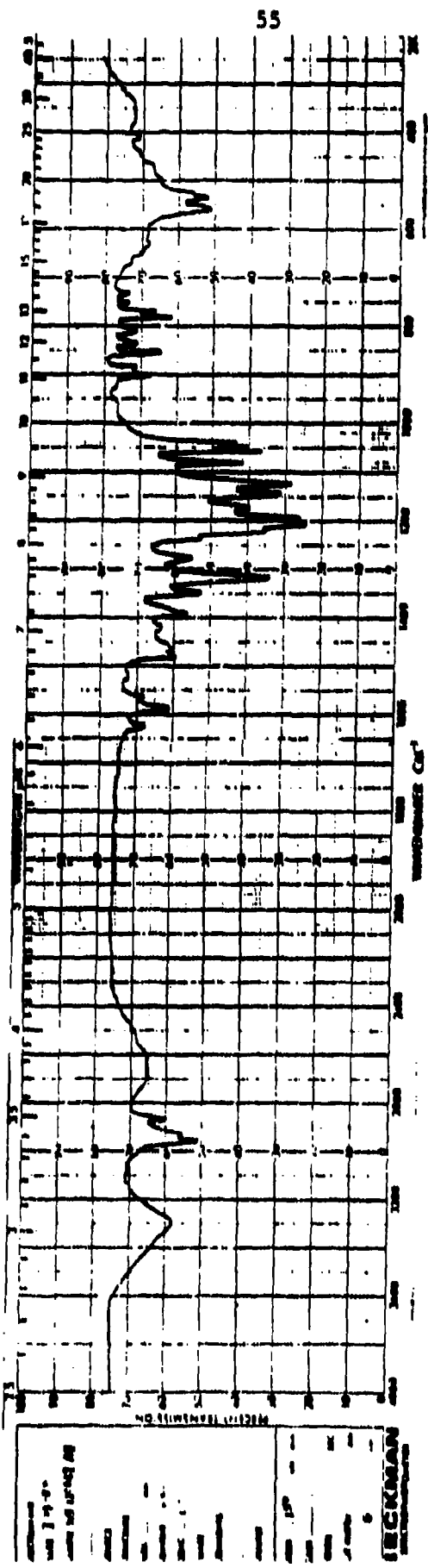


Figure 26. Infrared spectrum of Halofantrine Hydrochloride (Lot AC) (KBr pellet)

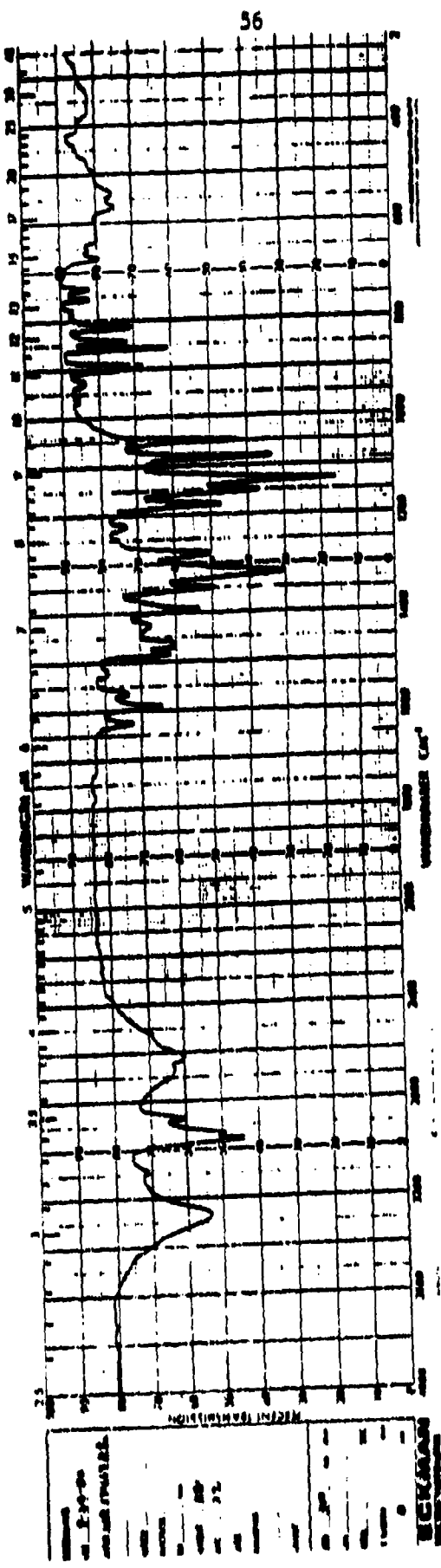


Figure 27. Infrared spectrum of Valofantrine Hydrochloride (Lot AL) (KBr pellet)

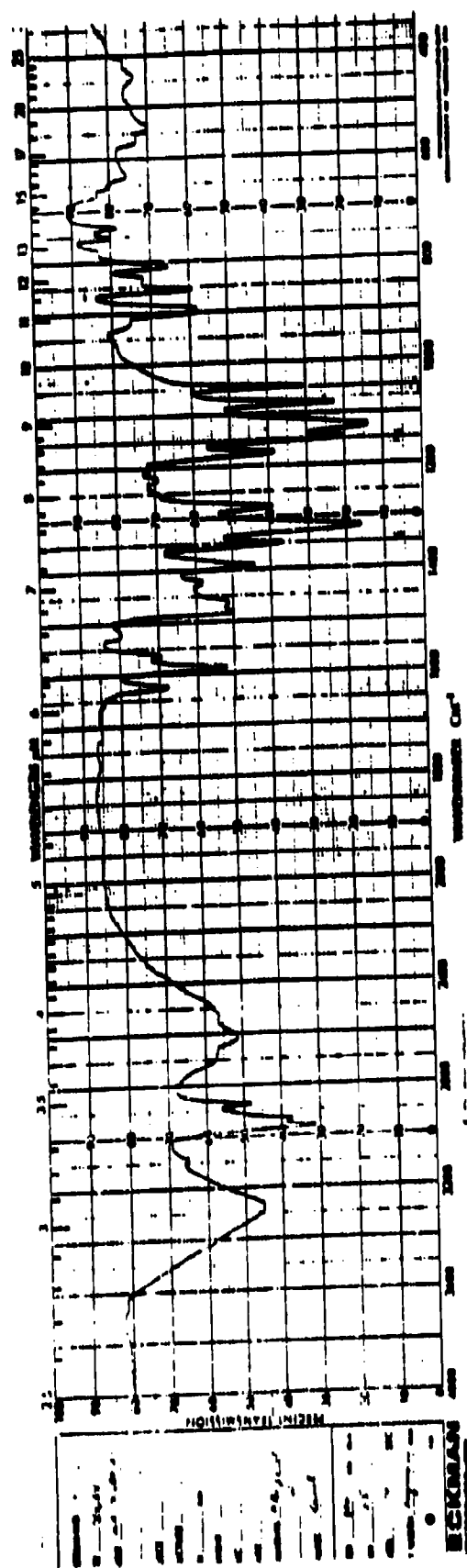


Figure 28. Infrared spectrum of Halofantrine Hydrochloride (Lot AH) (KBr pellet)

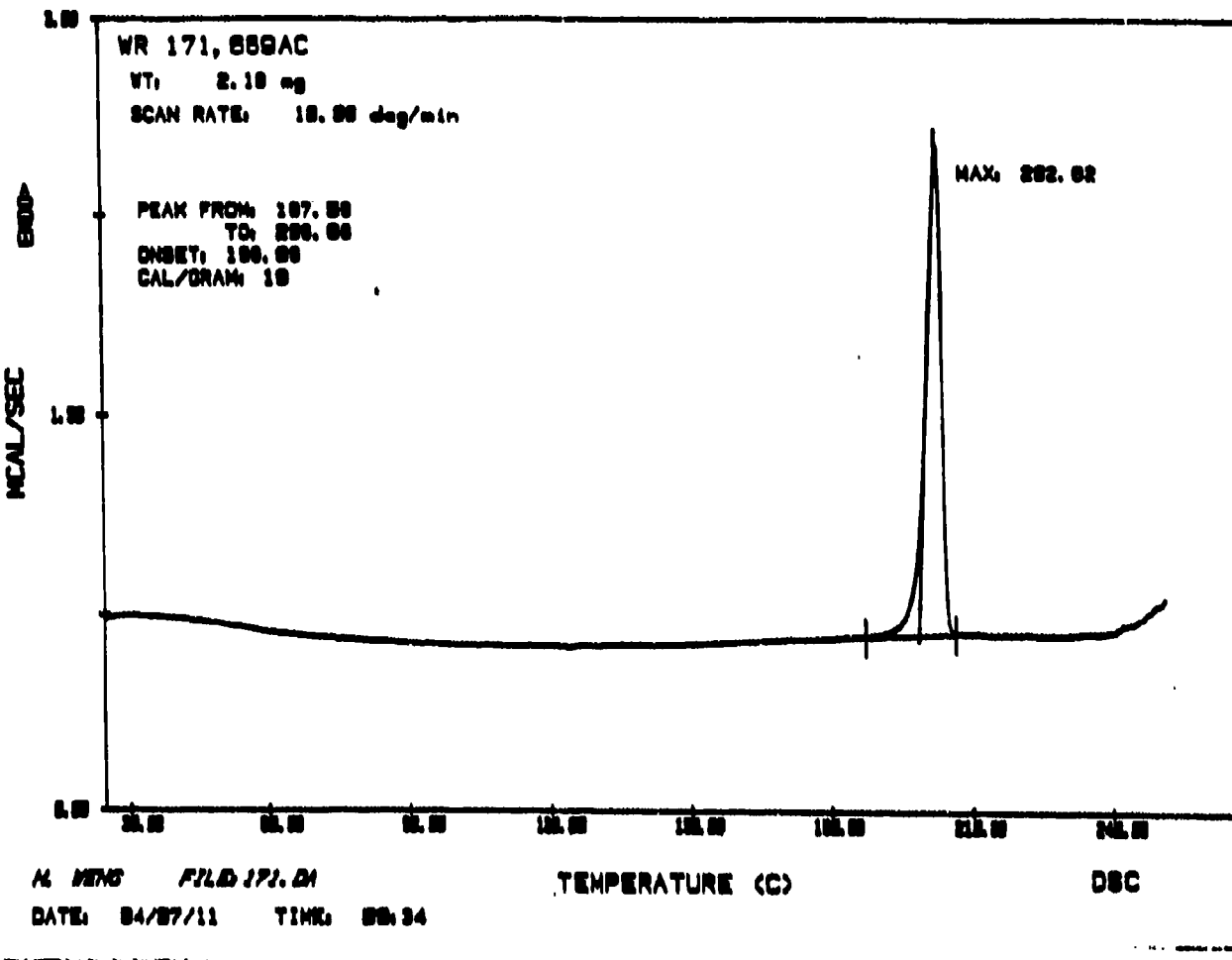


Figure 29. Thermogram of Halofantrine Hydrochloride (Lot AC)

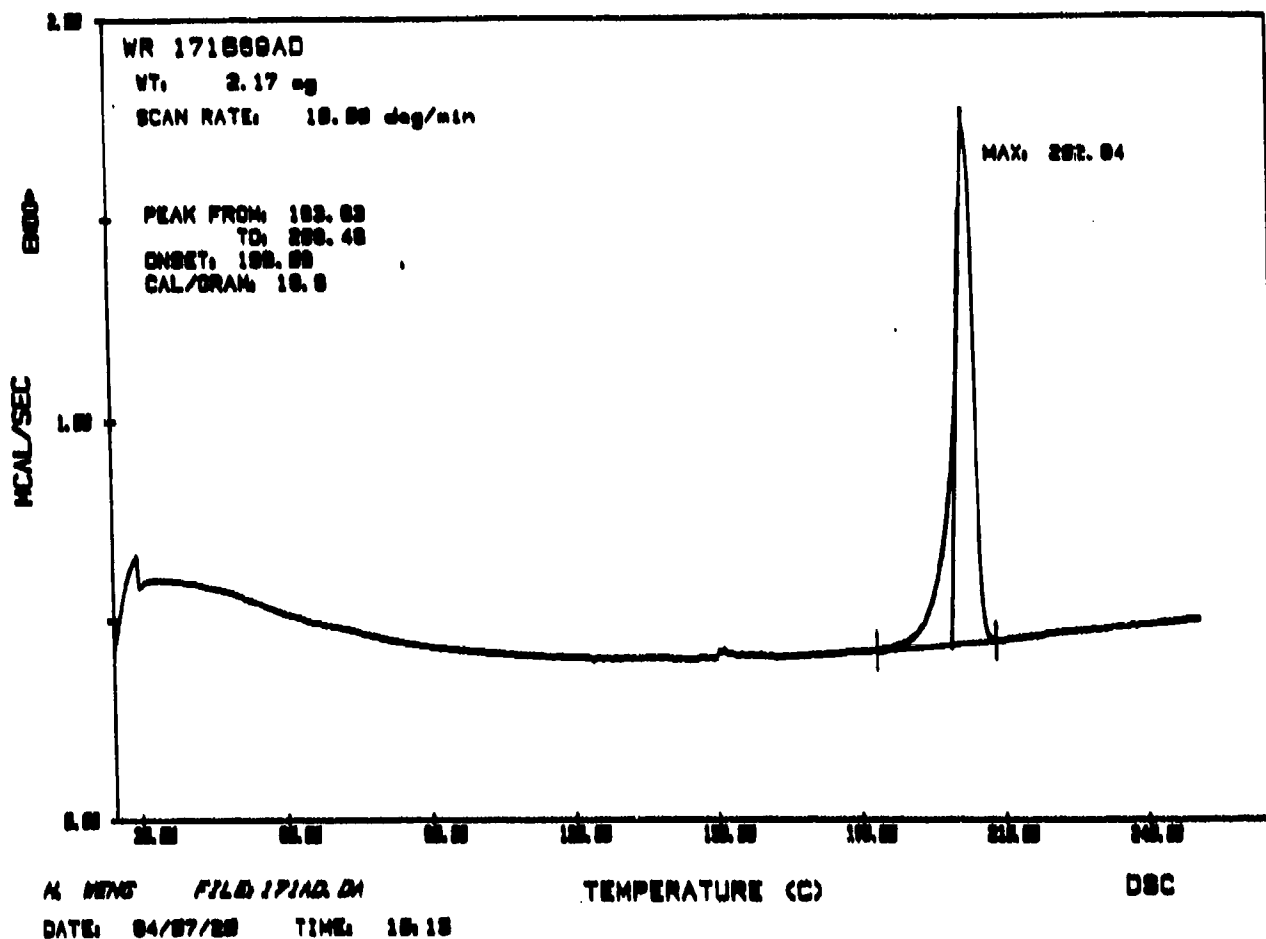


Figure 30. Thermogram of Halofantrine Hydrochloride (Lot AD)

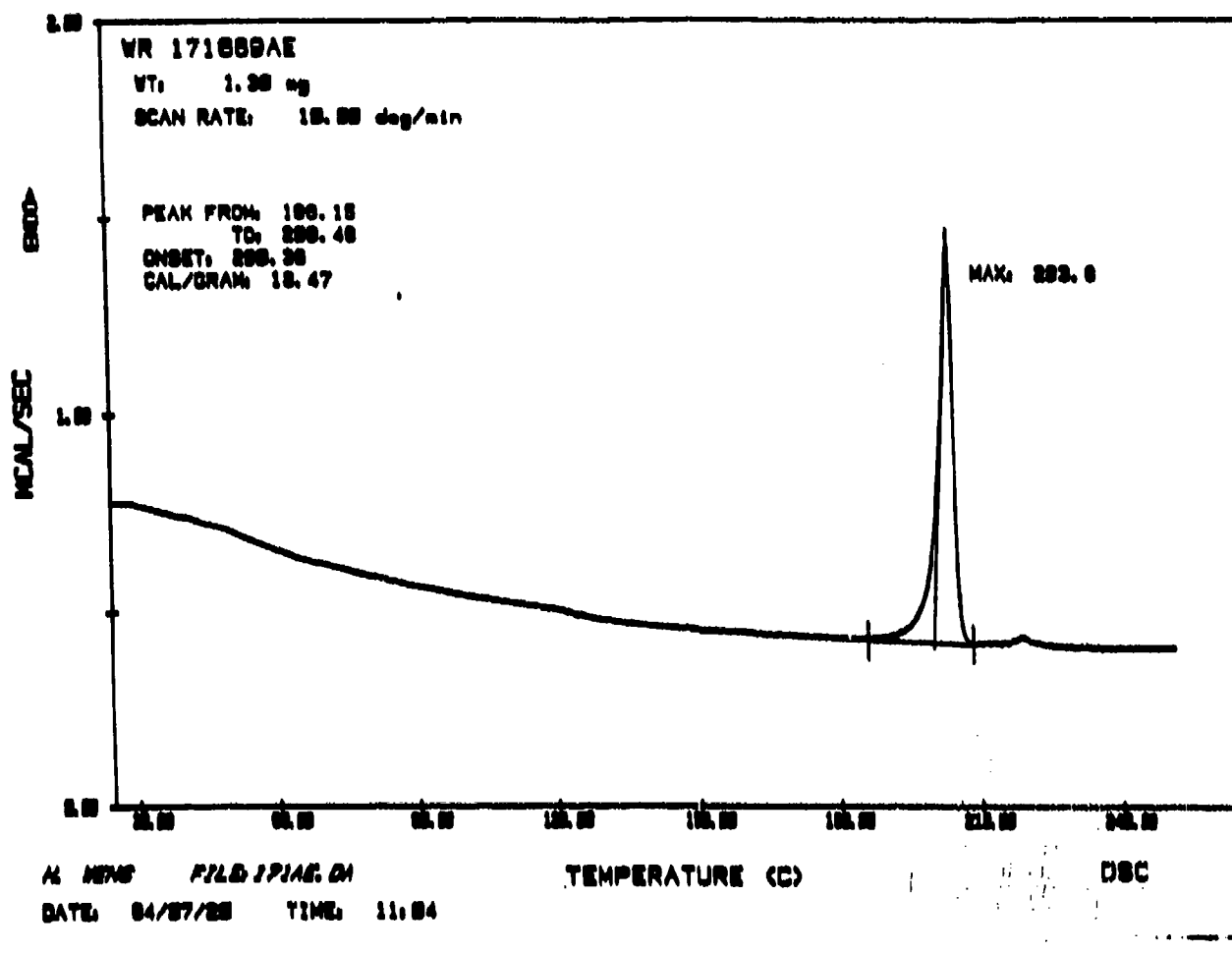


Figure 31. Thermogram of Halofantrine Hydrochloride (Lot AE)

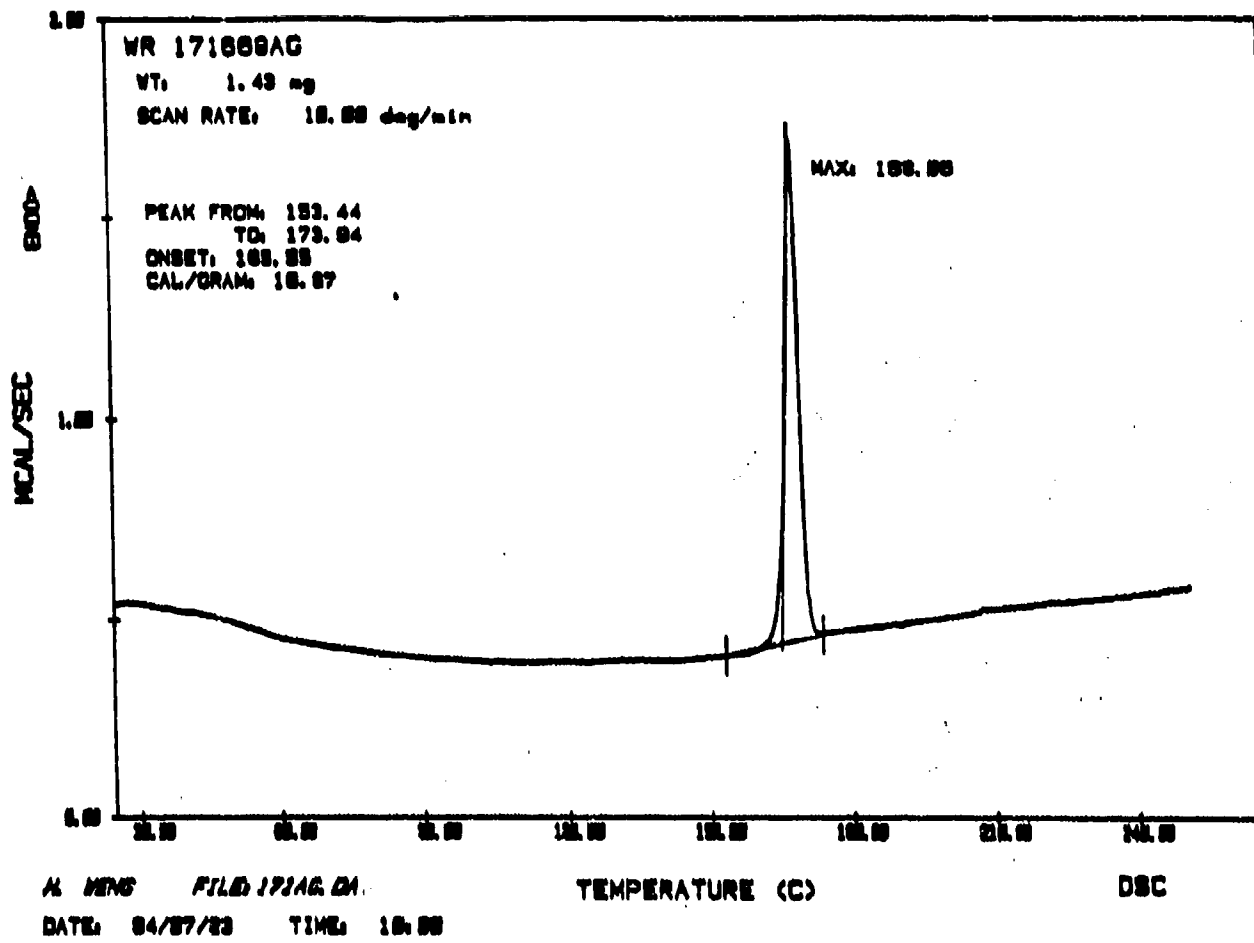


Figure 32. Thermogram of Halofantrine Hydrochloride (Lot AG)

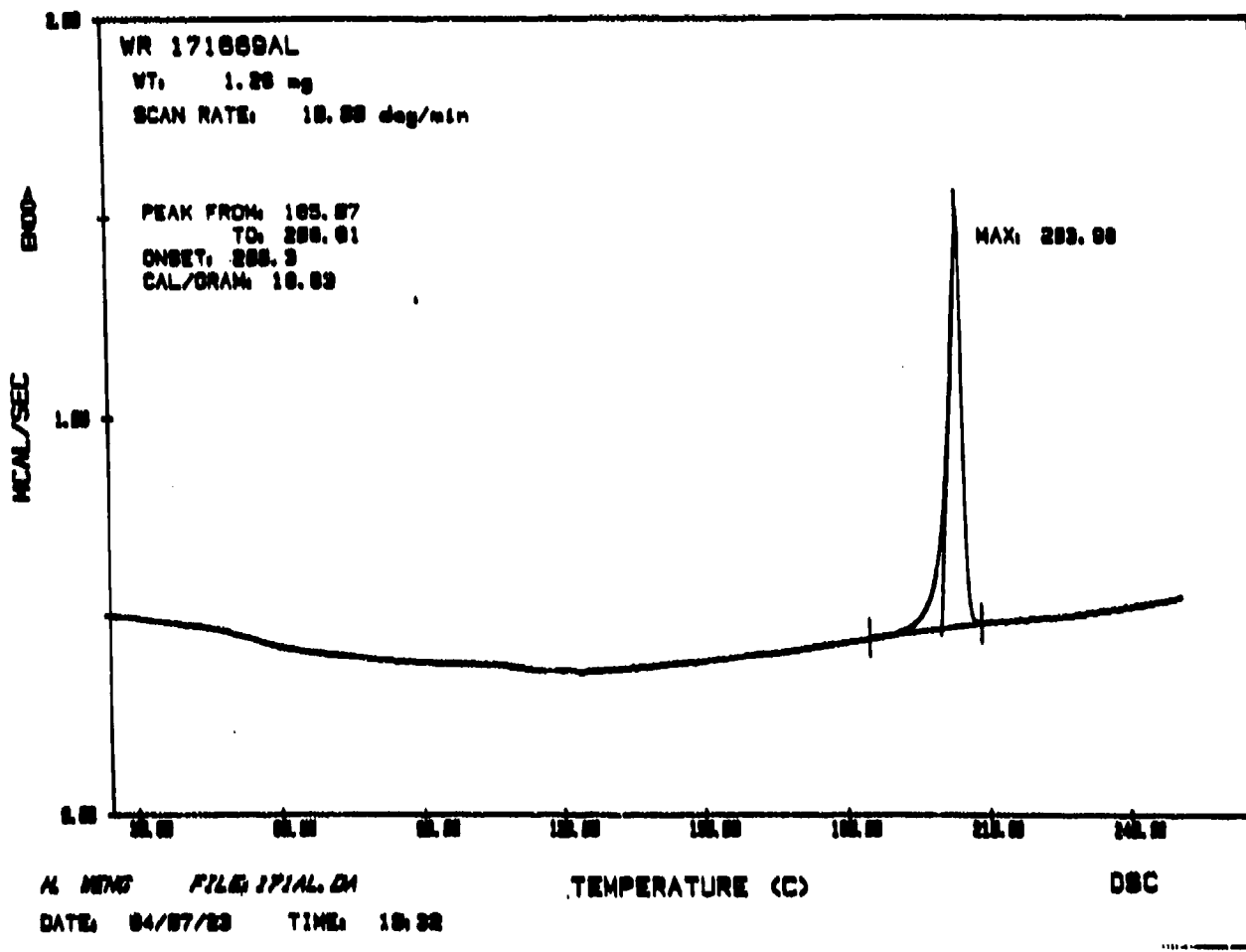


Figure 33. Thermogram of Halofantrine Hydrochloride (Lot AL)

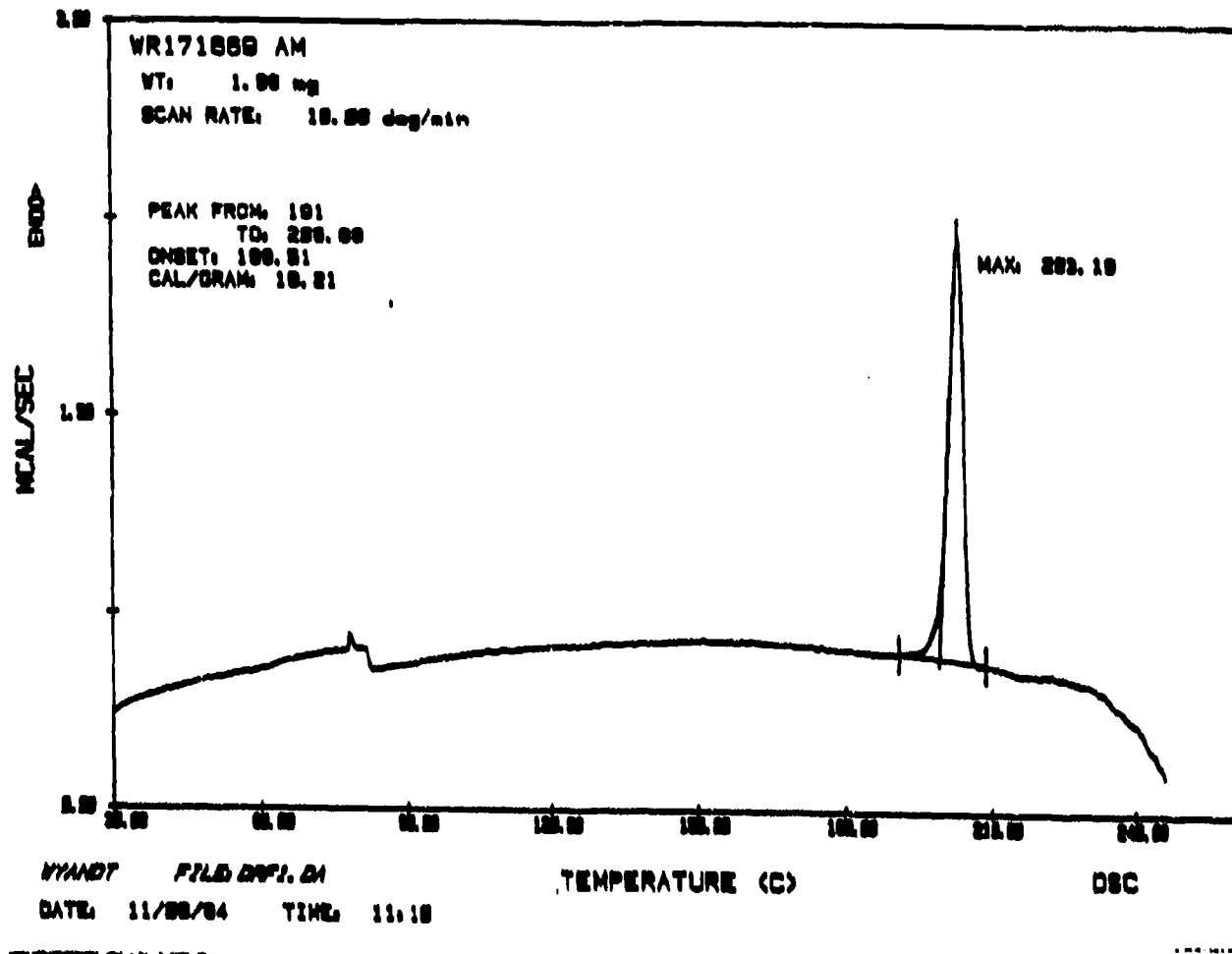


Figure 34. Thermogram of Halofantrine Hydrochloride (Lot AM)

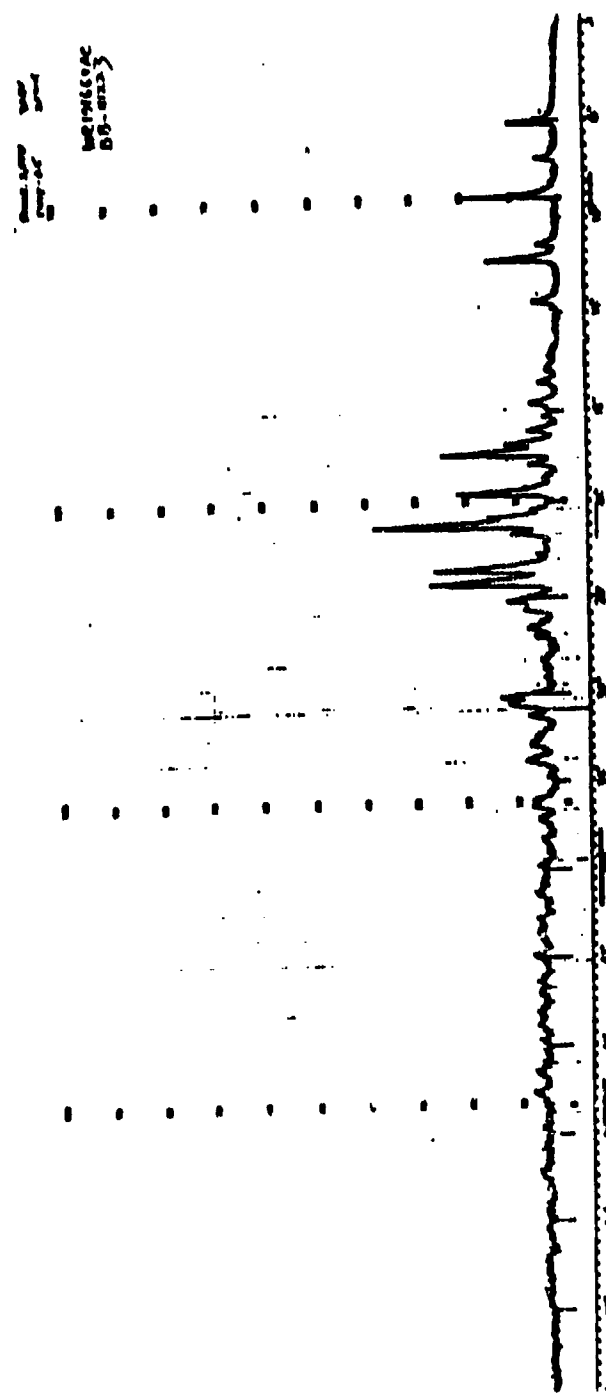


Figure 35. X-ray powder diffraction pattern for Halofantrine Hydrochloride (Lot AC)

Table 9. X-ray Diffraction Data for Halofantrine Hydrochloride
(Lot AC)

BKG	PEAK	TWO-THETA	
	182	5.642	1
128	922	6.076	14.
128	459	7.496	11.793
128	1425	9.051	9.770
120	442	11.162	7.927
120	1332	11.834	7.478
120	523	13.563	6.528
132	4413	16.713	5.305
132	576	17.595	5.041
244	672	18.842	4.710
244	1022	19.427	4.569
344	2041	19.877	4.467
344	628	20.355	4.363
344	1765	21.562	4.121
412	1219	22.606	3.933
412	1214	22.680	3.921
412	3117	22.950	3.875
412	2150	24.839	3.584
412	2222	25.397	3.507
296	920	26.068	3.418
296	926	26.116	3.4
340	1091	30.157	2.9
340	994	30.339	2.9
340	1054	30.398	2.9

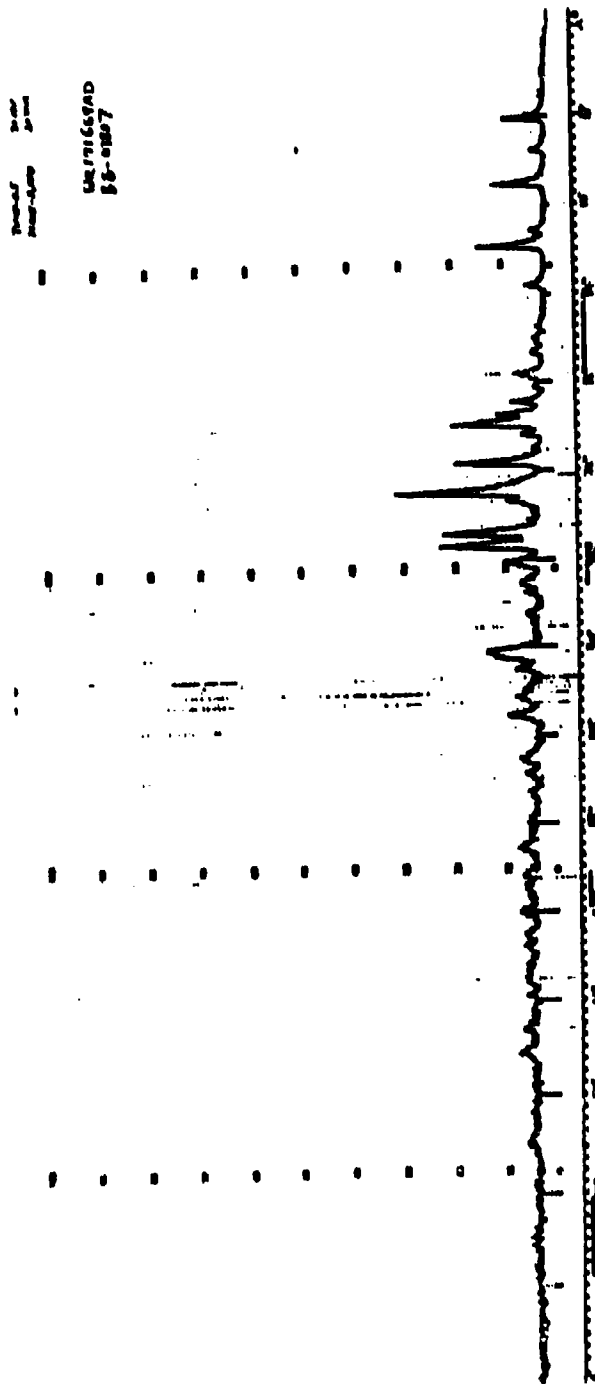


Figure 36. X-ray powder diffraction data for Halofantrine Hydrochloride (Lot AD)

Table 10. X-ray Diffraction Data for Halofantrine Hydrochloride
(Lot AD)

BKG	PEAK	TWO-THETA	
60	150	5.522	16
60	172	5.652	15.664
60	176	5.722	15.445
112	759	6.076	14.546
112	315	7.464	11.844
112	333	7.514	11.765
112	962	9.062	9.739
132	1304	11.856	7.464
132	456	13.601	6.510
168	660	17.642	5.027
276	840	19.419	4.571
276	1640	19.915	4.458
276	1631	21.632	4.108
384	2535	22.944	3.876
384	1784	24.840	3.5
384	1758	25.378	3.5
368	1200	30.227	2.9
368	1035	30.391	2.9

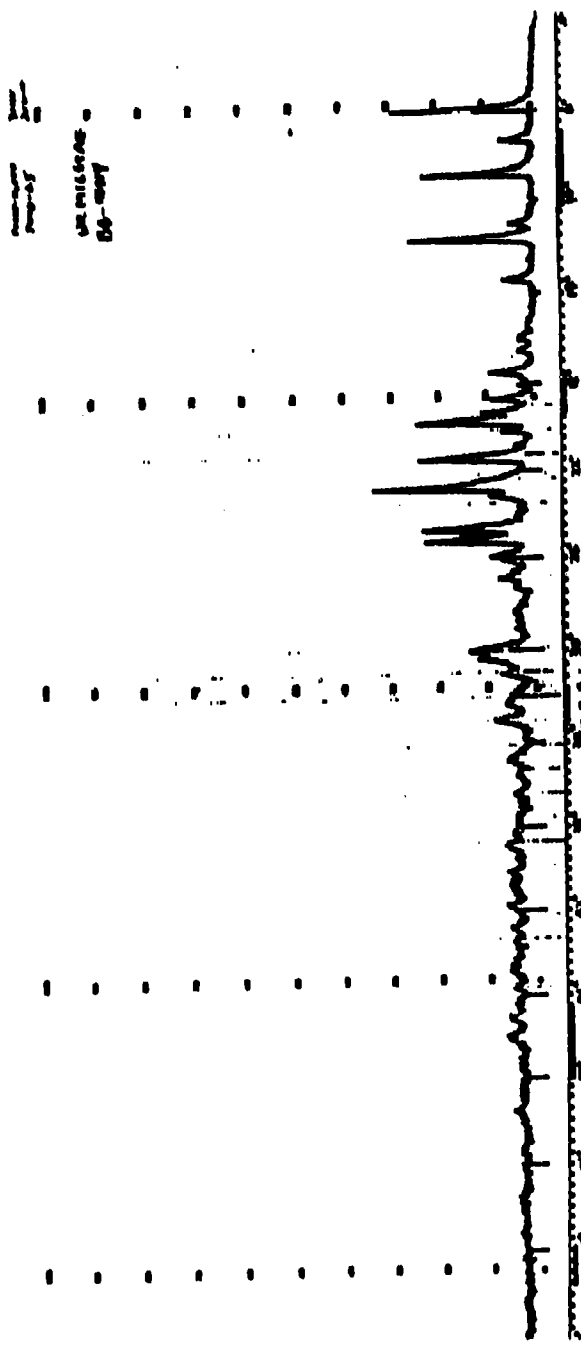


Figure 37. X-ray powder diffraction data for Halofantrine Hydrochloride (Lot AF)

Table 11. X-ray Diffraction Data for Halofantrine Hydrochloride
(Lot AE)

BKG	PEAK	TWO-THETA	
76	256	5.459	16.
76	2552	5.940	14.
136	737	7.345	12.1
136	2047	8.916	9.918
136	487	11.025	8.025
136	2156	11.681	7.576
136	576	13.423	6.596
169	792	17.481	5.073
276	792	18.680	4.750
276	978	19.273	4.605
276	2129	19.738	4.498
276	2030	21.440	4.144
420	1184	22.496	3.952
420	2790	22.793	3.901
420	1906	24.691	3.606
420	1922	25.223	3.581
356	1143	29.928	2
352	1250	29.983	2
352	1028	30.243	2

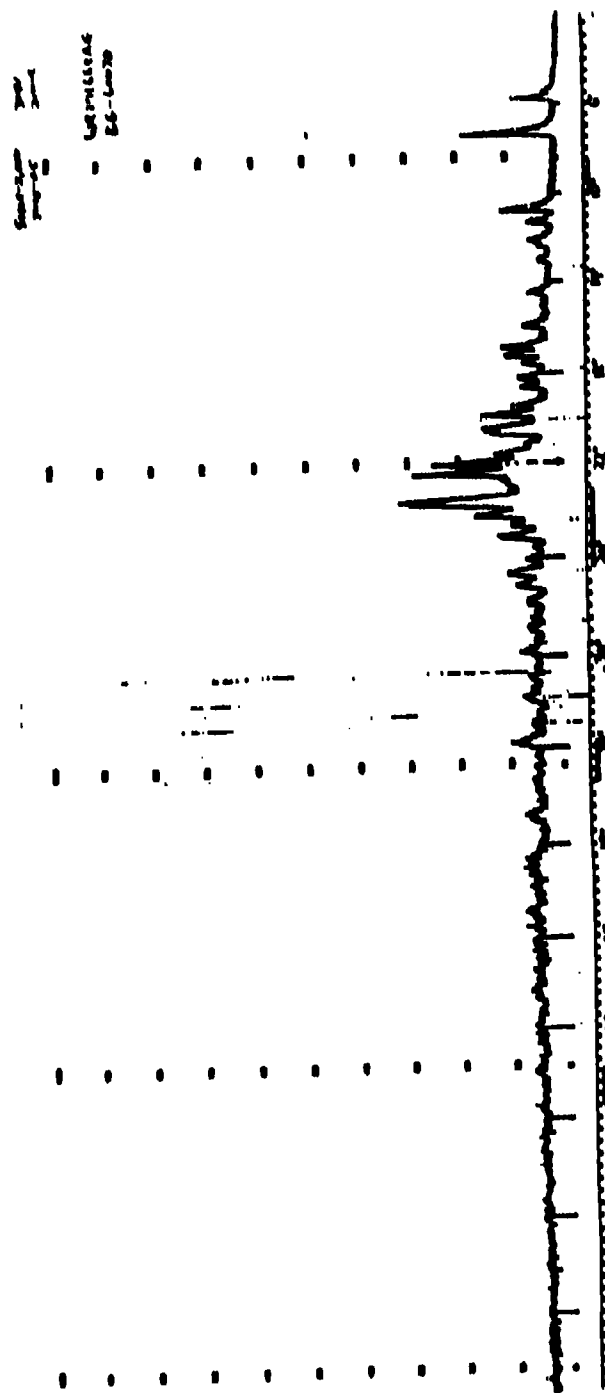


Figure 38. X-ray powder diffraction data for Halofantrine Hydrochloride (Lot AG)

Table 12. X-ray Diffraction Data for Halofantrine Hydrochloride
(Lot AG)

BKG	PEAK	TWO-THETA	
76	332	1.960	45.0
76	218	5.283	16.7
76	277	5.365	16.4
76	318	5.523	16.00
76	780	5.738	15.402
160	1575	7.293	12.122
244	939	10.675	8.287
336	966	16.856	5.260
336	922	17.179	5.161
436	1308	19.256	4.471
436	1312	20.439	4.345
436	1198	20.616	4.308
436	1178	21.578	4.118
476	2076	21.999	4.
476	2318	22.420	3.
476	2570	23.599	3.
476	2590	23.657	3.7
476	1404	24.182	3.6

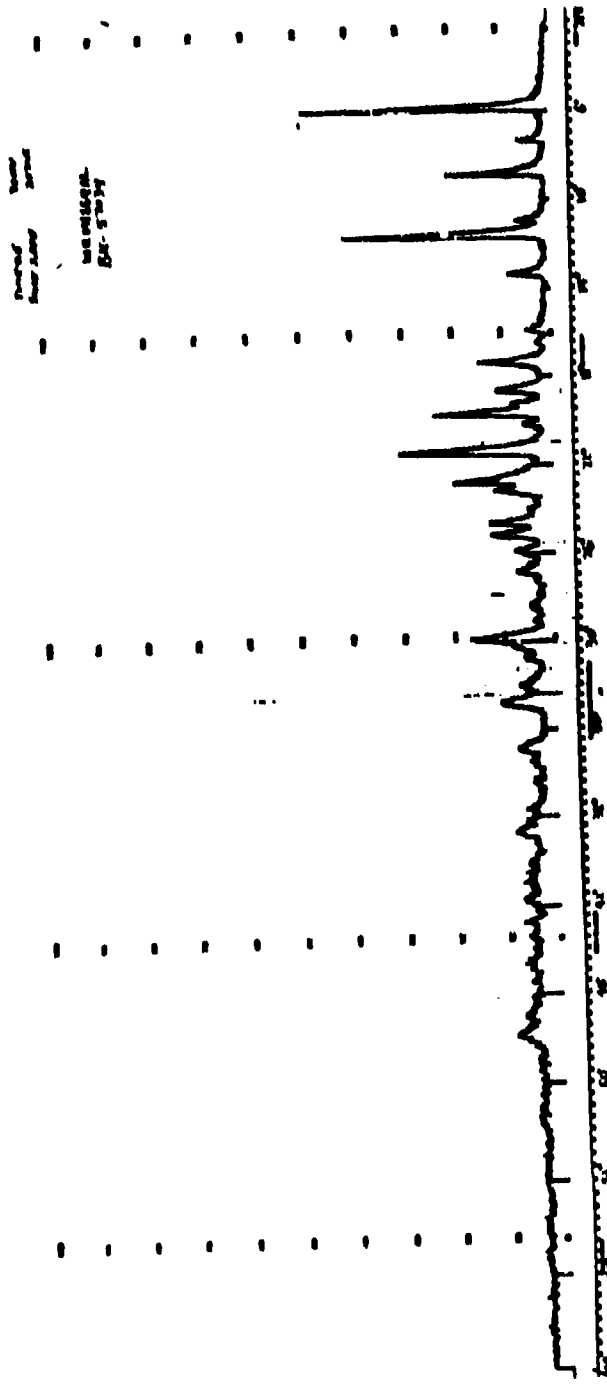


Figure 39. X-ray powder diffraction data for Halofantrine Hydrochloride (Lot AL)

Table 13. X-ray Diffraction Data for Halofantrine Hydrochloride
(Lot AL)

BKG	PEAK	TWO-THETA	
96	3916	5.843	15
144	490	7.264	12
144	1680	8.838	10
128	558	10.956	
128	3344	11.567	7.650
128	684	13.321	6.646
168	1138	17.344	5.113
268	951	18.570	4.778
268	1919	19.612	4.526
268	2507	21.326	4.166
360	1557	22.711	3.915
360	926	23.136	3.844
360	1067	24.606	3.618
360	1076	24.654	3.
360	1070	25.177	3.
316	1272	29.838	2.
332	934	32.752	2.

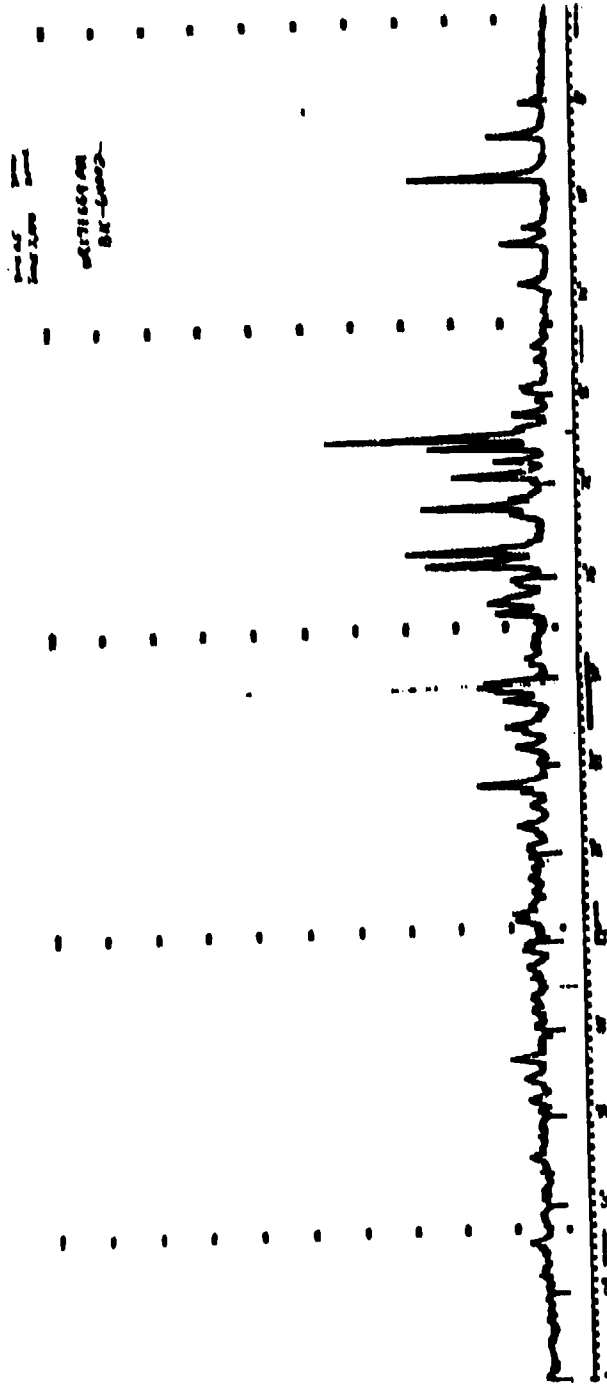


Figure 40. X-ray powder diffraction data for Halofantrine Hydrochloride (Lot AH)

Table 14. X-ray Diffraction Data for Halofantrine Hydrochloride
(Lot AM)

BKG	PEAK	TWO-THETA	
128	470	.119	14.
128	986	7.526	11.
128	2358	9.092	9.
128	436	11.213	7.890
128	882	11.861	7.461
128	554	13.614	6.504
128	486	17.682	5.016
128	458	17.882	4.960
128	358	17.911	4.952
200	652	18.866	4.704
200	560	19.496	4.553
200	3676	19.899	4.462
200	2038	20.330	4.368
200	976	20.959	4.239
200	1734	21.637	4.107
316	2217	23.004	3.866
316	2488	24.880	3.579
316	2110	25.435	3.502
284	730	26.081	3.417
284	802	26.820	3.324
284	1132	27.022	3.300
284	982	27.476	3.246
296	1065	30.192	2.960
296	1209	30.428	2.
296	837	31.017	2.
296	842	32.161	2.
328	1316	34.791	2.

AD _____

Quarterly Report Number 21

Effect of Antioxidants on the Stability of Cholinesterase Reactivator Oximes**Part I: Screening of Antioxidants for Enhancement of WR249,943·2Cl****(MMB-4·2Cl) and WR249,655·2Cl (HI-6·2Cl) Stability****Part II: Enhancement of WR249,943·2Cl (MMB-4·2Cl) Stability with
Antioxidants****Part III: Effect of Thioglycerol on WR249,655·2Cl (HI-6·2Cl) Stability****Submitted by:****John L. Lach, Principal Investigator****Douglas R. Flanagan, Assistant Principal Investigator****Lloyd E. Matheson, Jr., Assistant Principal Investigator****January 1985****Supported by:****U.S. Army Medical Research and
Development Command
Fort Detrick
Frederick, Maryland 21701-5012****Contract No. DAMD 17-85-C-5003****College of Pharmacy
University of Iowa
Iowa City, IA 52242
(319/353-4520)**

Further dissemination only as directed by Commander, US Army Medical Research and Development Command, ATTN: SGRD-RM1-S, Fort Detrick, Frederick, Maryland 21701-5012, 16 September 1986, or higher DOD authority.

The findings in this report are not to be construed as an Official Department of the Army position unless so designated by other authorized documents.

Table of Contents

	<u>Page</u>
List of Tables	78
Resumé of Progress	79
PART I: Screening of Antioxidants for Enhancement of WR249,943·2C1 (MMB-4·2C1) and WR249,655·2C1 (HI-6·2C1) Stability	
Objective	80
Summary	80
Methodology	80
Results	81
Conclusions	85
PART II: Enhancement of WR249,943·2C1 (MMB-4·2C1) Stability with Antioxidants	
Objective	86
Summary	86
Methodology	86
Results	89
Conclusions	91
PART III: Effect of Thioglycerol on WR249,655·2C1 (HI-6·2C1) Stability	
Objective	92
Summary	92
Methodology	92
Results	94
Conclusions	94

List of Tables

<u>Table</u>	<u>Title</u>	<u>Page</u>
1	Antioxidant Solutions	82
2	Antioxidant Screen Results for WR249,943·2C1 (MMB-4·2C1)	83
3	Antioxidant Screen Results for WR249,655·2C1 (HI-6·2C1)	84
4	Percent Remaining of WR294,943·2C1 (MMB-4·2C1) at 60°C for Formulations A, B, E and F	89
5	Percent Remaining of WR294,943·2C1 (MMB-4·2C1) at 40°C for Formulations A, B, C and D	90
6	Percent Remaining of WR294,943·2C1 (MMB-4·2C1) at Room Temperature for Formulations A and B	90
7	Percent Remaining of WR294,655·2C1 (HI-6·2C1) at 60°C for Formulations G and H	95
8	Percent Remaining of WR294,655·2C1 (HI-6·2C1) at 40°C for Formulations G and H	95
9	Percent Remaining of WR294,655·2C1 (HI-6·2C1) at Room Temperature for Formulations G and H	96

Resumé of Progress

Work has begun on the formulation of a sustained release oral dosage form for pyridostigmine. A comparison of the solid state properties of several lots of WR142,490·HCl is in progress.

Part I: Summary of Antioxidants for Enhancement of WR249,943·2Cl (MMB-4·2Cl)
WR249,655·2Cl (HI-6·2Cl) Stability

Objectives

The objectives of this work were 1) to screen a series of antioxidants singly and in combination to aid in the stabilization of HI-6·2Cl (WR249,655·2Cl) and MMB-4·2Cl (WR249,943·2Cl); and 2) to determine the stability of these materials using the best formulation conditions.

Summary

Eight antioxidants were screened singly and in combination for their ability to enhance the stability of both MMB-4·2Cl and HI-6·2Cl. Instability is observed visually by changes in the color of the original solutions. Propyl gallate was the best antioxidant for MMB-4·2Cl. A combination of sodium bisulfite/thioglycerol was also tested further. None of the antioxidants or their combination appeared as promising for the HI-6·2Cl, but thioglycerol and the thioglycerol/cysteine combination were chosen for further testing.

Methodology

Antioxidant Solutions

A large number of antioxidant solutions were screened for their effect on the stabilization of both MMB-4·2Cl and HI-6·2Cl. The materials and concentrations are given in Table 1. The concentrations in the table are double what they were during the actual experiment since the solution was diluted by a factor of two by the addition of the requisite volume of oxime solution. Citrate buffer at pH 2.26 (room temperature) was used as the solvent.

MMB-4·2Cl and HI-6·2Cl Solution

These solutions were prepared at a drug concentration of 200 mg/mL pH 2.26 citrate buffer.

Final Screening Solution

0.25 mL of each antioxidant solution and 0.25 mL of drug solution were placed into a clear one dram glass vial. The vials were protected from light by placing them into amber bottles, which were immersed in a 60°C water bath. The vial contents were examined periodically for a color change. MMB-4·2C1 changes from a light tan or deep yellow color to dark brown while HI-6·2C1 changes from light yellow to green upon degradation.

Results

The results of the screening procedure are given in Table 2 for MMB-4·2C1 and in Table 3 for HI-6·2C1.

Table 1. Antioxidant Solutions

Number	Code	Composition
1	SB	2% Sodium Bisulfite
2	SM	0.3% Sodium Metabisulfite
3	AA	1.0% Ascorbic Acid
4	TG	1.0% Thioglycol
5	TU	0.1% Thiourea
6	TGA	1.0% Thioglycolic Acid
7	PG	0.2% Propyl Gallate
8	C	1.0% Cysteine
9	SB/E	No. 1 + 0.1% Na ₂ EDTA·2H ₂ O (E)
10	SM/E	No. 2 + E
11	AA/E	No. 3 + E
12	TG/E	No. 4 + E
13	TU/E	No. 5 + E
14	TGA/E	No. 6 + E
15	PG/E	No. 7 + E
16	C/E	No. 8 + E
17	SR/SM	No. 1 + No. 2
18	SB/AA	No. 1 + No. 3
19	SB/TG	No. 1 + No. 4
20	SB/TU	No. 1 + No. 5
21	SB/TGA	No. 1 + No. 6
22	SB/PG	No. 1 + No. 7
23	SB/C	No. 1 + No. 8
24	SM/AA	No. 2 + No. 3
25	SM/TG	No. 2 + No. 4
26	SM/TU	No. 2 + No. 5
27	SM/TGA	No. 2 + No. 6
28	SM/PG	No. 2 + No. 7
29	SM/C	No. 2 + No. 8
30	AA/TG	No. 3 + No. 4
31	AA/TU	No. 3 + No. 5
32	AA/TGA	No. 3 + No. 6
33	AA/PG	No. 3 + No. 7
34	AA/C	No. 3 + No. 8
35	TG/TU	No. 4 + No. 5
36	TG/TGA	No. 4 + No. 6
37	TG/PG	No. 4 + No. 7
38	TG/C	No. 4 + No. 8
39	TU/TGA	No. 5 + No. 6
40	TU/PG	No. 5 + No. 7
41	TU/C	No. 5 + No. 8
42	TGA/PG	No. 6 + No. 7
43	TGA/C	No. 6 + No. 8
44	PG/C	No. 7 + No. 8

Table 2. Antioxidant Screen Results for WR249,943·2C1 (MMB-4·2C1)

Number	Code	Color Change	First Day Observed
1	SB	Brown	7
2	SM	Light Brown	7
3	AA	Brown	7
4	TG	Brown	7
5	TU	Brown	7
6	TGA	Brown	7
7	PG	Brownish Yellow	13
8	C	Brown	7
9	SB/E	Reddish Brown	1
10	SM/E	Brown	1
11	AA/E	Brown	2
12	TG/E	Brown	2
13	TU/E	Brownish Yellow	3
14	TGA/E	Reddish Brown	1
15	PG/E	Light Brown	16
16	C/E	Reddish Brown	1
17	SB/SM	Brown	1
18	SB/AA	Brown	1
19	SB/TG	Brownish Yellow	3
20	SB/TU	Light Brown	1
21	SB/TGA	Brown	1
22	SB/PG	Brown	1
23	SB/C	Light Brown	1
24	SM/AA	Brown	1
25	SM/TG	Brownish Yellow	1
26	SM/TU	Light Brown	1
27	SM/TGA	Brown	1
28	SM/PG	Brownish Yellow	1
29	SM/C	Brown	1
30	AA/TG	Brown	1
31	AA/TU	Brown	1
32	AA/TGA	Brown	1
33	AA/PG	Brown	1
34	AA/C	Brown	1
35	TG/TU	Brown	1
36	TG/TGA	Brown	1
37	TG/PG	Brown	1
38	TG/C	Brown	1
39	TU/TGA	Brown	1
40	TU/PG	Brown	2
41	TU/C	Brown	1
42	TGA/PG	Brown	1
43	TGA/C	Brown	1
44	PG/C	Brown	1

Table 3. Antioxidant Screen Results for WR249,655·2C1 (HI-6·2C1)

Number	Code	Color Change	First Day Observed
1	SB	Green	7
2	SM	Green	7
3	AA	Green	7
4	TG	Green	7
5	TU	Green	7
6	TGA	Green	7
7	PG	Green	7
8	C	Green	4
9	SB/E	Green	1
10	SM/E	Light Green	1
11	AA/E	Brown	3
12	TG/E	Brown	3
13	TU/E	Green	1
14	TGA/E	Brown	2
15	PG/E	Green	2
16	C/E	Light Green	3
17	SB/SM	Green	1
18	SB/AA	Brownish Green	2
19	SB/TG	Brown	1
20	SB/TU	Green	1
21	SB/TGA	Brown	1
22	SB/PG	Green	1
23	SB/C	Green	2
24	SM/AA	Light Brown	2
25	SM/TG	Brown	2
26	SM/TU	Green	2
27	SM/TGA	Brown	1
28	SM/PG	Green	2
29	SM/C	Green	3
30	AA/TG	Brown	2
31	AA/TU	Brown	2
32	AA/TGA	Brown	1
33	AA/PG	Brown	2
34	AA/C	Light Brown	2
35	TG/TU	Brown	2
36	TG/TGA	Brown	1
37	TG/PG	Brown	2
38	TG/C	Brownish Yellow	3
39	TU/TGA	Brown	1
40	TU/PG	Green	2
41	TU/C	Green	3
42	TGA/PG	Brown	1
43	TGA/C	Brownish Yellow	1
44	PG/C	Greenish Yellow	3

Conclusions

The propyl gallate (Number 7) was by far the best antioxidant for the MMB-4·2Cl. The sodium bisulfite/thioglycerol system (Number 19) was also chosen to carry out a stability study.

Results for HI-6 are not as conclusive. Numbers 1-7 were first observed on day 7 and probably would yield much shorter times like they did in Number 9-16. None of the antioxidants or their combinations appear very promising, but thioglycerol (Number 4) and thioglycerol/cysteine (Number 38) were chosen to carry out a stability study.

Part II: Enhancement of WR249,943·2Cl (MMB-4·2Cl) Stability with Antioxidants

Objective

The objective of this work was to examine the stability of MMB-4·2Cl using the best antioxidants as determined in the screening study.

Summary

Six formulations of MMB-4·2Cl were tested for stability at various temperatures for extended periods. Propyl gallate was found to be the best antioxidant. The presence of hydroxylamine further stabilized the solution. An acceptable field product can now be made.

Methodology

Reagents

MMB-4·2Cl (WRAIR); tetrahydrofuran, UV grade (MCB); 1-octanesulfonic acid, sodium salt (Eastman Kodak); hydroxylamine HCl, (Sigma); glacial acetic acid, A.C.S., methyl paraben, sodium hydroxide, citric acid monohydrate, concentrated hydrochloric acid (Mallinckrodt); sodium bisulfite, (Aldrich); propyl gallate, (Pfaltz and Bauer). All reagents were used as received.

Apparatus

The high pressure liquid chromatographic system consisted of a Waters system with a Model 6000A pump and a Model 440 absorbance detector; a Fisher Recordall Series 5000 recorder; a Rheodyne 7125 injector with a 20 μ L loop and an Altex Ultrasphere 1.P 5 μ (25 cm x 4.6 mm I.D.) column. The concentrated solution kinetic studies were carried out by placing the drug solution into clear 1 mL vials (Pierce Chemical) sealed with Teflon[®]/Silicone discs (Pierce Chemical). The vials, in turn, were placed into amber bottles and stored in the appropriate waterbath. An adjustable sampler system (Oxford) was used

to pipet the required volumes. A Fisher pH meter was used for pH measurements. Haake E2 heater circulators were used to maintain waterbath temperature.

Solution Preparation

Citrate Buffers. Solution A was prepared by dissolving 21.01 grams of citric acid monohydrate and 8 grams of sodium hydroxide in enough distilled water to make 1000 mL of a pH 5.0 solution. Solution B was prepared by diluting concentrated hydrochloric acid to 0.1N (8.33 mL per liter) to produce a solution of pH 1.0. The pH 2.0 buffer was prepared by mixing 75.5 mL of solution A with enough solution B to make 250 mL of solution. These pH values are theoretical values. Actual pH values were measured at the appropriate temperatures.

MMB-4·2Cl Formulations

<u>Formulation A</u>		
MMB-4·2Cl		100 mg
Hydroxylamine		40 mg
Propyl gallate		1 mg
Citrate Buffer (pH 2)	qs ad	1 mL

<u>Formulation B</u>		
MMB-4·2Cl		100 mg
Propyl gallate		1 mg
Citrate Buffer (pH 2)	qs ad	1 mL

<u>Formulation C</u>		
MMB-4·2Cl		100 mg
Hydroxylamine		40 mg
Sodium Bisulfite		10 mg
Thioglycerol		5 mg
Citrate Buffer (pH 2)	qs ad	1 mL

Formulation D

MMB-4·2Cl	100 mg
Sodium Bisulfite	10 mg
Thioglycerol	5 mg
Citrate Buffer (pH 2) qs ad	1 mL

Formulation E

MMB-4·2Cl	100 mg
Hydroxylamine	20 mg
Propyl gallate	1 mg
Citrate Buffer (pH 2) qs ad	1 mL

Formulation F

MMB-4·2Cl	100 mg
Hydroxylamide	10 mg
Propyl gallate	1 mg
Citrate Buffer (pH 2) qs ad	1 mL

Internal Standard. The stock solution was prepared by dissolving 16 mg of methyl paraben in 2-3 mL of methanol and diluting to a volume of 1000 mL with distilled water.

Standard Curve Stock Solution. 25 mg of drug was dissolved in distilled water and diluted to 250 mL in a volumetric flask giving a 10 mg % solution.

Standard Curve Solutions. Four concentrations of MMB-4·2Cl were prepared in distilled water. The solutions were made by mixing either 1, 5, 8 or 10 mL of MMB-4·2Cl standard curve stock solution with 20 mL of internal standard solution and enough distilled water to make 100 mL. Appropriate concentrations of other components were added as demanded by a particular set of study conditions. These dilutions resulted in concentrations of 0.10, 0.50, 0.80 and 1.0 mg %, respectively, of MMB-4·2Cl and a constant 0.32 mg % concentration of internal standard.

Mobile Phase. Mobile phase was prepared by dissolving 4.325 gm of 1-octanesulfonic acid, sodium salt in about 500 mL of distilled water, adding 25.2 mL of

glacial acetic acid and 344 mL of tetrahydrofuran, (UV grade) and finally diluting up to a volume of 1000 mL with distilled water. This solution was filtered before using.

Assay Method

The kinetic solutions were analyzed by removing 10 μ L of solution from a vial and adding it to a 100 mL volumetric flask containing 20 mL of internal standard solution. The flasks were brought to volume with distilled water. The flow rate was 1 mL per minute and the analytical wave length was 280 nm.

Results

Long term stability was determined for the six MMB-4·2C1 formulations described earlier. The results are shown in Tables 4-6.

Table 4. Percent Remaining of WR249,943·2C1 (MMB-4·2C1) at 60°C for Formulations A, B, E and F

Time(Days)	<u>Percent Remaining</u>			
	A	B	E	F
0	100.0	100.0	100.0	100.0
2	103.4	98.5	-	-
5	100.8	98.4	-	-
15	100.6	92.9	-	-
16	-	-	106.2	107.8
30	99.0	85.5	-	-
56	-	-	92.5	97.8
59	100.6	73.0	-	-
80	105.0	62.3	-	-
97	-	-	105.1	104.1
120	93.6	40.3	-	-
156	-	-	99.8	94.0
161	105.8	30.6	-	-
220	95.1	18.3	-	-

Table 5. Percent Remaining of WR249,943·2C1 (MMB-4·2C1)
at 40°C for Formulations A, B, C and D

Time (Days)	Percent Remaining			
	A	B	C	D
0	100.0	100.0	100.0	100.0
14	100.6	97.1	-	-
21	-	-	51.5	7.5
35	99.0	96.8	-	-
60	93.9	93.4	-	-
88	99.7	92.8	-	-
120	96.1	92.1	-	-
209	102.9	97.3	-	-

Table 6. Percent Remaining of WR249,943·2C1 (MMB-4·2C1) at
Room Temperature for Formulations A and B

Time (Days)	Percent Remaining	
	A	B
0	100.0	100.0
39	105.4	101.0
48	109.3	103.4
85	106.9	-
117	107.2	107.4
206	114.7	114.5

It is clear from the data in Table 4 that when the stability of Formulation A (with hydroxylamine) is compared to that of Formulation B (without hydroxylamine) that the inclusion of hydroxylamine is very helpful in stabilizing the MMB-4·2C1. Lesser amounts of hydroxylamine as shown in Table 4 for Formulations E and F are also effective indicating that as little as 10 mg/mL of hydroxylamine will be needed. Even though there appears to be little difference between Formulations A and B in Tables 5 and 6 at lower temperatures, there is no doubt that the 60°C temperature is able to discriminate between the formulations.

The data in Table 5 clearly demonstrates the superiority of propyl gallate (Formulations A and B) as an antioxidant compared to that of the combination of sodium bisulfite and thioglycerol (Formulations C and D).

Conclusions

MMB-4·2Cl can be stabilized for extended periods of time even at elevated temperatures using propyl gallate, hydroxylamine and a pH 2 citrate buffer. An acceptable field product containing MMB-4·2Cl can now be formulated.

Part III: Effect of Thioglycerol on WR249,655·2Cl (HI-6·2Cl) Stability

Objective

The objective of this work was to examine the stability of HI-6·2Cl using the best antioxidant as determined in the screening study.

Summary

Two formulations of HI-6·2Cl were tested at various temperatures for extended periods. No effective antioxidant was found. The presence of hydroxylamine appeared to further destabilize the HI-6·2Cl. No acceptable product can be formulated at this time.

Methodology

Reagents

HI-6·2Cl, (WRAIR); tetrahydrofuran, UV grade (Burdick and Jackson); 1-octane-sulfonic acid, sodium salt (Eastman Kodak); glacial acetic acid, A.C.S., methyl paraben, sodium hydroxide, citric acid monohydrate, concentrated hydrochloric acid, (Mallinckrodt); thioglycerol, (Pfaltz and Bauer). All reagents were used as received.

Apparatus

The high pressure liquid chromatographic system consisted of a Waters system with a Model 6000A pump and a Model 440 absorbance detector; a Fisher Recordall Series 5000 recorder; a Rheodyne 7125 injector with a 20 µL loop and an Altex Ultrasphere I.P. 5µ (25 cm x 4.6 mm I.D.) column. The kinetic studies were carried out by placing the drug solution into clear 1 mL vials (Pierce Chemical) sealed with Teflon®/Silicone discs (Pierce Chemical). The vials were, in turn, were placed into amber bottles and stored in the appropriate waterbath. An adjustable sampler system (Oxford) was used to pipet the

required volumes. A Fisher pH meter was used for pH measurements. Haake E2 heater circulators were used to maintain waterbath temperature.

Solution Preparation

Citrate Buffers. Solution A was prepared by dissolving 21.01 grams of citric acid monohydrate and 8 grams of sodium hydroxide in enough distilled water to make 1000 mL of a pH 5.0 solution. Solution B was prepared by diluting concentrated hydrochloric acid to 0.1N (8.33 mL/L) to produce a solution of pH 1.0. The pH 2.0 buffer was prepared by mixing 75.5 mL of solution A with enough solution B to make 250 mL of solution.

HI-6·2C1 Formulations

<u>Formulation G</u>		
HI-6·2C1	100 mg	
Hydroxylamine	40 mg	
Thioglycerol (90% aqueous solution)	5.6 mg	
Citrate Buffer (pH 2) qs ad	1 mL	

<u>Formulation H</u>		
HI-6·2C1	100 mg	
Thioglycerol (90% aqueous solution)	5.6 mg	
Citrate Buffer (pH 2) qs ad	1 mL	

These pH values are theoretical values. Actual pH values were measured at the appropriate temperatures.

Internal Standard. The stock solution was prepared by dissolving 16 mg of methyl paraben in 2-3 mL of methanol and diluting up to a volume of 1000 mL with distilled water.

Standard Curve Stock Solution. 20 mg of HI-6·2C1 was dissolved in distilled water and diluted to 100 mL in a volumetric flask giving a 20 mg % solution.

Standard Curve Solutions. Four concentrations of HI-6·2Cl were prepared in distilled water mixing in a 50 mL volumetric flask using either 0.5, 2, 4 or 5 mL of stock solution with 10.0 mL of internal standard solution and enough distilled water to make 50 mL. These dilutions resulted in concentrations of 0.2, 0.8, 1.6 and 2.0 mg %, respectively, and a constant concentration of 0.32 mg % of internal standard.

Mobile Phase. Mobile phase was prepared by dissolving 4.325 mL of 1-octanesulfonic acid, sodium salt in a solvent system consisting of 300 mL of tetrahydrofuran, 21 mL of glacial acetic acid and enough distilled water to make a volume of one liter.

Assay Method

The apparatus and mobile phase have been previously described. The analytical wavelength was 280 nm; the flow rate was 1.0 mL/min. and the chart speed was one cm/min. The kinetic solutions were analyzed by removing 10 μ l of solution from a vial and adding it to a 50 mL volumetric flask containing 10 mL of internal standard solution. The flasks were brought to volume with distilled water and carried out in duplicate.

Results

Long term stability was determined for the two HI-6·2Cl formulations described earlier. The results are shown in Tables 7-9. It is clear from the results in the Tables that thioglycerol does not function as an effective antioxidant for HI-6·2Cl. It is also interesting to note that the presence of hydroxylamine in Formulation G appears to destabilize the HI-6·2Cl compared to Formulation H.

Conclusions

No effective antioxidant has been found to stabilize HI-6·2Cl.

Table 7. Percent Remaining of WR249,655·2Cl (HI-6·2Cl) at 60°C
for Formulations G and H.

Time(Days)	<u>Percent Remaining</u>	
	G	H
0	100.0	100.0
1	90.4	98.8
2	81.3	94.7
4	52.4	70.0
6	39.1	61.5
10	22.3	46.3
18	5.8	20.7
50	-	2.9

Table 8. Percent Remaining of WR249,655·2Cl (HI-6·2Cl) at 40°C
for Formulations G and H.

Time(Days)	<u>Percent Remaining</u>	
	G	H
0	100.0	100.0
1	97.7	97.9
4	87.7	91.5
7	87.8	91.7
14	75.3	84.5
21	62.6	80.2
28	54.4	75.3
38	43.1	65.9
45	40.5	63.8
55	28.8	52.1
71	18.7	42.3
99	9.5	30.6
105	-	27.9
118	-	19.3
134	-	22.3

Table 9. Percent Remaining of WR249,655·2C1 (HI-6·2C1) at Room Temperature for Formulations G and H.

Time(Days)	Percent Remaining	
	G	H
0	100.0	100.0
2	87.8	89.6
5	95.4	92.3
12	90.9	93.7
35	82.0	88.4
43	71.3	82.3
56	62.3	79.2
72	55.0	73.5

Quarterly Report Number 22

**Comparison of the Solid-State Properties of Lots AE, AH and AN
of Mefloquine Hydrochloride (WR 142,490·HCl)**

Submitted by:

John L. Lach, Principal Investigator
Douglas R. Flanagan, Assistant Principal Investigator
Lloyd E. Matheson, Assistant Principal Investigator

April 1985

Supported by:

U.S. Army Medical Research and Development Command
Fort Detrick
Frederick, Maryland 21701-5012

Contract DAMD 17-85-C-5003

College of Pharmacy
University of Iowa
Iowa City, Iowa 52242
(319/353-4520)

Further dissemination only as directed by Commander, US Army Medical Research and Development Command, ATTN: STRD-RMI-S, Fort Detrick, Frederick, Maryland 21701-5012, 16 September 1986, or higher DOD authority.

The findings in this report are not to be construed as an Official Department of the Army position unless so designated by other authorized documents.

Table of Contents

	<u>Page</u>
List of Tables	99
List of Figures	100
Resumé of Progress	101
Objective	102
Summary	102
Experimental Procedures and Results	102
Conclusions	120

List of Tables

<u>Table</u>	<u>Title</u>	<u>Page</u>
1	Powder X-ray diffraction data summary for mefloquine hydrochloride, Lot AE	116
2	Powder X-ray diffraction data summary for mefloquine hydrochloride, Lot AH	117
3	Powder X-ray diffraction data summary for mefloquine hydrochloride, Lot AN	119

List of Figures

<u>Figure</u>	<u>Title</u>	<u>Page</u>
1a	Scanning electron micrograph at 200X magnification of mefloquine hydrochloride, Lot AE	103
1b	Scanning electron micrograph at 400X magnification of mefloquine hydrochloride, Lot AE	103
2a	Scanning electron micrograph at 200X magnification of mefloquine hydrochloride, Lot AH	104
2b	Scanning electron micrograph at 400X magnification of mefloquine hydrochloride, Lot AH	104
3a	Scanning electron micrograph at 200X magnification of mefloquine hydrochloride, Lot AN	105
3b	Scanning electron micrograph at 400X magnification of mefloquine hydrochloride, Lot AN	105
4	Infrared spectrum of mefloquine hydrochloride, Lot AE	107
5	Infrared spectrum of mefloquine hydrochloride, Lot AH	108
6	Infrared spectrum of mefloquine hydrochloride, Lot AN	109
7	Differential scanning calorimetry thermogram of mefloquine hydrochloride, Lot AE	110
8	Differential scanning calorimetry thermogram of mefloquine hydrochloride, Lot AH	111
9	Differential scanning calorimetry thermogram of mefloquine hydrochloride, Lot AN	112
10	Powder X-ray diffraction pattern of mefloquine hydrochloride, Lot AC	113
11	Powder X-ray diffraction pattern of mefloquine hydrochloride, Lot AH	114
12	Powder X-ray diffraction pattern of mefloquine hydrochloride, Lot AN	115

Resumé of Progress

Work is progressing on the development of a pyridostigmine sustained release dosage form.

Objective

Three lots of mefloquine hydrochloride (Lots AE, AH and AN) were evaluated to determine if there was any difference in solid-state properties among the lots.

Summary

The solid-state properties of mefloquine hydrochloride (WR 142,490·HCl) investigated were physical appearance, particle size and morphology, thermal behavior, infrared spectrum and X-ray diffraction pattern. There does not appear to be any significant difference in the physical solid-state properties of these three lots (AE, AH and AN) of mefloquine hydrochloride.

Experimental Procedures and Results

1. Physical Appearance: All three lots were white powders with no noticeable odor
2. Scanning Electron Microscopy (SEM): SEMs were obtained using the Jeol 35C scanning electron microscope. Solid powder samples were coated with a thin gold-platinum film in a vacuum sputtering system at 1×10^{-5} mm Hg. Magnifications of 200-600x were obtained at 13KV. Figures 1-3 show the crystal morphology and size for each lot at two magnifications. All lots appear to be composed of flat prismatic plates with long dimensions of 30-100 microns and narrow dimensions of 10-30 microns (the white bar in the lower right of each micrograph indicates the length equivalent to 10 or 100 microns). Much of the particle mass in each lot appears to be broken pieces from larger crystals which contributes to a significant portion of the material being somewhat irregular in size and shape. There is no observable difference in the crystal morphology or particle size among these three lots of mefloquine.

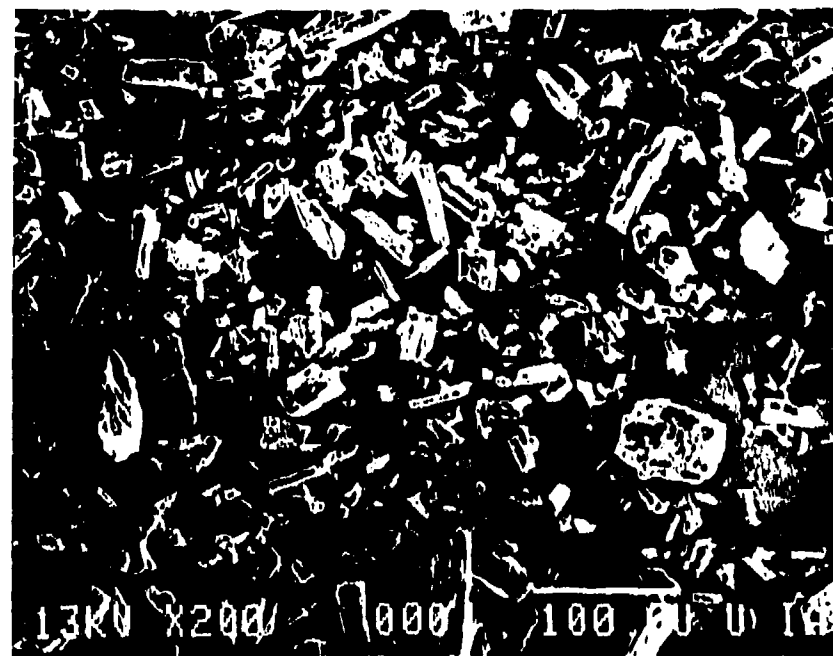


Figure 1a. Scanning electron micrograph at 200X magnification of mefloquine hydrochloride, Lot AE

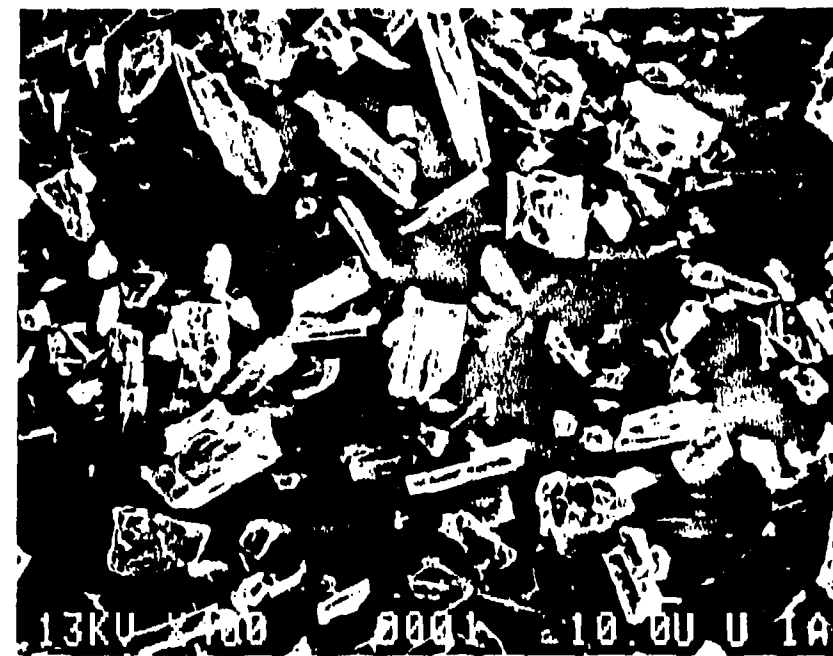


Figure 1b. Scanning electron micrograph at 400X magnification of mefloquine hydrochloride, Lot AE



Figure 2a. Scanning electron micrograph at 200X magnification of mefloquine hydrochloride, Lot AH



Figure 2b. Scanning electron micrograph at 400X magnification of mefloquine hydrochloride, Lot AH

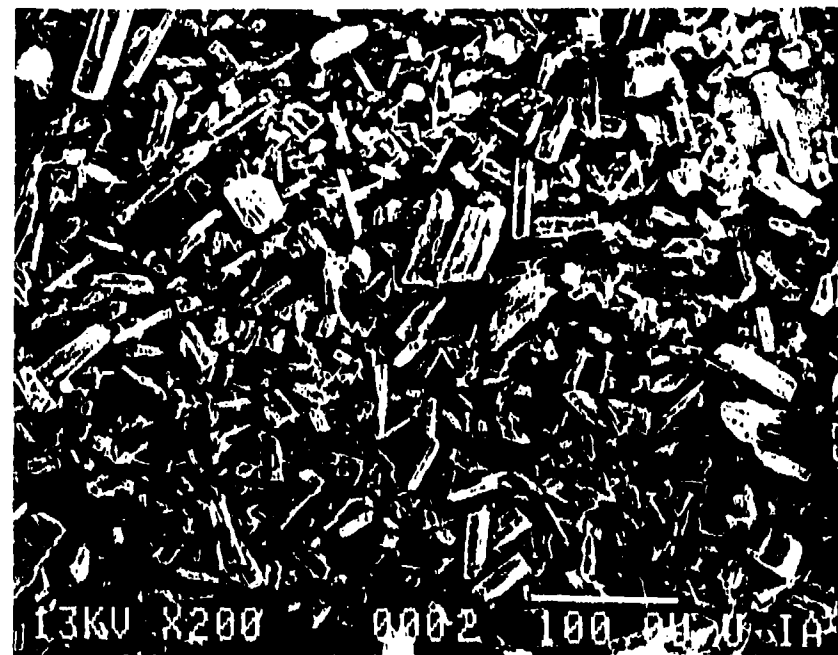


Figure 3a. Scanning electron micrograph at 200X magnification of mefloquine hydrochloride, Lot AN



Figure 3b. Scanning electron micrograph at 400X magnification of mefloquine hydrochloride, Lot AN

3. Infrared Spectrum: Figures 4-6 are the infrared spectra on each lot taken at a 1% concentration in a KBr pellet on a Beckman Model 4240 infrared spectrophotometer. There is no difference in any region of the infrared spectrum among these three lots.
4. Differential Scanning Calorimetry (DSC): DSC thermograms were taken at 10°C/min on a Perkin-Elmer DSC-2C. They show similar melting behavior among the three lots. Figures 7-9 are the DSC thermograms for each lot. Lots AH and AN are almost identical while the lot AE appears to have an approximately 7-8°C lower melting onset. This difference is probably not significant since mefloquine melts with decomposition. Such melting behavior is difficult to reproduce from lot-to-lot and is not indicative of any difference in crystal form.
5. Powder X-Ray Diffraction: Powder X-ray diffraction patterns were obtained using a Phillips APD 3500 automated diffractometer with monochromatized $\text{CuK}\alpha(\lambda=15418 \text{ \AA})$ radiation. Patterns were obtained from $2-62^\circ$ ($2-\theta$) at a scanning speed of $2.4^\circ (\text{2}\theta) \text{ min}^{-1}$. Figures 10-12 show the powder X-ray diffraction patterns for each lot.

Tables I-III give the data summary from these diffraction patterns in terms of 2θ angles, D values (\AA) and relative intensities of the diffraction maxima (I/I'). There is no significant difference in the X-ray diffraction patterns of these three lots. In the data summary, the difference in the number of maxima can be accounted for on the basis of the slight splittings in certain peaks which may be recorded as separate peaks. These slight differences in each lot are not indicative of any significant difference in crystal properties.

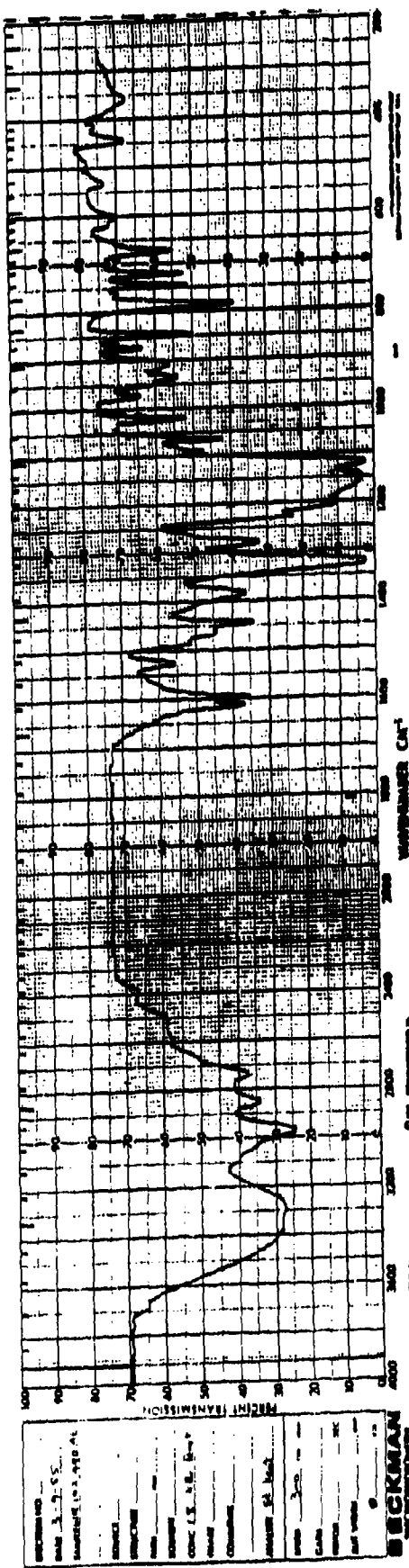


Figure 4. Infrared spectrum of nefloquine hydrochloride, Lot AE

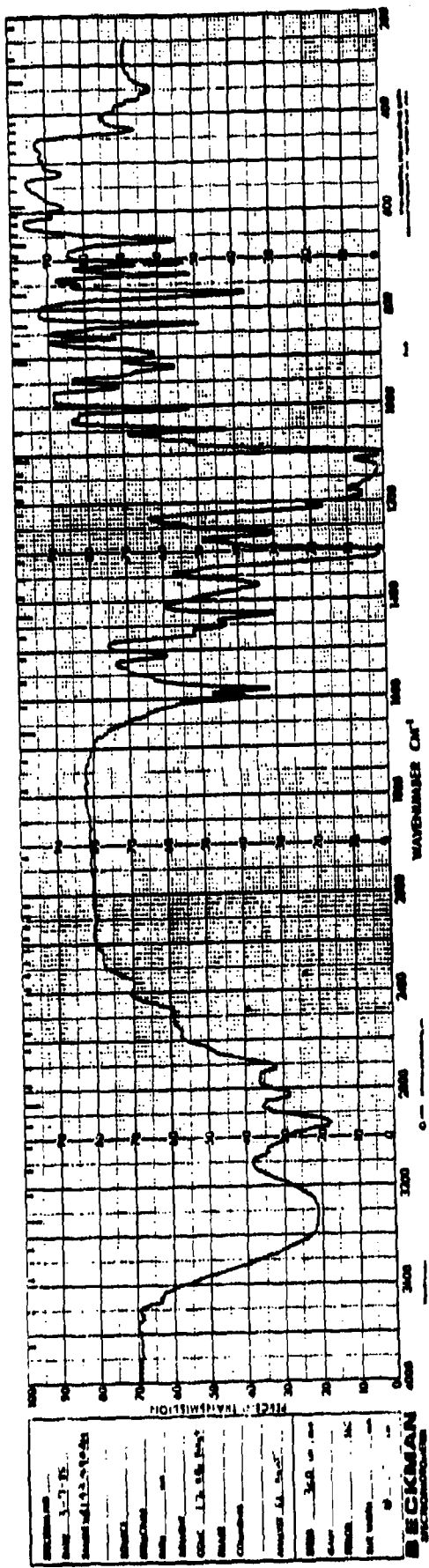


Figure 5. Infrared spectrum of mafloquine hydrochloride, Lot AH

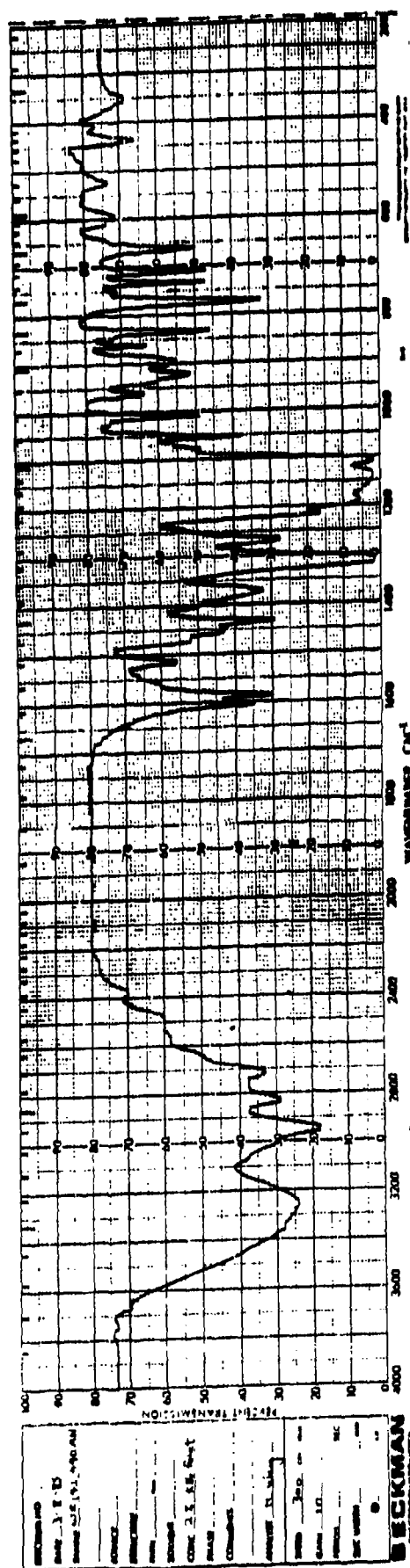


Figure 6. Infrared spectrum of nefloquine hydrochloride, Lot AN

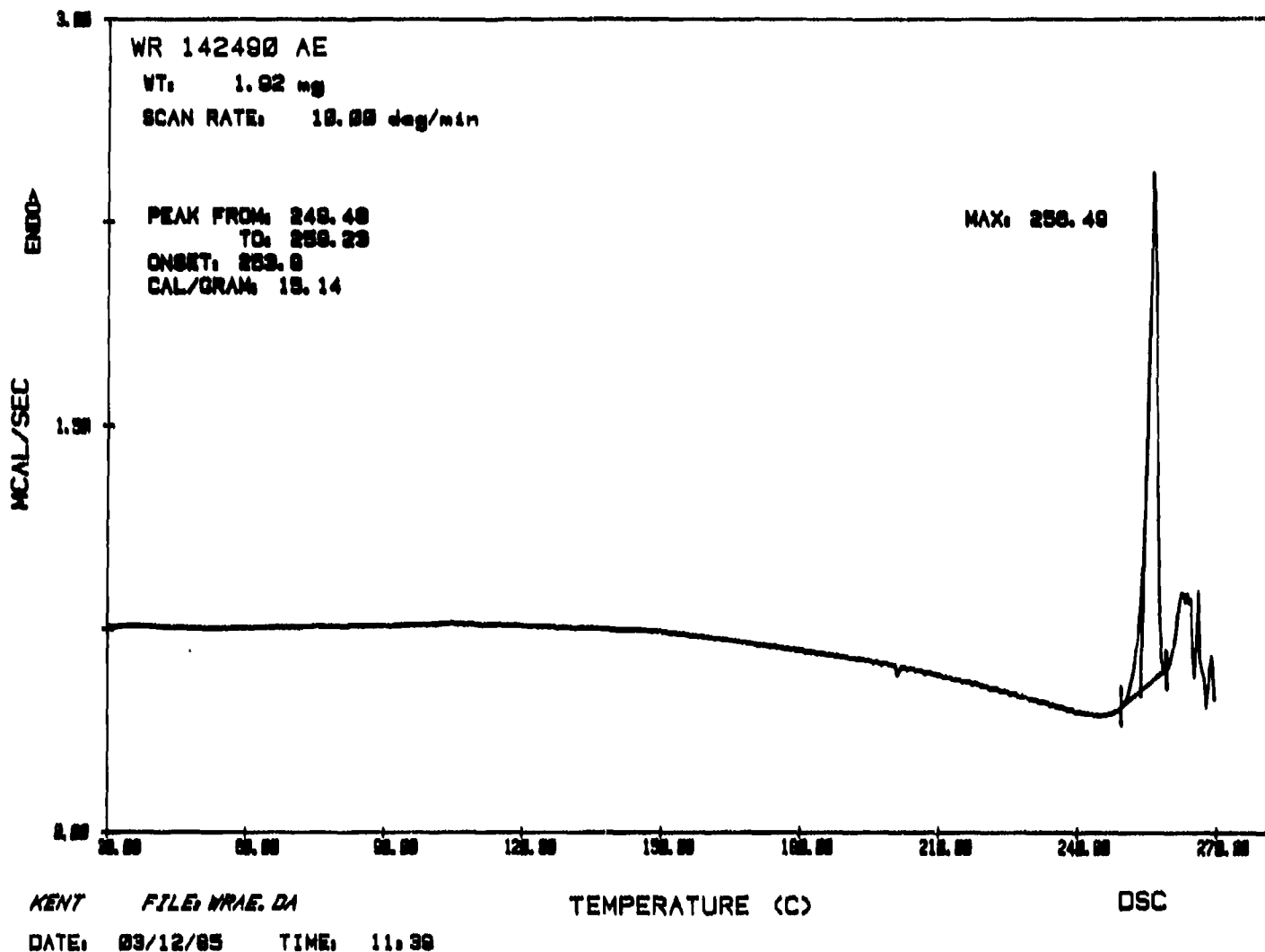
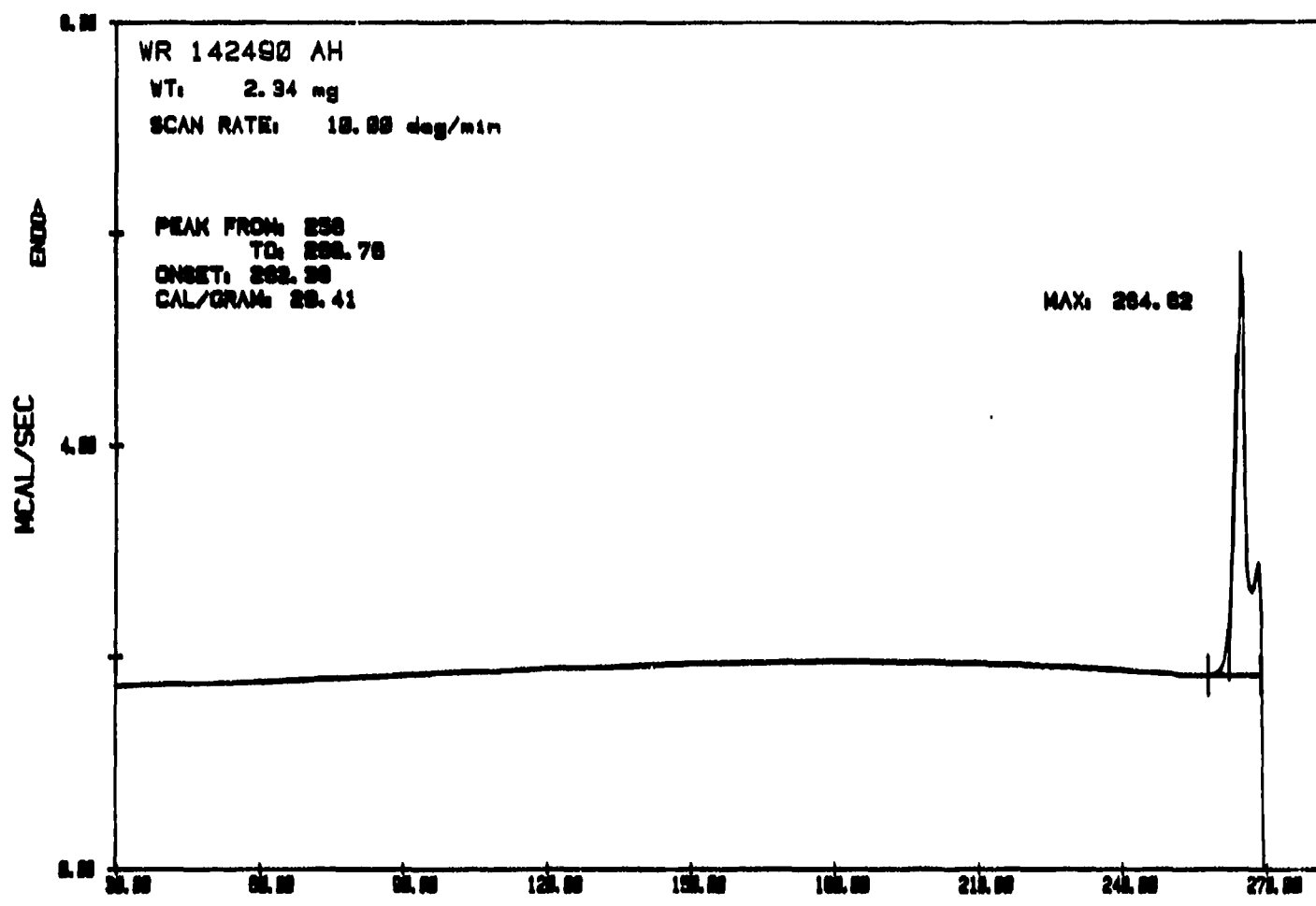


Figure 7. Differential scanning calorimetry thermogram of mefloquine hydrochloride, Lot AE



KENT FILED: MRAH.DA
DATE: 03/12/05 TIME: 12:24

TEMPERATURE (C)

DSC

Figure 8. Differential scanning calorimetry thermogram of mefloquine hydrochloride, Lot AH

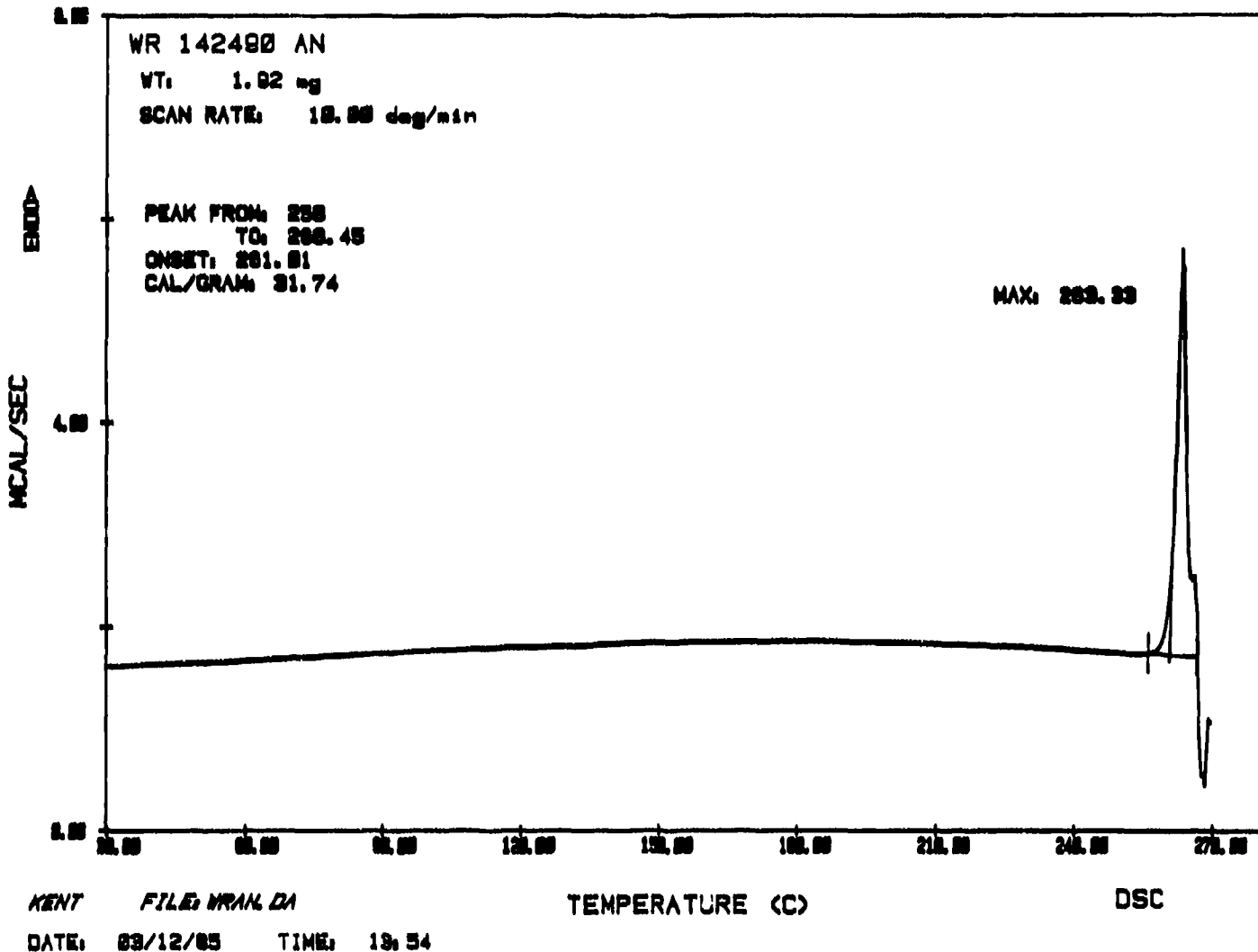


Figure 9. Differential scanning calorimetry thermogram of mefloquine hydrochloride, Lot AN

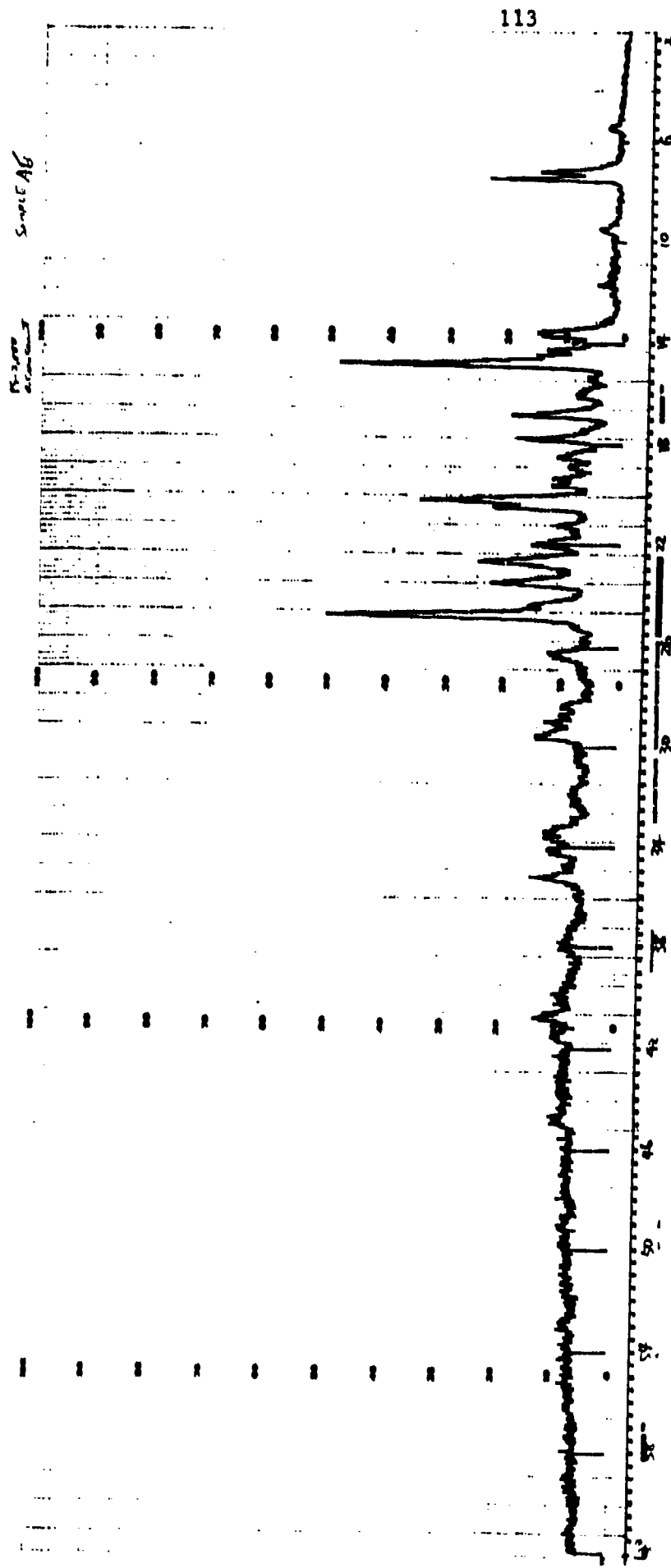


Figure 10. Powder X-ray diffraction pattern of nefloquine hydrochloride, Lot AF

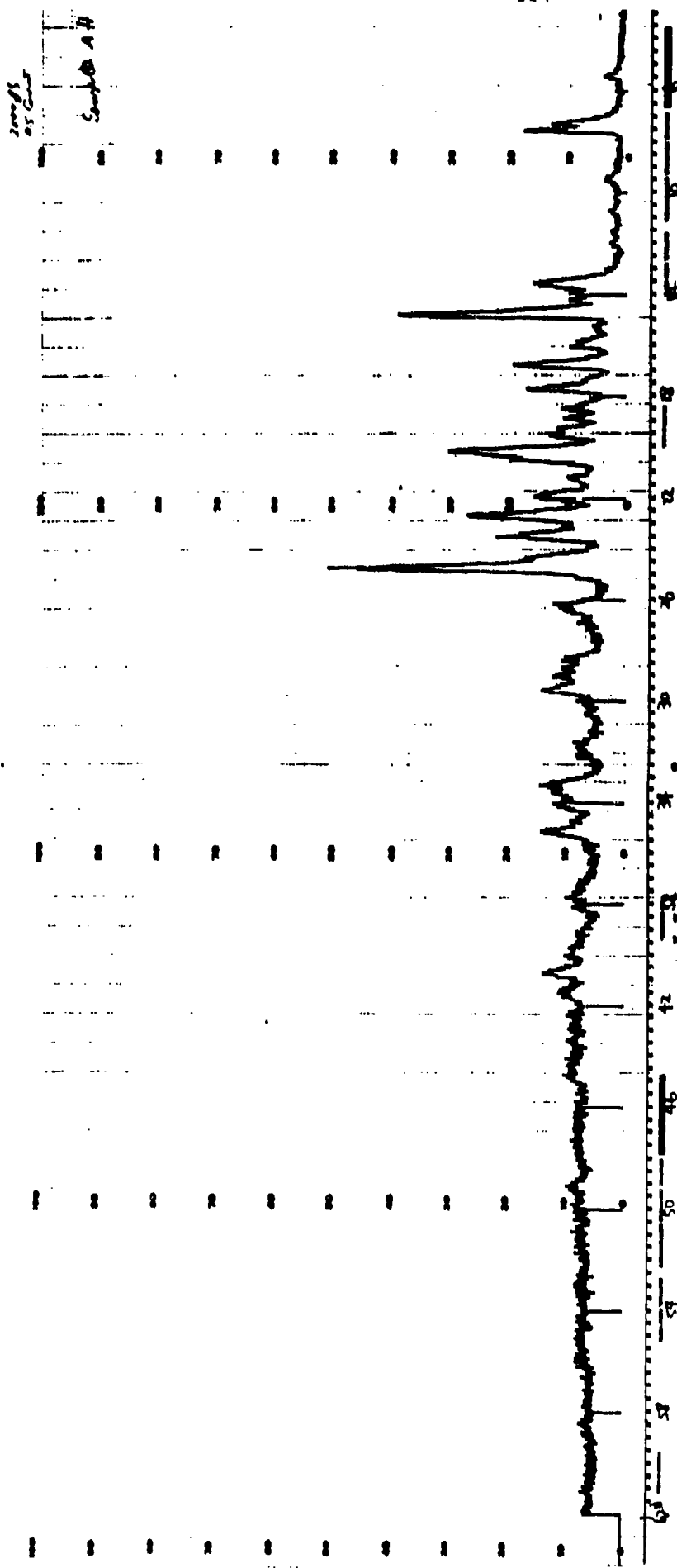


Figure 11. Powder X-ray diffraction pattern of nefloquine hydrochloride, Lot AH

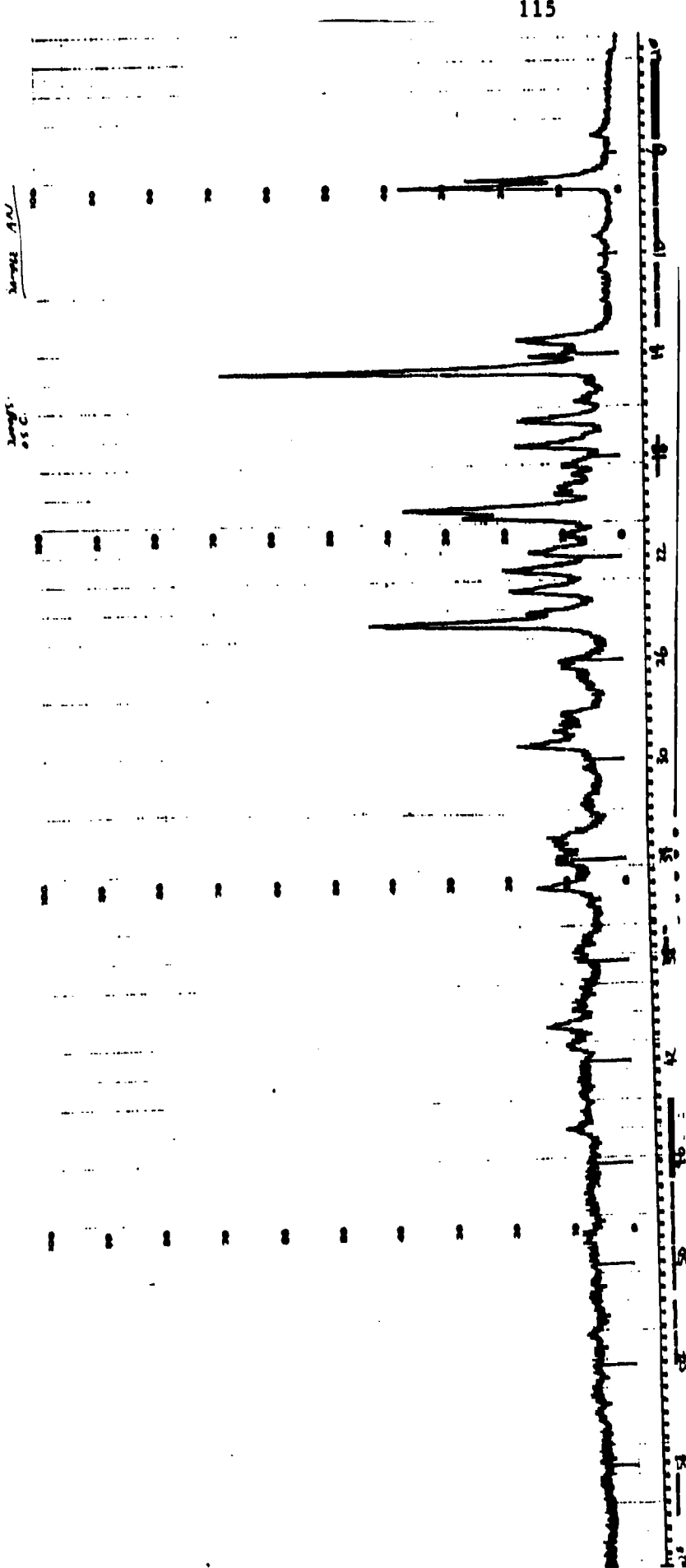


Figure 12. Powder X-ray diffraction pattern of mefloquine hydrochloride, Lot AN.

Table 1. Powder X-ray Diffraction Data Summary for Mefloquine Hydrochloride, Lot AE

BKG	PEAK	TWO-THETA	"D"
68	470	1.960	45.073
68	208	5.343	16.540
68	288	5.502	16.061
132	1260	7.249	12.185
132	1885	7.543	11.719
132	354	9.466	9.343
132	346	9.516	9.294
132	375	9.583	9.229
180	1195	13.564	6.528
180	1176	13.662	6.481
180	762	13.940	6.353
416	1215	14.478	6.118
416	3908	14.824	5.976
416	1584	16.806	5.275
416	1456	17.782	4.988
580	2691	20.230	4.389
580	1810	20.508	4.331
532	1916	22.675	3.921
532	1849	23.496	3.786
532	1340	24.339	3.657
532	3871	24.756	3.596
		"D"	I/I/
		5.975	100
		3.596	99
		4.389	68
		45.072	12
		16.540	5
		16.061	7
		12.195	32
		11.719	48
		9.342	9
		9.294	8
		9.228	9
		6.527	30
		6.481	30
		6.352	19
		6.118	30
		5.975	
		5.275	40
		4.987	37
		4.389	
		4.330	46
		3.921	49
		3.786	47
		3.657	34
		3.596	21

Table 2. Powder X-ray Diffraction Data Summary for Mefloquine Hydrochloride, Lot AH

BKG	PEAK	TWO-THETA	"D"
48	134	4.816	18.348
48	126	4.894	18.056
48	144	4.960	17.817
48	146	5.042	17.527
48	180	5.222	16.922
48	328	5.422	16.298
48	120	5.594	15.797
48	128	5.669	15.590
48	126	5.720	15.450
48	121	5.887	15.013
48	130	5.939	14.882
132	1044	7.215	12.252
132	1395	7.484	11.813
156	1201	13.517	6.551
156	1188	13.662	6.500
156	782	13.873	6.383
408	3074	14.744	6.008
408	1571	16.726	5.300
408	1384	17.713	5.007
532	2504	20.175	4.401
412	2192	22.680	3.921
412	994	22.875	3.887
412	1656	23.461	3.792
412	1402	24.371	3.652
412	3947	24.704	3.604
412	974	24.932	3.571

"D"	I/I
3.604	100
6.007	78
4.401	63

18.348	3	1
18.055	3	2
17.816	3	3
17.527	3	4
16.921	5	5
16.297	8	6
15.796	3	7
15.590	3	8
15.450	3	9
15.012	3	10
14.882	3	11
12.252	26	12
11.812	35	13
6.550	30	14
6.500	30	15
6.383	19	16

Table 2 (Continued)

6.007		17
5.300	39	18
5.007	35	19
4.401		20
3.921	55	21
3.887	25	22
3.792	42	23
3.642	35	24
3.604		25
3.571	27	26

Table 3. Powder X-ray Diffraction Data Summary for Mefloquine Hydrochloride, Lot AN

BKG	PEAK	TWO-THETA	"D"
100	382	5.320	16.612
148	2133	7.064	12.514
148	3168	7.365	12.002
184	1443	13.376	6.619
184	740	13.779	6.426
408	1218	14.062	6.298
408	5558	14.656	6.044
408	1440	16.618	5.334
408	1487	17.585	5.043
576	3087	20.047	4.429
576	2190	20.357	4.362
388	1654	22.516	3.949
388	931	22.702	3.917
388	1605	23.303	3.817
388	1210	24.128	3.688
388	1208	24.179	3.681
388	3617	24.570	3.623
432	1420	29.449	3.033
"D"		I/I/	
6.043		100	
3.623		65	
12.001		57	
16.611		6	1
12.611		38	2
12.001		3	
6.619		26	4
6.426		13	5
6.298		22	6
6.043		7	
5.334		26	8
5.043		26	9
4.429		56	10
4.362		39	11
3.949		29	12
3.917		17	13
3.817		29	14
3.688		21	15
3.691		21	16
3.623		17	
3.033		25	18

Conclusions

Even though there were small differences observed in the DSC thermograms of lot AE compared to lots AH and AN, other physical tests of the solid-state properties of these lots indicated no difference in crystal form. Thus, these mefloquine hydrochloride lots do not appear to have any solid-state differences that could be attributed to polymorphism or crystal solvates being present.

Quarterly Report Number 23

Part I: Formulation of Pyridostigmine Sustained-Release
Oral Dosage Forms

Part II: Comparison of the Solid State Properties of Lots
AC, AF, AG and AH of HI-6 (WR249,655·2C1)

Submitted by:

John L. Lach, Principal Investigator
Douglas R. Flanagan, Assistant Principal Investigator
Lloyd E. Matheson, Assistant Principal Investigator

July 1985

Supported by:

U.S. Army Medical Research and Development Command
Fort Detrick
Frederick, Maryland 21701-5012

Contract DAMD 17-85-C-5003

College of Pharmacy
University of Iowa
Iowa City, Iowa 52242
(319/353-4520)

Further dissemination only as directed by Commander, US Army Medical Research and Development Command, ATTN: SGRD-RMI-S, Fort Detrick, Frederick, Maryland 21701-5012, 16 September 1986, or higher DOD authority.

The findings in this report are not to be construed as an Official Department of the Army position unless so designated by other authorized documents.

Table of Contents

	<u>Page</u>
List of Tables	123
List of Figures	124
Resumé of Progress	125
PART I: Formulation of Pyridostigmine Sustained-Release Oral Dosage Forms	
Objective	126
Summary	126
Experimental	126
Results and Discussion	130
PART II: Comparison of the Solid State Properties of Lots AC, AF, AG, and AH of HI-6 (WR249,655·2C1)	
Objective	135
Summary	135
Solid State Properties	135
Conclusions	136

List of Tables

<u>Table</u>	<u>Title</u>	<u>Page</u>
1	Pyridostigmine Bromide 40 mg Sustained-Release Tablets-Hydrophilic Polymer Formulations	128
2	Pyridostigmine Bromide 40 mg Sustained-Release Tablets-Inert Matrix Formulations	129
3	Cumulative Amount (mg) of Pyridostigmine Dissolved-Hydrophilic Polymer Formulations	132
4	Cumulative Amount (mg) of Pyridostigmine Dissolved-Inert Matrix Formulations	134
5	X-Ray Diffraction Data for HI-6 (WR249,655·2C1), Lot AC	150
6	X-Ray Diffraction Data for HI-6 (WR249,655·2C1), Lot AF	152
7	X-Ray Diffraction Data for HI-6 (WR249,655·2C1), Lot AG	154
8	X-Ray Diffraction Data for HI-6 (WR249,655·2C1), Lot AH	156

List of Figures

<u>Figure No.</u>	<u>Caption</u>	<u>Page</u>
1a & b	Scanning electron micrograph of HI-6 (WR249,655·2C1), Lot AC; 40X & 320X magnification	137
2a & b	Scanning electron micrograph of HI-6 (WR249,655·2C1), Lot AF, 48X and 480X magnification	138
3a & b	Scanning electron micrograph of HI-6 (WR249,655·2C1), Lot AG; 20X and 400X magnification	139
4a & b	Scanning electron micrograph of HI-6 (WR249,655·2C1), Lot AH; 20X and 160X magnification	140
5	Infrared spectrum of HI-6 (WR249,655·2C1), Lot AC (KBr pellet)	141
6	Infrared spectrum of HI-6 (WR249,655·2C1), Lot AF (KBr pellet)	142
7	Infrared spectrum of HI-6 (WR249,655·2C1), Lot AG (KBr pellet)	143
8	Infrared spectrum of HI-6 (WR249,655·2C1), Lot AH (KBr pellet)	144
9	DSC thermogram of HI-6 (WR249,655·2C1), Lot AC	145
10	DSC thermogram of HI-6 (WR249,655·2C1), Lot AF	146
11	DSC thermogram of HI-6 (WR249,655·2C1), Lot AG	147
12	DSC thermogram of HI-6 (WR249,655·2C1), Lot AH	148
13	X-ray powder diffraction pattern for HI-6 (WR249,655·2C1), Lot AC	149
14	X-ray powder diffraction pattern for HI-6 (WR249,655·2C1), Lot AF	151
15	X-ray powder diffraction pattern for HI-6 (WR249,655·2C1), Lot AG	153
16	X-ray powder diffraction pattern for HI-6 (WR249,655·2C1), Lot AG	155

Resumé of Progress

Work is continuing on the development of a sustained-release pyridostigmine tablet in order to refine the formulation for high speed production of the tablet.

Part I: Formulation of Pyridostigmine Sustained-Release Oral Dosage Forms

Objective

The objective of this study was to develop oral formulations of pyridostigmine bromide that would release at a constant rate over a 10-12 hour period for doses of 10, 20 and 40 mg.

Summary

Two approaches have been explored for achieving constant release tablet formulations of pyridostigmine. One employed the use of hydrophilic polymers and the other employed the use of an inert matrix system. While release rates have been slowed in these systems, additional work is still proceeding to optimize the system.

Experimental

Formulation Strategy

Two approaches have been explored for achieving constant release tablet formulations one employing hydrophilic polymers and one employing inert matrix systems.

The first approach, employing hydrophilic polymers, required the use of both nonionic and anionic polymers. The polymers used are given below:

Methocel K4M-----Hydroxypropylmethylcellulose, USP 2208(4,000 cps)
Methocel E4M-----Hydroxypropylmethylcellulose, USP 2910(4,000 cps)
Methocel K15M-----Hydroxypropylmethylcellulose, USP 2208(15,000 cps)
Methocel XD-30018.00--Hydroxypropylmethylcellulose, USP 2208(100,000 cps)
Sodium CMC 7HP-----Sodium carboxymethylcellulose (DS-0.7, high viscosity)
Geltab F-----Mixture of carrageenans, locust bean gum and dextrose

The Methocel derivatives are nonionic cellulose polymers which are marketed by Dow Chemical for a variety of formulation applications, including oral sustained-release products. Sodium CMC and Geltab are anionic polymers in wide use in the food and drug industry. Formulations are detailed in Table 1.

The second approach of preparing inert polymeric matrix tablets is an application of principles developed as part of a doctoral thesis project in our department. In these systems the polymer does not swell or in any way interact with the drug or medium. When the drug dissolves in release medium that has permeated the porous matrix, it diffuses from the matrix. The extended release is obtained by the continuously increasing path length for release as drug deeper in matrix is released. In a constant surface area matrix, this continuous increase in diffusional path length results in a continuously decreasing release rate. In the systems we have developed this increasing diffusion path is compensated by an increase in releasing surface area as the drug boundary moves into the matrix. An increasing surface area is achieved by using cylindrical tablets with a hole in the middle from which the drug is released. Thus, the entire tablet is coated with a water-impermeable coat (polyethylene) except for the area surrounding the central hole. Formulations are detailed in Table 2.

Table 1: Pyridostigmine Bromide 40 mg Sustained-Release Tablets-Hydrophilic Polymer

Formulation #1

Pyridostigmine Bromide	40 mg
Methocel K4M	180 mg
Sodium CMC 7HP	<u>180 mg</u>
Weight of one tablet	400 mg

Formulation #2

Pyridostigmine Bromide	40 mg
Methocel E4M	180 mg
Sodium CMC 7HP	<u>180 mg</u>
Weight of one tablet	400 mg

Formulation #3

Pyridostigmine Bromide	40 mg
Methocel K15M	180 mg
Sodium CMC 7HP	<u>180 mg</u>
Weight of one tablet	400 mg

Formulation #4

Pyridostigmine Bromide	40 mg
Sodium CMC 7HP	<u>360 mg</u>
Weight of one tablet	400 mg

Formulation #5

Pyridostigmine Bromide	40 mg
Geltab F (carageenan)	<u>360 mg</u>
Weight of one tablet	400 mg

Formulation: #6 #7 #8

Pyridostigmine Bromide	40 mg	40 mg	40 mg
Methocel K4M	360 mg	-	-
Methocel K15M	-	360 mg	-
Methocel XD	-	-	360 mg

Table 2: Pyridostigmine Bromide 40 mg Sustained-Release Tablets-Inert Matrix Formulations

Formulation #9

Pyridostigmine Bromide	40 mg
Ethycellulose	11 mg
Methocel K4M	180 mg
Sodium CMC 7HP	<u>180 mg</u>
Weight of one tablet	411 mg

Formulation #10

Pyridostigmine Bromide PSDVB/PPC (3/1)	40 mg (15%) <u>226.7 mg (85%)</u>
Weight of one tablet	226.7 mg

Formulation #11

Pyridostigmine Bromide PSDVB/PPC (3/1)	40 mg (10%) <u>360 mg (90%)</u>
Weight of one tablet	400 mg

Formulation #12

Pyridostigmine Bromide PSDVB/PPC (3/3)	40 mg (10%) <u>360 mg (90%)</u>
Weight of one tablet	400 mg

Formulation #13

Pyridostigmine Bromide PPC	40 mg (5%) <u>760 mg (95%)</u>
Weight of one tablet	800 mg

Tablet Preparation

Component powders were dry-blended with the drug with a mortar and pestle and then further blended by tumbling the powdered mixture in a test tube on a rotating sample mixer for 2-3 hours. The appropriate weight of the mixture was weighed and compressed on a hydraulic press (15,000 psi) with a stainless steel punch and die (13 mm dia.) to form a disc-shaped tablet. The tablets were stored in a vacuum desiccator over P₂O₅ until tested for release characteristics.

Dissolution Test System

All release studies were conducted in a Hanson six-station dissolution apparatus which conforms to the requirements of the USP(USP XXI, p. 1243-1244). Apparatus II was chosen which employs paddles for agitation. The stirring speed was maintained at 100 rpm with the bottom of the paddle blade centered and maintained at 2.5 cm from the bottom of the dissolution vessel. The dissolution medium was distilled water (500 mL) which was maintained at 37°C. At frequent time intervals, samples were removed for assay by UV spectrophotometry and the sample volume replaced with an equal volume of distilled water.

Results and DiscussionHydrophilic Polymer Approach

Initial studies (Formulations #6-8) using the Methocel derivatives alone in a tablet showed that they did not sufficiently retard pyridostigmine release, although release with K4M and K15M was extended over 8-10 hours. It was felt that the addition of an anionic polymer to these formulations would retard pyridostigmine release by electrostatic interaction. Thus, if the cationic pyridostigmine could be bound to an anionic polymer, its release could be retarded sufficiently that the Methocel derivative would have adequate time to

hydrate and further retard the release. Pure anionic polymer (Formulation #4-5) did not perform as well as the mixtures with the Methocels (Formulations #1-3). Formulations #1 and #2 give almost constant release after an initial burst in the first 30 minutes.

Since such formulations would first contact gastric pH upon ingestion, it was decided to determine if there was any pH effect on the release profiles. Simulated gastric fluid (USP XXI, p. 1424) without pepsin was used at the dissolution medium in place of distilled water. As can be seen, its release rate was increased significantly over that in water. We are now in the process of evaluating the pH effect of other such systems to determine which are least affected by acidic pH media.

A final formulation (#9) employing hydrophilic polymers involved first coating the pyridostigmine with ethylcellulose (approximately 20%) in cyclohexane before incorporating the coated powder in a polymeric system equivalent to formulation #1. This powder coating was studied to determine if a very water-impermeable polymer like ethylcellulose could retard the initial rapid release of pyridostigmine in the first hour. As can be seen this formulation released completely in about 8 hours with the first hour exhibiting faster release than that observed later. Upon closer examination of this system, we have found that the pyridostigmine dissolves in the coating solution and subsequently precipitates in the ethylcellulose upon evaporation. Thus, the pyridostigmine used in formulation #9 is actually of smaller particle size than the untreated drug and this particle size reduction probably accounts for the initial faster release rate. We are exploring other means to coat pyridostigmine with ethylcellulose so that we can retard its initial rapid release rate.

Data is shown in Table 3.

Table 3: Cumulative Amount (mg) of Pyridostigmine Dissolved-Hydrophilic Polymer Formulations

Time (hrs)	Formulation Number								Mestinon Timespan 180 mg
	1	2	3	4	5	6	7	8	
0.25	2.5	2.90	4.40	1.84	6.15	8.47	8.93	16.69	44.09
0.5	4.14	4.54	6.99	4.13	10.24	13.95	11.99	24.06	58.86
0.75	5.54	6.03	9.28	6.26	13.56	17.18	14.47	26.05	66.95
1	6.60	7.18	11.24	9.43	15.97	18.99	16.00	28.24	74.47
2	10.54	11.84	17.81	17.58	22.56	24.84	21.40	34.66	93.69
3	14.72	16.09	23.61	25.03	27.46	28.42	25.18	39.30	108.54
4	18.66	19.85	28.62	31.22	30.18	31.61	28.81		116.74
5	23.50	24.07	34.57	37.25	32.63	33.58	31.35		129.72
6	26.58	27.59	39.81	40.00	34.08	35.27	33.49		138.95
7	30.18	30.86	40.00		40.00	36.12	35.03		146.31
8	35.16	35.44					36.26		152.35
9	38.12	38.72					37.25		156.46
10	40.00	40.00					38.66		161.86
11									167.98
12									

Inert Matrix Approach

The polymers used were chlorinated polypropylene and a mixture of chlorinated polypropylene and polystyrene divinylbenzene. These polymers are available as powders and have been evaluated in other drug formulations which give constant release profiles. Formulations #10 and #11 are examples of two of the inert cylindrical matrix systems - one with 15% drug-loading and the other with 10% drug-loading. The lower loaded system gave a release profile that extended for over 12 hours but was not zero-order. A different ratio of polystyrene divinylbenzene/chlorinated polypropylene was also evaluated (Formulation #12) and its release rate is significantly slower than formulation #11. If pure chlorinated polypropylene is used as a matrix (Formulation #13) the matrix is so impermeable (low porosity, high tortuosity and low wettability) that only 8% of the pyridostigmine is released in 12 hours. We are exploring

means by which the chlorinated polypropylene matrix can be made more permeable to enhance its rate of release. The more permeable matrices do not give the constant release profiles expected because of the high solubility of pyridostigmine in water. The diffusional models for such systems depend upon undissolved drug existing inside the matrix and the boundary of undissolved drug receding slowly as a function of time. With pyridostigmine having a solubility in excess of 500 mg/mL, it probably dissolves completely in the matrix pores that are filled with release medium. We are considering preparing lower solubility salts of pyridostigmine (i.e., salicylate, citrate and pamoate) to achieve better release characteristics from these inert matrix tablets.

We have also investigated the release characteristics of the commercially available pyridostigmine bromide product which is sustained release (Mestinon Timespan,® Roche). Its release characteristics are not zero-order and the tablet appears to be an inert matrix system since it retains its shape as drug is released. It releases 1/3 of its contents (60 mg) in less than one hour which corresponds to a priming dose for its therapeutic application. The balance of the tablets contents (120 mg) are then released over 12 hours.

Data is shown in Table 4.

Table 4: Cumulative Amount (mg) of Pyridostigmine Dissolved-Inert Matrix Formulations

Time(hrs)	Formulation Number						
	9	10	11	11(repeat)	12	13	1(pH 1.2)
0.25	2.30	7.09	2.50	-----	-----	-----	9.48
0.5	8.52	10.97	4.68	-----	-----	-----	15.10
0.75	10.99	14.67	6.87	-----	-----	-----	19.53
1	12.78	17.62	8.60	11.09	4.43	0.70	23.37
2	17.44	27.03	14.96	17.92	8.63	1.00	30.57
3	21.07	32.73	19.49	-----	-----	-----	34.90
4	26.68	36.25	23.15	26.08	15.58	1.30	37.39
5	32.32	38.51	26.10	-----	-----	-----	39.21
6	36.05	39.97	28.76	30.62	21.08	1.80	40.00
7	39.39		30.71	-----	-----	-----	
8	40.00		32.34	33.41	25.46	2.10	
9			33.72	-----	-----	-----	
10			35.00	35.23	28.82	2.60	
11			36.13	-----	-----	-----	
12			37.33	36.42	31.46	3.20	

Part II: Comparison of the Solid State Properties of Lots AC, AF, AG and AH of HI-6 (WR249,655·2Cl)

Objective

The objective of this work was to determine if there were any differences in the solid state properties of various lots of HI-6 (WR249,655·2Cl). The lots examined were AC, AF, AG, and AH.

Summary

The solid state properties of HI-6 (WR249,655) determined include color, odor, taste, appearance, particle size, thermal behavior, infrared spectrum and X-ray diffraction pattern. There appear to be differences among the various lots based on the thermograms, X-ray diffraction patterns and infrared spectra.

Solid State Properties

All four lots were white, bitter powders with no odor.

Scanning electron micrographs are shown for each lot at two magnifications in Figures 1-4. There is a broad range in particle size with small (~10 μ) particles fused to the surface of larger particles (up to 400 μ). The small particles of Lot AG in Figure 3b appear somewhat different in morphology than those of the other lots. Lots AC and AH have better defined crystal morphology, indicative of slower crystallization.

The infrared spectra shown in Figures 5-8 appear to have differences. For example, lot AG has a large doublet at 8.4 μ that does not appear in the IR spectra of the other lots. The region around 13 μ also shows significant differences from lot-to-lot.

The DSC thermograms are shown in Figures 9-12. HI-6 (WR249,655) exhibits a large exotherm ranging from about 152°C to 172°C indicating decomposition

after the onset of melting. A small endotherm, indicative of melting, appears in each case before decomposition begins. Unfortunately, it is not possible to obtain the heat of fusion for these lots because of the decomposition that occurs soon after melting begins. Nevertheless, from the differences in the onset of melting (AC, 147.8°C; AF, 140.3°C; AG, 162.98°C and AH, 146.7°C), it does appear that there are variations in the solid-state properties.

The X-ray powder diffraction patterns are shown in Figures 13-16. The 2 θ angles, D values (\AA) and relative intensities ($I/I' \times 100$) for all diffraction maxima over 2-40° are presented in Tables I-IV. The peak between 26° and 30° in Figures 13-16 appear to vary from one lot to another. This too is indicative of different crystalline forms.

Conclusions

Differences in solid-state properties of various lots of HI-6 (WR249,655-2C1) were observed. These differences may be various polymorphs obtained through alteration of crystallization methods for these lots. Further studies may be warranted of whether these solid-state property differences influence other properties of HI-6 such as solubility or solid-state stability.



Figure 1a. Scanning electron micrograph of HI-6 (WR249,655-2C1),
Lot AC; 40X magnification

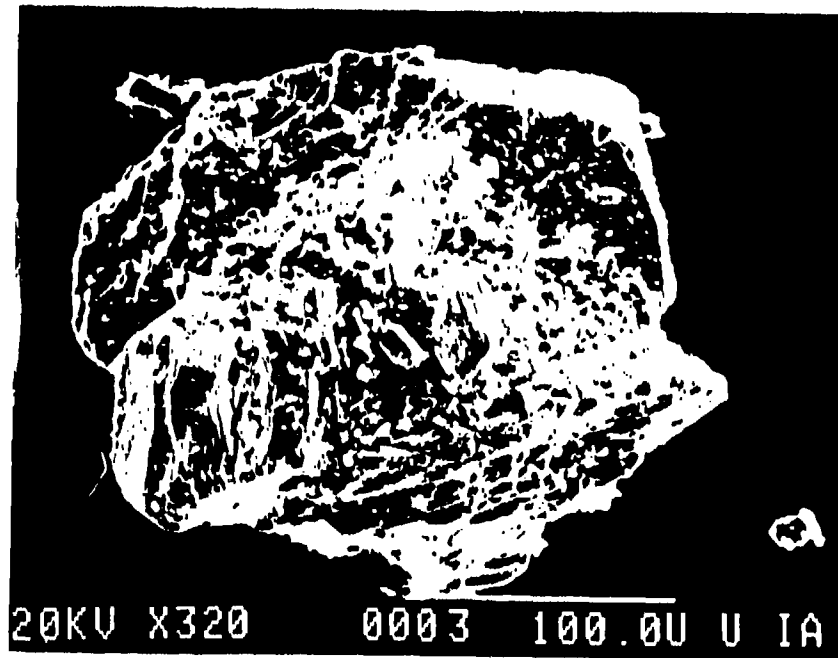


Figure 1b. Scanning electron micrograph of HI-6 (WR249,655-2C1),
Lot AC; 320X magnification

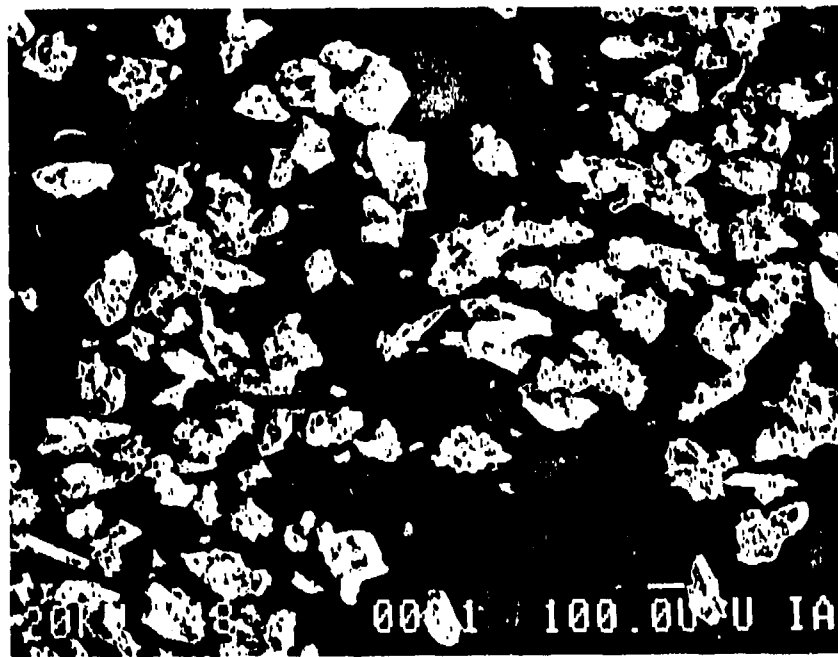


Figure 2a. Scanning electron micrograph of HI-6 (WR249,655-2C1),
Lot AF; 48X magnification

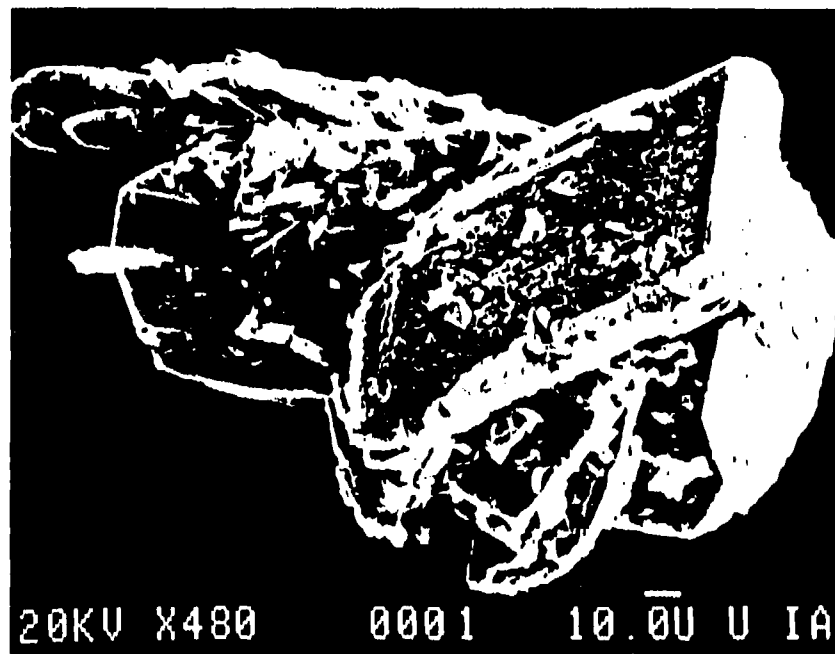


Figure 2b. Scanning electron micrograph of HI-6 (WR249,655-2C1),
Lot AF; 480X magnification



Figure 3a. Scanning electron micrograph of HI-6 (WR249,655-2C1),
Lot AG; 20X magnification

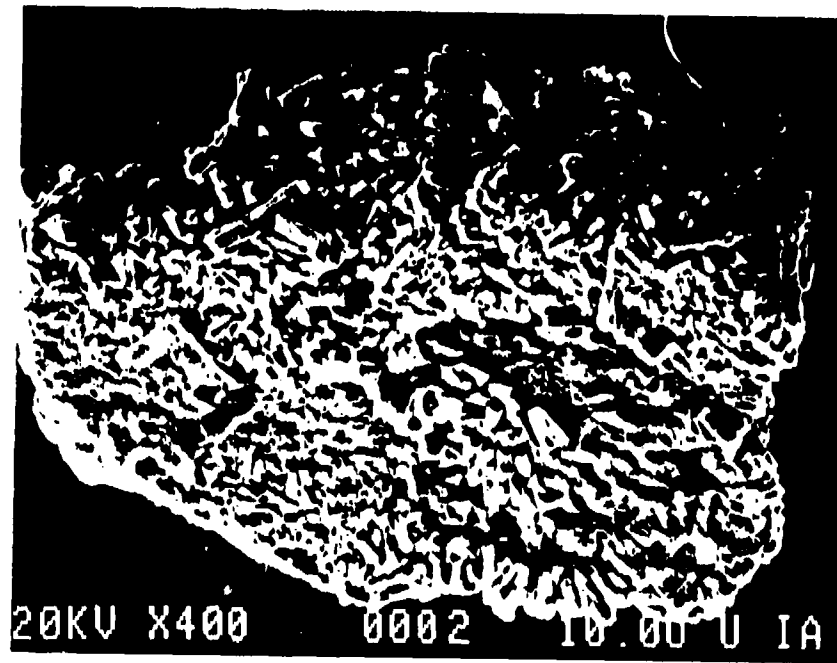


Figure 3b. Scanning electron micrograph of HI-6 (WR249,655-2C1),
Lot AG; 2000X magnification



Figure 4a. Scanning electron micrograph of HI-6 (WR249,655-2C1),
Lot AH; 400X magnification

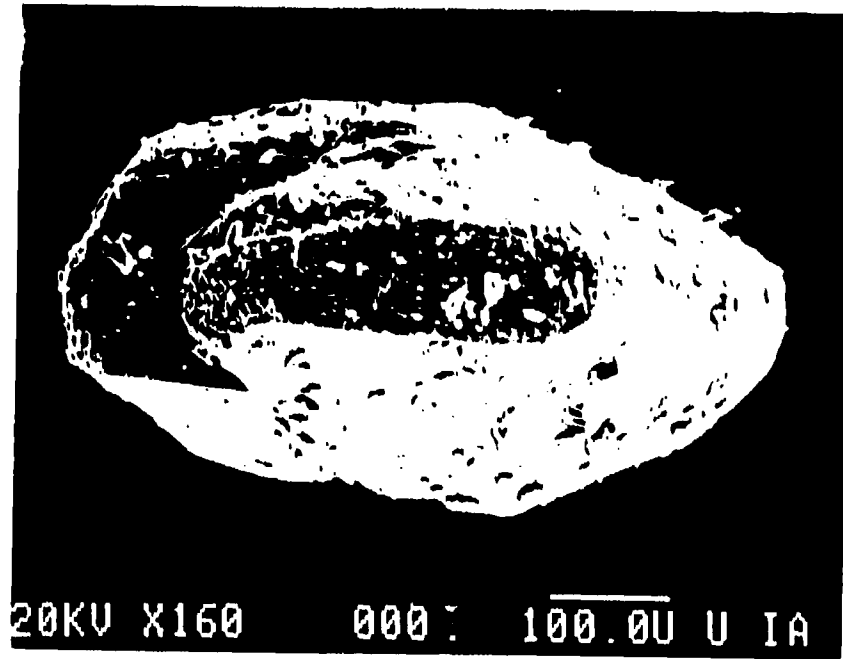


Figure 4b. Scanning electron micrograph of HI-6 (WR249-655-2C1),
Lot AH; 160X magnification

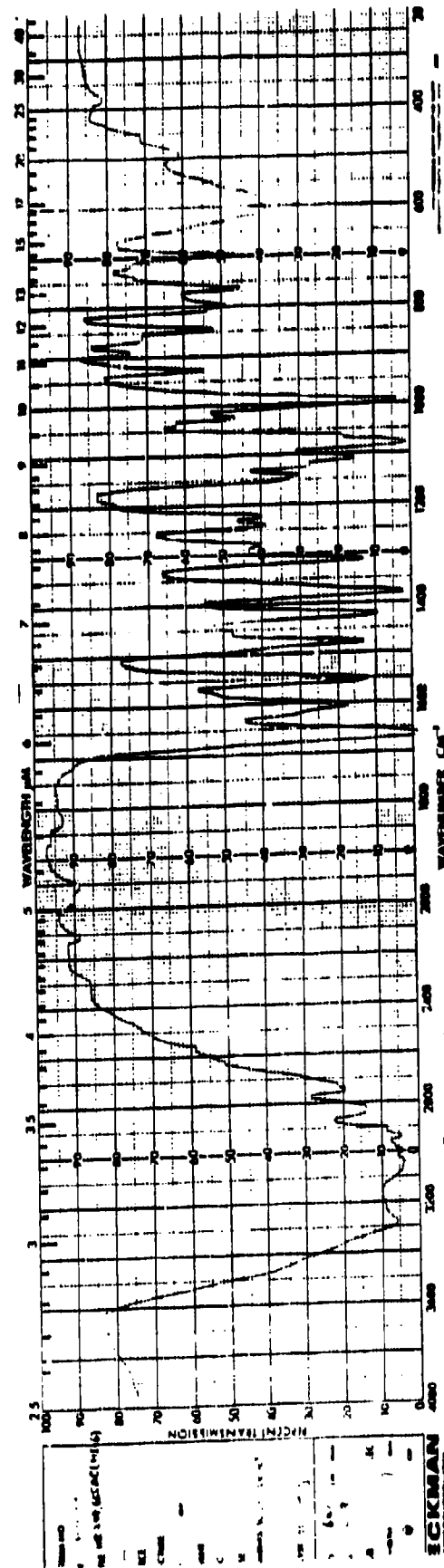


Figure 5. Infrared spectrum of HI-6 (WR249,655-2C1), Lot AC (KBr pellet)

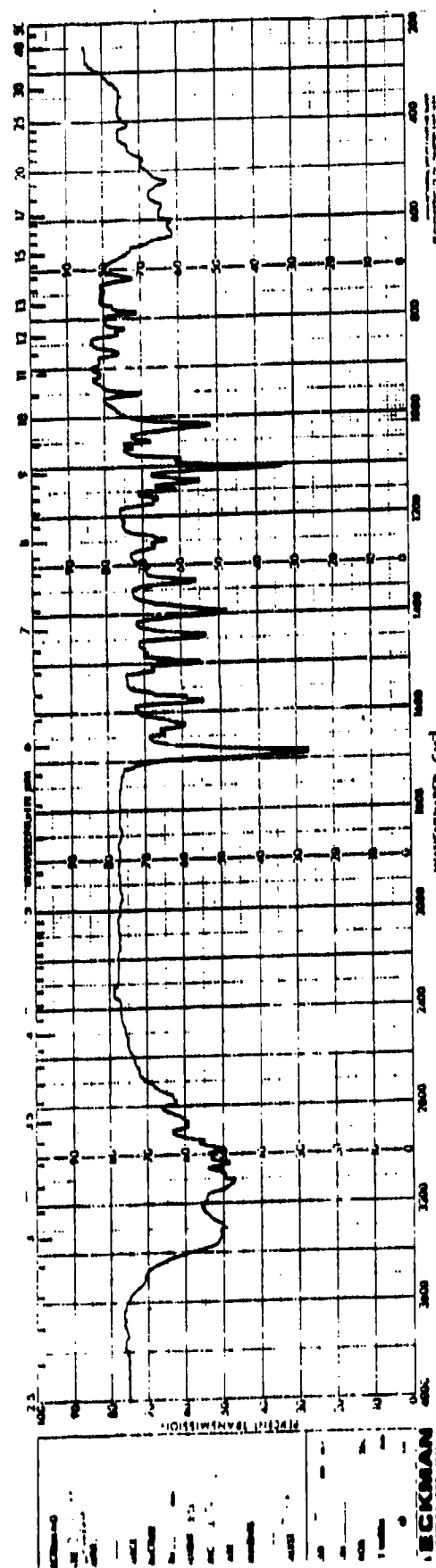


Figure 6. Infrared spectrum of HI-6 (WR249,655·2Cl), Lot AF

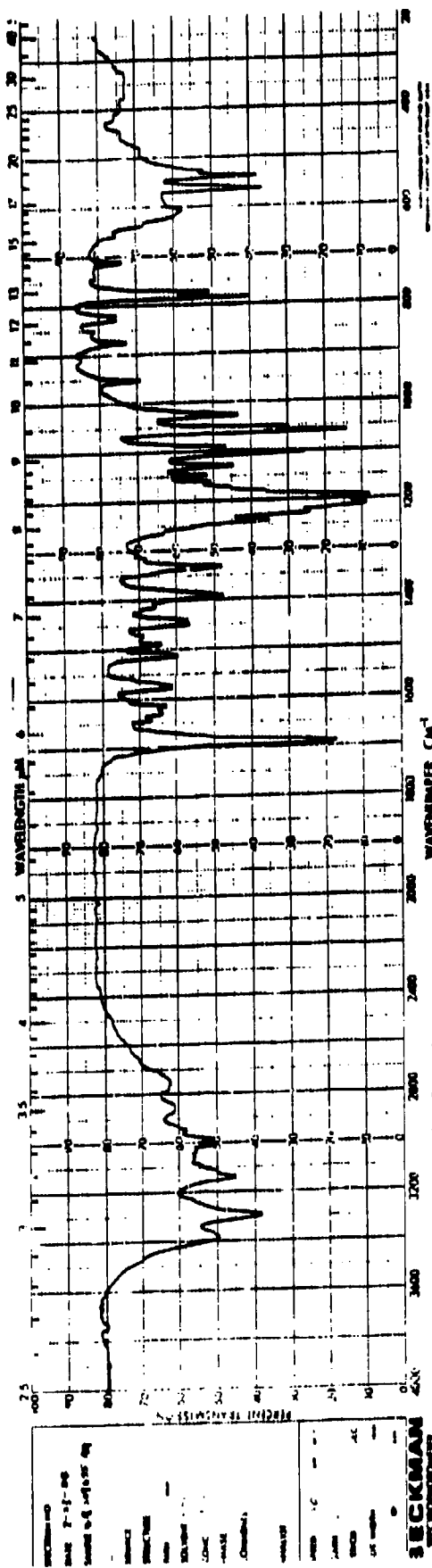


Figure 7. Infrared spectrum of HI-6 (WR249,655+2C1), Lot AG

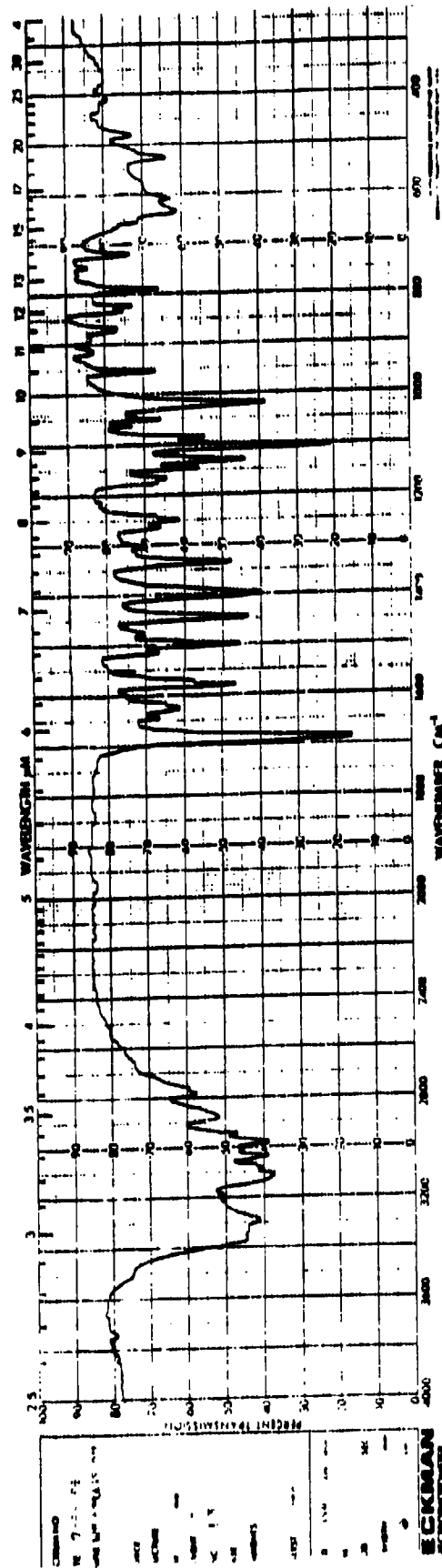


Figure 8. Infrared spectrum of HI-6 (MR249,655-2C1), Lot AH

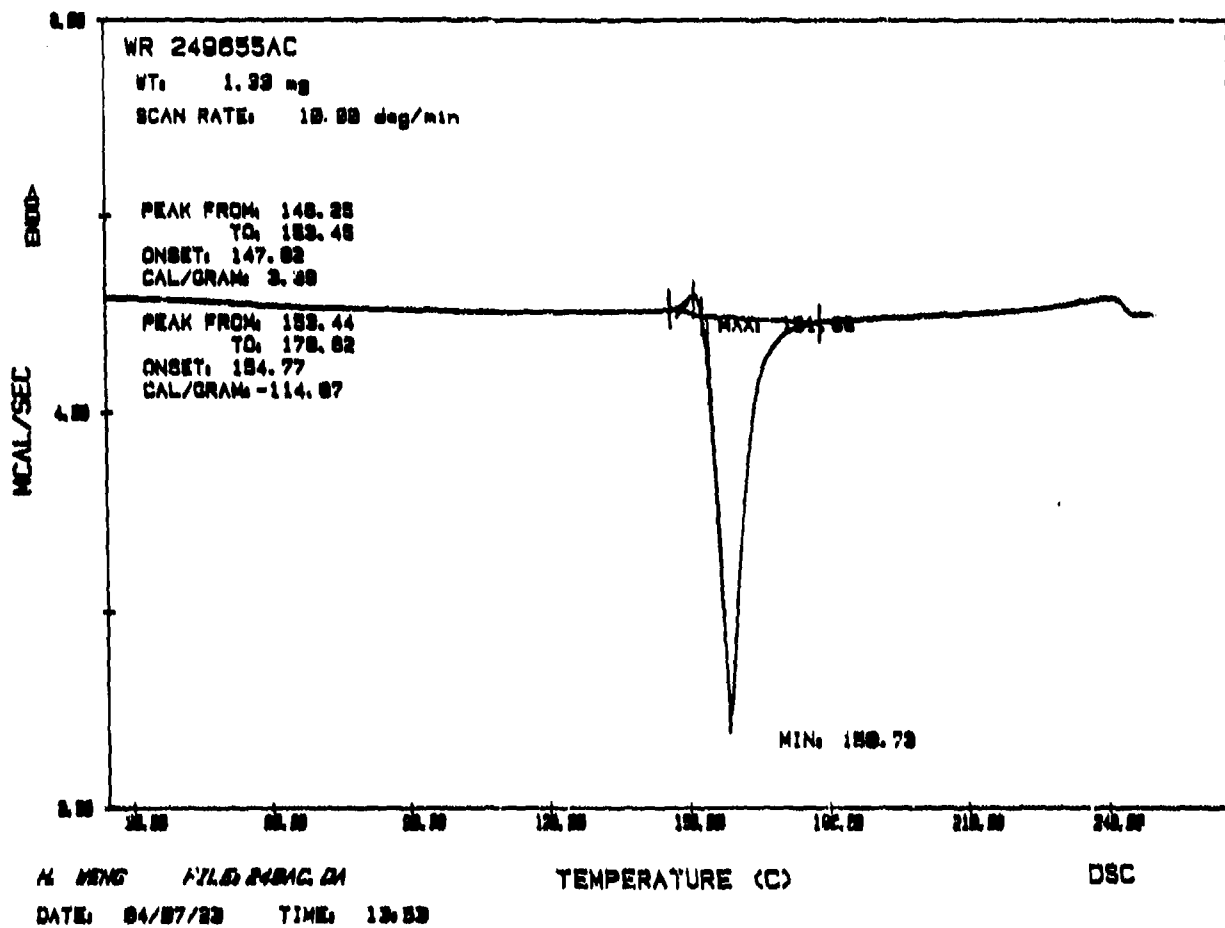


Figure 9. DSC Thermogram of HI-6 (WR249,655-2C1), Lot AC

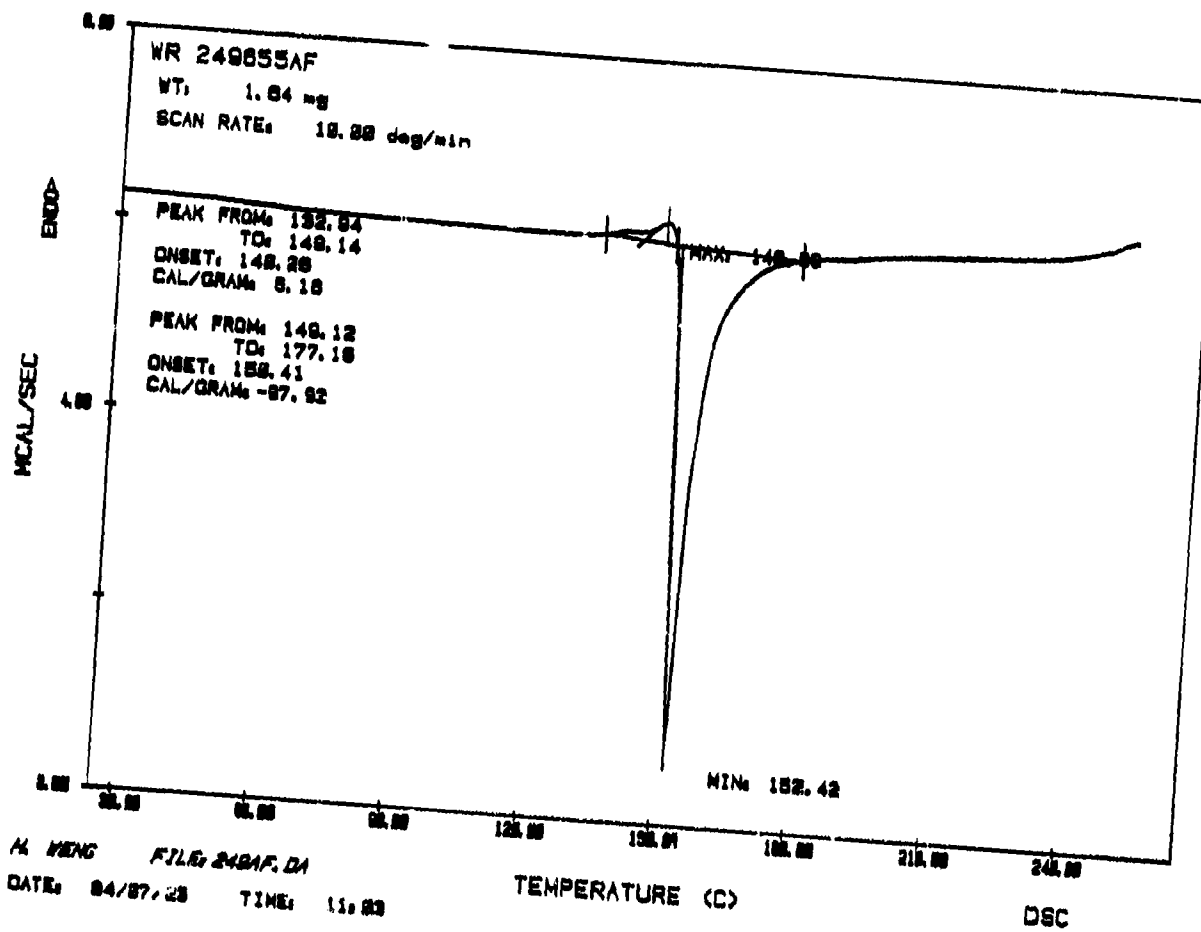


Figure 10. DSC Thermogram of HI-6 (WR249,655-2C1), Lot AF

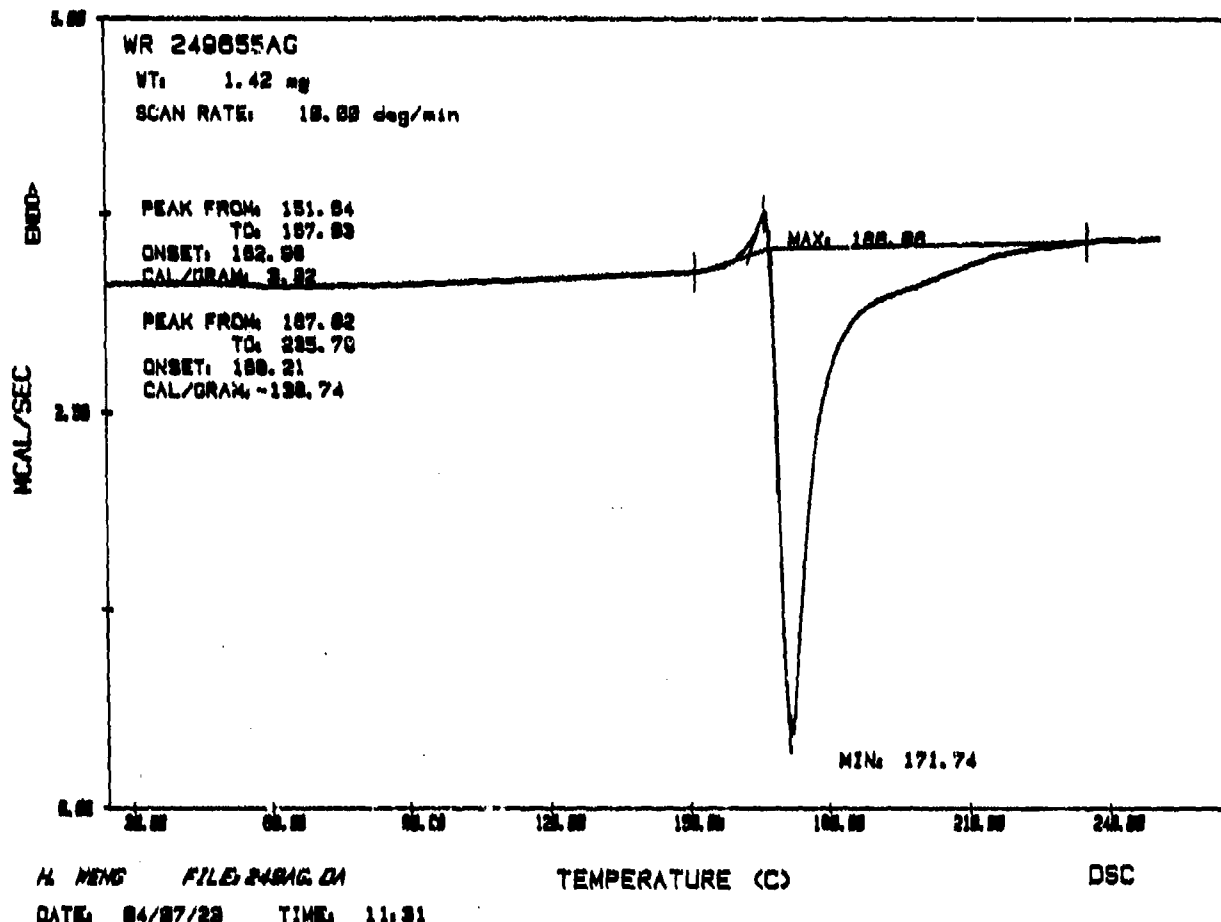


Figure 11. DSC Thermogram of HI-6 (WR249,655-2C1), Lot AG

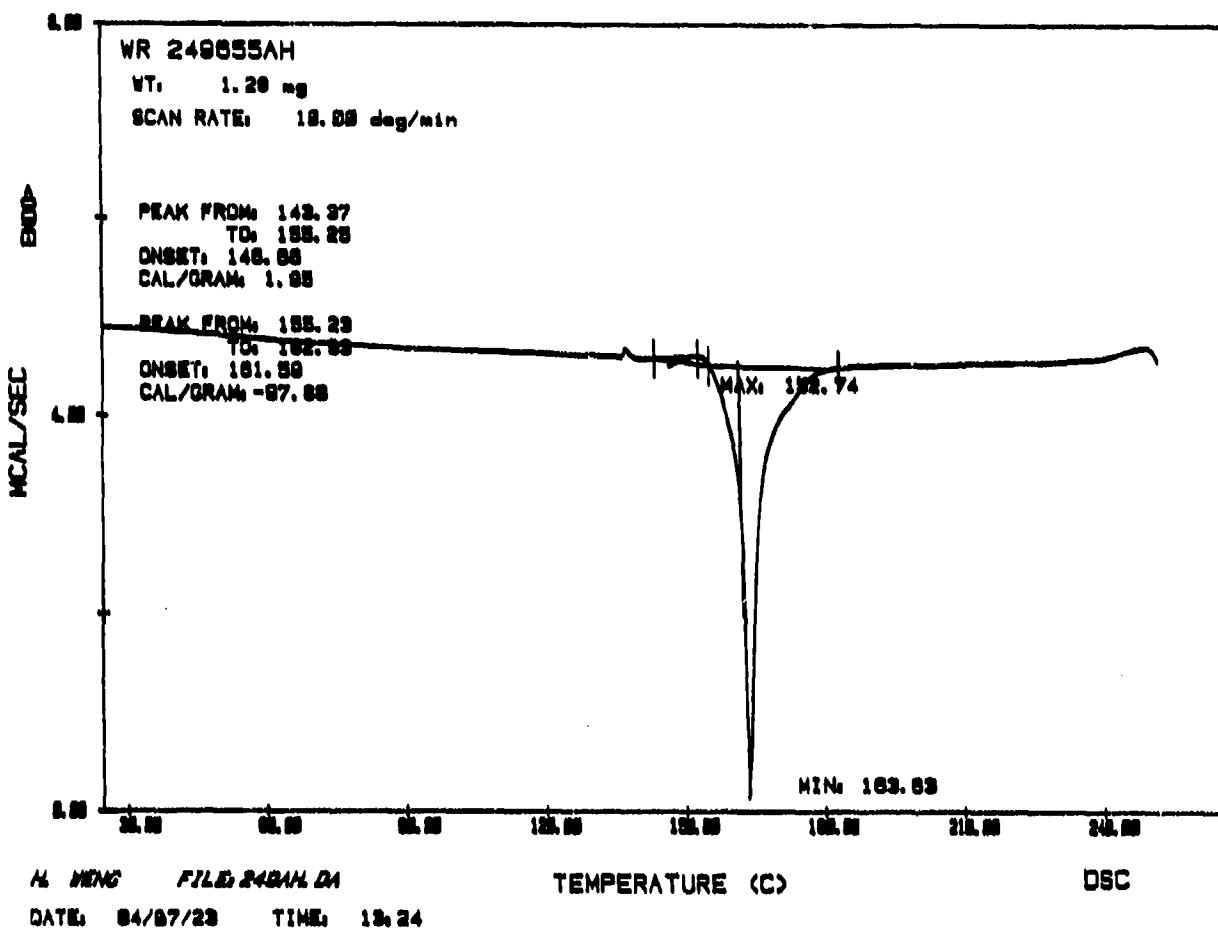


Figure 12. DSC Thermogram of HI-6 (WR249,655-2C1), Lot AH

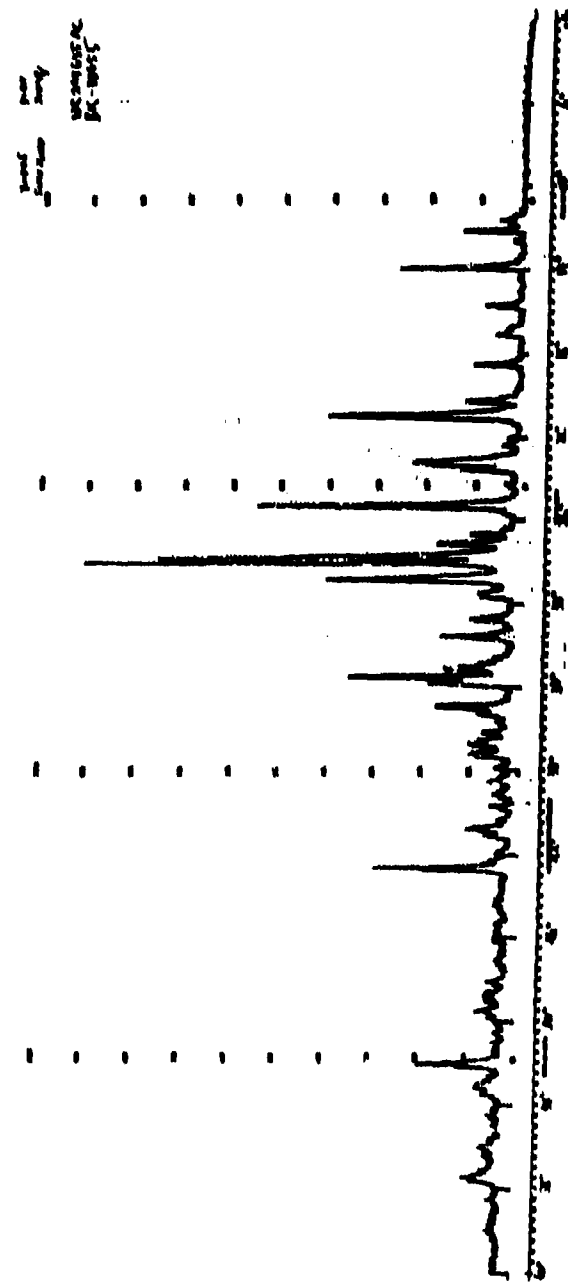


Figure 13. X-ray powder diffraction pattern for HI-6 (MR249, 655-2CL), Lot AC

Table 5. X-ray Diffraction Data for HI-6 (WR249,655·C1), Lot AC

2θ	D-Value (Å)	Peak Intensity (I)	Intensity Ratio (I/I' × 100)
11.616	7.618	313	1.06
11.765	7.522	220	0.75
12.111	7.308	951	3.23
13.885	6.378	2074	7.04
15.640	5.666	536	1.82
17.035	5.205	370	1.26
18.459	4.806	708	2.40
20.216	4.392	886	3.01
20.257	4.327	268	0.91
20.897	4.251	3201	10.86
21.180	4.195	236	0.80
23.158	3.841	1643	5.54
23.278	3.821	1406	4.77
23.519	3.782	816	2.77
25.296	3.521	4242	14.39
26.614	3.349	617	2.09
27.062	3.295	1080	3.66
28.867	3.202	29470 (I')	100.00
28.743	3.106	2997	10.17
30.681	2.914	572	1.94
31.520	2.838	1006	3.41
33.074	2.708	1001	3.40
33.466	2.678	2555	8.67
33.789	2.653	1339	4.54
34.883	2.572	1151	3.91
35.180	2.551	478	1.83
36.716	2.448	538	2.12
37.217	2.416	626	2.15
40.727	2.215	635	1.22
40.845	2.209	361	7.35
42.570	2.124	2165	4.51
42.670	2.119	1328	4.57
52.002	1.758	1346	2.10
52.152	1.754	620	1.86
57.453	1.604	549	

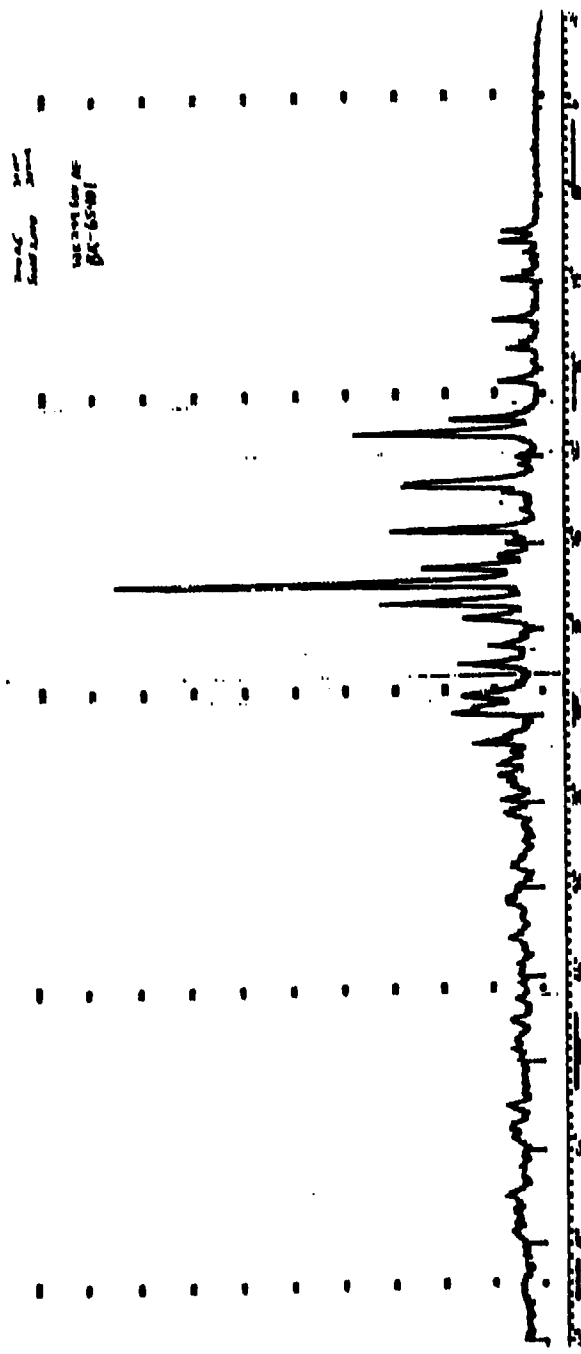


Figure 14. X-ray powder diffraction pattern for HI-6 (WR249,655-2C1), Lot AF

Table 6. X-ray Diffraction Data for HI-6 (WR249,655·Cl), Lot AF

2θ	D-Value (Å)	Peak Intensity (I)	Intensity Ratio (I/I' × 100)
11.605	7.625	540	8.12
12.062	7.337	636	9.56
13.838	6.350	516	7.76
15.696	5.646	727	10.93
16.738	5.297	248	3.44
17.024	5.208	438	6.58
18.474	4.803	562	8.45
20.219	4.392	1432	21.53
20.877	4.255	2945	44.27
21.178	4.195	240	3.61
23.122	3.847	2004	30.13
23.267	3.823	2134	32.08
25.319	3.518	2258	33.94
27.115	3.289	1688	25.38
27.860	3.202	6652 (I')	100.00
28.761	3.104	2234	33.58
29.433	3.035	1028	15.45
31.501	2.840	868	13.05
33.021	2.713	1036	15.57
33.525	2.673	779	11.71
33.787	2.653	1111	16.70
35.177	2.551	807	12.13

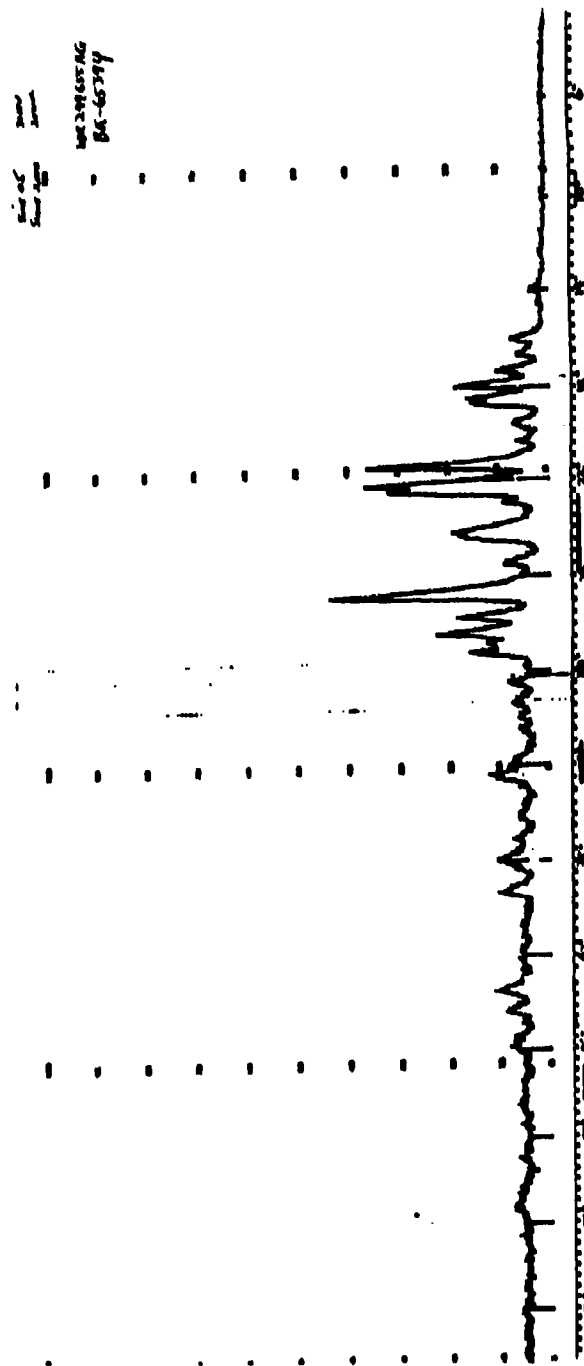


Figure 15. X-ray powder diffraction pattern for HI-6 (WR249, 655-2C1), Lot AG

Table 7. X-ray Diffraction Data for HI-6 (WR249,655-C1), Lot AG

2θ	D-Value (Å)	Peak Intensity (I)	Intensity Ratio (I/I' × 100)
16.011	5.535	468	15.46
16.596	5.342	448	14.80
17.258	5.138	744	24.57
17.431	5.088	406	13.41
17.880	4.961	1398	46.17
18.459	4.806	1082	35.73
18.640	4.760	830	27.41
18.714	4.741	888	29.33
21.434	4.146	2524	83.36
22.198	4.005	2640	87.19
22.458	3.959	2294	75.76
24.044	3.701	1059	34.97
24.157	3.684	1203	39.73
24.218	3.675	1216	40.16
24.324	3.659	1132	37.38
26.725	3.336	3028 (I')	100.00
27.665	3.224	1044	34.48
28.397	3.143	1392	45.97
29.181	3.060	886	29.26

Table 8. X-ray Diffraction Data for HI-6 (WR249,655·C1), Lot AH

20	D-Value (Å)	Peak Intensity (I)	Intensity Ratio (I/I' × 100)
11.718	7.552	292	0.12
12.070	7.332	542	0.23
12.161	7.278	554	0.24
13.955	6.346	6944	2.96
15.782	5.615	272	0.12
16.784	5.282	259	0.11
16.840	5.265	286	0.12
17.097	5.186	2223	0.95
18.503	4.795	268	0.11
20.314	4.372	665	0.28
20.810	4.268	2713	1.16
20.927	4.245	4339	1.85
23.200	3.834	2090	0.89
23.367	3.807	6859	2.92
24.936	3.571	1405	0.60
25.384	3.509	3569	1.52
27.185	3.280	989	0.42
27.339	3.262	692	0.29
27.942	3.193	234614 (I')	100.00
28.627	3.118	3571	1.52
28.820	3.098	8154	3.48
29.490	3.029	626	0.27
29.554	3.022	580	0.25
30.771	2.906	824	0.35
32.856	2.726	494	0.21
33.134	2.704	1716	0.73
33.620	2.666	2184	0.93
33.820	2.650	1228	0.52
34.945	2.568	2975	1.27
35.036	2.561	1694	0.72
35.280	2.544	480	0.20
36.781	2.443	500	0.21
37.104	2.423	715	0.30
37.319	2.409	938	0.40
42.299	2.137	1884	0.80
42.403	2.132	941	0.40
52.039	1.757	774	0.33
55.995	1.642	905	0.39
57.347	1.607	1116	0.48
57.540	1.602	1438	0.61
57.697	1.598	645	0.27

SUPPLEMENTARY

INFORMATION



DEPARTMENT OF THE ARMY
U.S. ARMY MEDICAL RESEARCH AND DEVELOPMENT COMMAND
FORT DETRICK, FREDERICK, MD 21702 5012



REPLY TO
ATTENTION OF:

ERRATA

SGRD-RMI-S

(70-1y)

B 113 186

18 1 JUL 1992

MEMORANDUM FOR Administrator, Defense Technical Information Center, ATTN: DTIC-HDS/William Bush, Cameron Station, Bldg. 5, Alexandria, VA 22304-6145

SUBJECT: Request Change in Distribution Statement

1. The U.S. Army Medical Research and Development Command (USAMRDC), has reexamined the need for the limited distribution statement on technical reports for Contract No. DAMD17-85-C-5003. Request the limited distribution statement for AD No. ~~DAD113186~~ be changed to "Approved for public release; distribution unlimited," and that copies of these reports be released to the National Technical Information Service.
2. Point of contact for this request is Ms. Virginia Miller, DSN 343-7325.

ERRATA

Carey O. Leverett
CAREY O. LEVERETT
LTC, MS
Deputy Chief of Staff for
Information Management

CF:

Dr. Ruthann Smejkal/WRAIR

ERRATA:

B 113 186

100-20114